Carbon Dioxide Intensified Hydrolysis of Secondary Phytochemicals

Dissertation

zur

Erlangung des Grades

Doktor-Ingenieur

der

Fakultät für Maschinenbau

der Ruhr-Universität Bochum

von

Markus Maier

aus Baierdorf bei Anger

Bochum 2017

Summary

»An apple a day keeps the doctor away«. This saying has been the impetus for numerous studies. The focus of many of these studies lays on flavonoids and tannins (condensed or hydrolyzable tannins), so-called secondary phytochemicals. Flavonoids (occurring mostly as glycosides) and tannins are widespread in flora, e.g. in medicinal plants. Throughout centuries medicinal plants have been utilized for self-treatments of human diseases, e.g. diarrhea and inflammations, and were the basis of a daily nutrition, which acted to prevent infections and strengthen the immune system.

For utilization of those secondary phytochemicals, in particular tannins, a screening study of 47 European medicinal herbs and spice plants was conducted to identify plants with high tannin contents. 16 plants were identified with measurable tannin content. Out of those 16 plants, four plants were identified with tannin contents above 7 w% in the dried plant and tannin contents of up to 38.4 w% in the dried extracts. Furthermore, the flavonoid (quercetin) content of those plants was analyzed by hydrolyzing the extracts.

In the conventional production process of quercetin, the extracts are hydrolyzed with mineral acids (HCl, H_2SO_4, HNO_3). This requires a neutralization step with alkaline or salts after hydrolyzing the extract. The neutralization forms salts in high concentrations that have to be later removed during the wastewater treatment. To avoid this neutralization step, an alternative methodology – CO_2-intensified hydrolysis – was investigated. CO_2-intensified hydrolysis requires only water and CO_2-pressure to form H+ ions for lowering the pH-value. To study that reaction in detail rutin, a flavonoid glycoside and the most common flavonoid in plants was selected as model substance and was dissolved in purified water prior to hydrolysis. The temperature- and the CO_2 pressure-dependence of the CO_2-intensified hydrolysis were investigated by varying

the temperature between 373.15 K and 433.15 K and the CO_2 pressure between ambient pressure and 150 bar. Thereby, a temperature and pressure dependence model were obtained. In this model, a new H^+-factor was introduced describing the influence of H^+ ions and concentrations of the model substance in the CO_2-intensified hydrolysis process. The optimum process parameters were found to be 413.15 K and 150 bar (100 % conversion of rutin to quercetin).

For assessing the potential of the CO_2-intensified hydrolysis, a mass balance for the conventional quercetin production process was made up considering a conventional source (*Fagopyrum*, rutin content 5%). For a production volume of one ton of quercetin (assumed that rutin is 100% hydrolyzed to quercetin), 20 tons of *Fagopyrum* weed is needed. The extraction in a ratio of 1:10 with water as extraction solvent would result in a consumption of 200 tons of water. Depending on the used acid, different salts could be formed due to neutralization. H_2SO_4 would form 2.84 tons of Na_2SO_4, HNO_3 would form 1.7 tons of $NaNO_3$ and HCl would form 1.2 tons of NaCl after neutralization, which have to be separated prior to introducing it to wastewater treatment plants.

For testing the CO_2-intensified hydrolysis on plant extracts, *Arctostaphylos uva-ursi* and *Fragaria* were investigated regarding the potential of a combined production process of hydrolyzed extracts rich in flavonoids and tannins. In addition, hydrolysis was performed with a strong acid (HCl) at 363.15 K and ambient pressure to compare the results with conventional acid hydrolysis. Furthermore, hydrolysis with a weak acid (CH_3COOH) was conducted at 363.15 K and ambient pressure inspired by the CO_2-intensified hydrolysis at pH 3. It was observed that hydrolyzable tannins degraded to 20% during hydrolyzing the extract at 413.15 K and 150 bar CO_2-pressure. In contrast, condensed tannins did not degrade to such a high extent (a loss of 20 % was observed after eight hours of CO_2-intensified hydrolysis). For *Fragaria,* a quercetin content of

0.23w% and a tannin content of 19.6w% in the dried extract was generated. For *Arctostaphylos uva-ursi,* a quercetin content of 0.35w% and a tannin content of 5.8w% in the dried extract was produced.

Acknowledgment

Table of Content

1 Introduction

1.1 Motivation

»An apple a day, keeps the doctor away« This famous idiom has been the impetus for numerous studies [2–4]. The positive effects of apples on the human body are not only limited to the presence of minerals and vitamins, but also to a great extent, to the presence of polyphenols that promote and intensify the positive effect of the vitamins and minerals [5]. The focus of the before mentioned studies referred to flavonoids and tannins (condensed or hydrolyzable tannins), also called secondary phytochemicals. Flavonoids and tannins are widespread in flora, e.g. in medicinal plants. For centuries medicinal plants have been utilized for self-treatments of human diseases, e.g. diarrhea [6] or inflammations [7] and were the basis of a daily nutrition, which acted to prevent infections and strengthen the immune system. Nowadays, flavonoids and tannins are also used in pharmaceuticals as an enhancer for the active pharmaceutical ingredient [8], in cosmetics [9, 10] and food supplements (mostly as plant extracts). Among these, quercetin is the most common flavonoid and can be found in a high abundance in fruits (e.g. apples and berries), vegetables (e.g. onions, broccoli, lettuce, tomatoes) [11] and medicinal herbs (e.g. buckwheat and bearberry leaves) [12]. Tannins occur in condensed (polymers of flavonoids) or as hydrolyzable (gallic or egallic acid bonded to a sugar) forms and can be found mainly in woods, barks, roots or in the leaves of plants. European medicinal herbs [13] were selected in a screening study to evaluate the potential of CO_2-intensified hydrolysis to obtain a flavonoid and tannin-rich extract. The screening was conducted to identify European medicinal plants with the highest tannin contents. Those plants were further analyzed regarding their flavonoid content (quercetin). The purpose of this study was the development of a

combined production process to obtain a flavonoid and tannin-rich powder. In the plant material, flavonoids and tannins are mostly present in their glycoside form and for later application in food supplements, etc… they have to be converted to their aglycone form by hydrolysis. In general, hydrolysis reactions are widely common in industrial processes, e.g. for sugar substitutes: hydrolysis of sucrose, starch to glucose or glucose syrup and starch to maltitol syrup [14, 15]. The conventional acid-hydrolysis can be carried out by adding hydrochloric acid [16], sulfuric acid [17] or nitric acid [18] and requires neutralization after hydrolysis with the addition of alkaline solutions [19]. Besides acid-catalyzed hydrolysis, enzymes can be an alternative for a specific hydrolysis of certain sugars [20] or hydrolysis of natural substances in pressurized and tempered water, e.g. hydrolysis of lignin, cellulose, hemicellulose [21–24]. Furthermore, several studies focused on glycosides cleavage via hydrothermal degradation or hydrolysis / pretreatment in subcritical water [25–28]. The applied pressures were achieved via static pressure, N_2 or CO_2. The latter was the focus of numerous studies [25, 29–35] and is applied by pressurized liquid CO_2 in water. The hydrolytic effect of CO_2-pressure in water is explained by the formation of H^+ ions due to dissociation. This formation of H^+ ions causes a decrease of the pH value to a minimum value of approximately 3. In combination with temperatures above 373.15 K, the hydrolytic effect is strong enough to cleave glycosidic bonds. In this work, the influence of CO_2-pressure applied on a model flavonoid glycoside (rutin) – water solution was examined. In particular, the influence of H^+ formation was investigated by varying pressure and temperature. Out of the experimental data, two kinetic models were compiled, one for the temperature and one for the pressure dependence. In the models, a »H^+-factor« was introduced to describe the excess of H^+ ions in comparison to the glycoside. The CO_2-intensified hydrolysis was further compared with conventional acid hydrolysis (hydrochloric and acetic acid). In order to understand

hydrolysis applied on tannins and the stability of tannins at temperatures above 413.15 K, the CO_2-intensified hydrolysis was investigated on tannins as well. For that purpose, tannic acid was used as a model substance to determine the hydrolytic degradation. The hydrolysis of flavonoids and tannins (model substances) was the basis for identifying suitable process parameters to apply it on plant extracts.

In the following chapters, relevant basics about European medicinal herbs and spice plants, secondary phytochemicals, different types of hydrolysis, including acid-catalyzed hydrolysis, enzymatic hydrolysis and CO_2-intensified hydrolysis are discussed.

1.2 European medicinal herbs and spice plants

According to Kew – Royal Botanical Gardens [36] there are more than 28.000 medicinal plants worldwide. The health benefits are mostly ascribed to phytochemicals, e.g. alkaloids, terpenes, diterpenoids, cardiac-glycosides, organic acids and coumarins. Besides, polyphenols, e.g. flavonoids and tannins, gain more and more importance in nutrition, as they may be beneficial for the human body, e.g. as anticancer or antiviral agents.

Since the medieval time, European medicinal herbs and spice plants (EMHSP) have been a basic element of European traditional medicine. EMHSP were mainly used in the preventive medicine and for strengthening the physical constitution. Back in the days, EMHSP were mixed with the meals to cleanse the body, strengthen the gastrointestinal tract and the bitter compounds of the plants conducted as an energy supplier for the human body. In general, the diet of humans was based on vegetables, fruit, herbs, crops and a small amount of meat.

In the last 10 years, the general interest of EMHSP gained more and more importance due to their potential positive effects and value for the human body. A major reason for the increase of cultivation is also explained by the increased fundings of research institutes by provincial governments. These realized funded research projects initiated a positive development within the federal states of Germany, especially in Bavaria and Thuringia. Changes in the German drug law, regulation of protection of species, residue amounts and crop protection, and the high environmental standards in Germany had a positive influence on the production of EMHSP. For the successful development of German cultivation of EMHSP the following market trends had a major impact: expansion of cultivation due to breeding and research activities; cultivation of usually wild collected species and enhanced exploitation as an industrial resource for technical and chemical purposes. [37]

In 2016, around 7.125 ha of cropland were used for cultivation of EMHSP (in Germany) [38]. In 2003 about 70 different species of EMHSP were cultivated [37]. Hoppe further classified the species into 6 groups, where the first four groups are the most important ones from the economical point of view [39]:

Table 1: Classification of species ordered to their cultivation area in 2003 [39] (supplemented in 2008)

Group	Cultivation area [ha]	Species
1	> 1000	Parsley
2	500 – 1000	Dill, marjoram, chives, flax camomile
3	100 – 500	Amber, thyme, celery, horseradish, fennel, basil, elder, ergot, mustard, chervil, peppermint, marian thistle
4	50 – 100	Willow (pharma), oregano, escallion, coriander, topinambour, caraway, woolly digitalis
5	10 – 50	e.g. sage, calendula, buckwheat, melissa, coneflower, stinging nettle,…
6	< 10	e.g. yarrow, baldmoney, rhubarb root, …

The German government declared in its action plan to increase the cultivation of EMHSP up to 20.000 ha in 2020 (Umsetzung der Drucksache 16/9757 of the German Bundestag, 25.08.2008). According to this action plan, a high potential can be derived and can be used for the search of new potential plants, which could be cultivated and used as a new renewable resource for the production of secondary phytochemicals.

1.3 Secondary phytochemicals

Secondary phytochemicals are secondary metabolic plant products, which are synthesized in specific plant cells at a specific time and are not essential for the survival of the plant. Those compounds serve in general as protection against herbivores, UV-

rays but also act as flavoring agents, attractants for insects, colorants, antioxidants, etc…In literature, more than 24.000 structures are described excluding oligomeric polyphenolic structures – condensed and hydrolyzable tannins – but including many antinutrients or toxic compounds [40]. According to RÖMPP, the most important secondary metabolites are: carotenoids, phytosterols, phytoestrogens, saponins, glucosinolates, monoterpenes, alkaloids, nonprotein amino acids, sulfides, protease inhibitors, lecithins and polyphenols [41]. The latter – polyphenols - can be subdivided into phenols (e.g. catechol), phenolic acids (e.g. gallic acid), hydroxycinnamic acids (e.g. caffeic acid), coumarins (e.g. umbelliferon), flavonoids and iso-flavonoids (e.g. quercetin and genistein), lignans (e.g. pinoresinol), lignins (e.g. lignin) and tannins (e.g. hydrolyzable and condensed tannins). Regularly, those compounds are bonded with sugars, to enhance their water solubility or their chemical stability, named »glycoside«. The sugar-free compound is called »aglycone«. Examples of glycosides[1] are hydrolyzable tannins (oligomer of gallic acid or egallic acid also called gallo tannins) or flavonoid – O – glycosides (rutin, hesperidin, naringin, etc.). Another possibility are polymerized structures, e.g. condensed tannins (proanthocyanidins – flavonoid – C – glycosides[2]). In the following subchapters, the substance classes flavonoids and tannins are described in more detail.

---

[1] Glycosides mainly occur as an aglycone bonded with an oxygen atom to a sugar. Further possible bonding atoms could be nitrogen, sulfur or selenium
[2] C-glycosides are difficult to be hydrolyzed by acids

1.3.1 **Flavonoids**

Flavonoids have in general a C15 body (Figure 1) and are divided, depending on their structure, into chalkones, flavan derivates, aurones and isoflavones.

Flavan derivates are the largest group of flavonoids and can be subdivided into flavanones, flavones, flavonols, leucoanthocyanidins, catechins and anthocyanidins. Furthermore,

Figure 1: General structure and numbering of flavonoids [1]

flavonoids differ in their amount of hydroxyl and methoxy substitutes and are mostly substituted on the A-ring with a C5 group. Flavonoids can occur as mono or oligo-glycosides. Glucose, galactose, rhamnose, uronic acids and further sugar derivates are mainly linked with an oxygen atom to the C3, C5 or C7 flavonoid basic structure. In some cases, glycosides are bonded with a carbon atom (C-glycoside) on the C8 atom. [42]

Flavonoids play an important role in plants and are responsible for an abundance of functions in the plant, e.g.:

- in the blossoms as vegetable colorants, which is crucial for the enticement of pollinators (e.g. anthocyanins (red to blue), flavones (white), flavonols (yellow))
- protection against herbivores due to their astringency (condensed tannins)
- repellent against herbivores due to toxicity (flavonols and flavonol-glycosides)
- protection against UV rays (flavones and flavonols)

Many of these flavonoids have antioxidative [43, 44], antibacterial [45, 46], antifungal [47, 48], antiviral [49, 50] or even anticarcinogenic [51, 52] properties.

A popular representative of flavonoids is quercetin. It is one of the most common flavonoids in fruits (e.g. apples and berries), vegetables (e.g. onions, broccoli, lettuce, tomatoes) [11] and medicinal herbs (e.g. buckwheat and bearberry leaves) and therefore, the reason for many studies. It has many health benefiting properties: anti-histaminic, anti-allergic and anti-inflammatory [53], anti-oxidative and anti-inflammatory [54], anti-allergic and anti-inflammatory [55], anti-thrombotic [56] and anti-sclerotic [57].

1.3.2 Tannins

Tannins are widespread in flora and occur in bushes, foliage, herbs and wood. They act as protection against herbivores due to their ability to deactivate proteins in the digestive system. Quideau et al. [58] classified tannins in three classes:

1) Proanthocyanidins: belong to condensed tannins (e.g. procyanidins, prodelphinidins and profisetinidins, which are oligomerized out of flavan-3-ol-units, see Figure 2) [59]
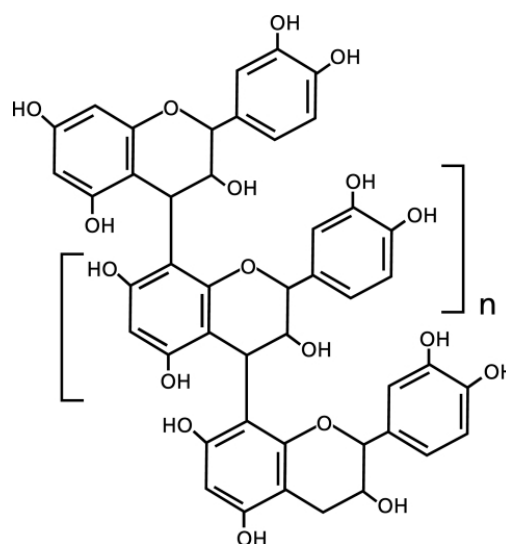
Figure 2: Structure of oligomeric proanthocyanidins [60]

2) Gallo- and ellagitannins: belong to hydrolyzable tannins, which contain gallic acid or egallic acid glycosides [61], (Figure 3)

3) Phlorotannins of red-brown algae (Figure 4).
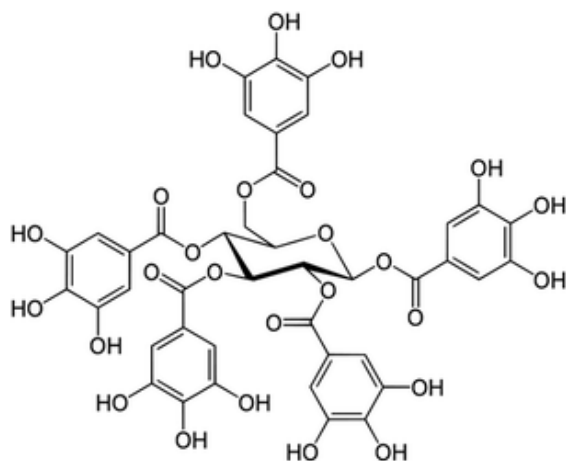
Figure 3: Penta-galloyl-glucose (PGG) [62]
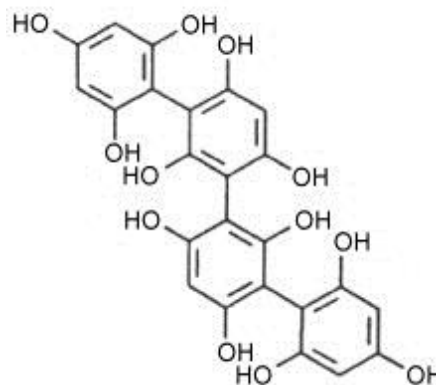
Figure 4: Tetrafucol A [63]

A further definition of Bate-Smith and Swain [64–66] for tannins implied: a molecular weight between 500 to 3 000 g/mol, the ability to precipitate alkaloids and build complexes with proteins and carbohydrates. In history, condensed and hydrolyzable tannins played an important role in the leather industry in order to prolong the stability of animal hides. Besides tanning of leather, Pizzi [67] summarized further possibilities for the usage of tannins: adhesives, especially wood adhesives [68–72], cement superplasticizers [73], wastewater treatment as tannin based coagulants [74–76] and drugs. Recently, tannins were investigated in-vivo and in-vitro for medical and pharmaceutical purposes due to their positive health effects: antimicrobial activity [77] – in vivo, antioxidant [78] – in-vivo, anti-caries [79] – in-vitro, anti-HIV [80] – in-vitro and anti-tumor [81] – in-vivo. Furthermore, extracts of fruits, berries and vegetables containing tannins are commonly used in food supplements for anti-aging and degenerative disease [72, 82, 83].

Choosing an appropriate assay for analyzing tannins

Many assays are available for quantifying tannins in extracts. In order to quantify the tannin content in plants, a distinction between hydrolyzable and condensed tannins and three main tannin reactions are required [84]:

The first reaction is a complexation on the phenolic ring (condensed tannins):

- complexation with metal ions, e.g. iron or titanium ions;

- reduction with iron ions (Prussian blue method [85]);

- reaction with vanillin (Vanillin method [86]) or

- complexation with formaldehyde (Stiasny method) [87].

The second reaction is depolymerization: that means oxidative depolymerization in butanol and hydrochloric acid with estimations of proanthocyanidins, or hydrolysis with estimations of gallic and egallic acid to draw interferences from gallic and egallic acid about hydrolyzable tannins, e.g. gallotannins or ellagitannins.

The third reaction is the complexation reaction of tannins with proteins (both hydrolyzable and condensed tannins). This can be caused by: adsorption of tannins with hide powder [88]; precipitation of tannins with proteins in a solution [89] or by diffusion of tannins in a protein containing gel (RDM) [90].

Besides the possible reactions with tannins, the number of samples should be taken into consideration. For the proposed screening of EMHSP, a big number of samples has to be analyzed. Hence, diffusion of tannins in a protein containing gel was selected to quantify tannins for the screening. The RDM-procedure is described in chapter 2.2.1. The benefits of RDM are:

- analysis of crude extracts

- preparation of Petri plates with the gel is simple and the used materials are less cost intense in comparison to HPLC analysis

- evaluation of tannin content is simple (precipitation ring area is compared with calibration curve)

- besides Petri plates, pipette and caliper, no further equipment is needed

- both, hydrolyzable and condensed tannins can be analyzed

1.4 Industrial quercetin production

Quercetin (Figure 5) from plant materials is obtained in the glycosidic form and has to be converted into its aglycone by hydrolysis prior to usage. A liquid rutin-containing extract is usually used as a raw material for the production of quercetin. Rutin (Figure 6) is present as a glycosidic compound of quercetin, rhamnose (naturally occurring 6-desoxy single sugar) and glucose in plants.
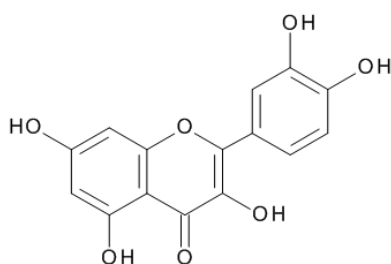
Figure 5: Quercetin
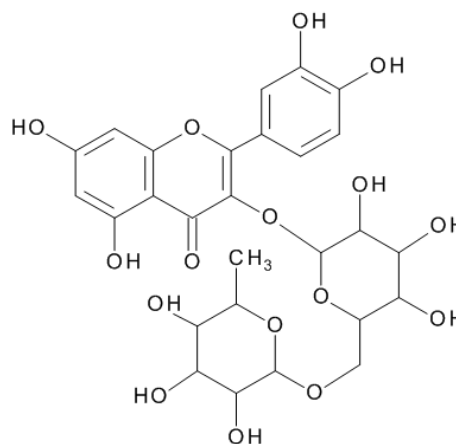
Figure 6: Rutin (quercetin-3-O-rutinosid)

The following plants or residues are considered as a source of raw material for quercetin (all content refers to the dry weight of plant material):

- Japanese lap (*Styphnolobium japonicum*): The Japanese lap is mainly found in China, Korea and Japan. A high rutin content could be detected both, in the flowers (12 to 30% by weight) and in the leaves (4% by weight) [12].

- Fava d'anta (*Dimorphandra mollis*): Fava d'anta is cultivated in Brazil. The plant has a rutin concentration of up to 8% by weight [91] and is used for the production of either rutin or quercetin.

- Genuine buckwheat (*Fagopyrum esculentum*): Genuine buckwheat is found all over the world. The leaves contain rutin in a concentration of up to 5% by weight [12].

Conventionally, an acid-catalyzed hydrolysis process produces the glycosides. Strong mineral acids, e.g. hydrochloric acid, sulfuric acid or nitric acid, are used for this purpose. These acids cause the cleavage of the sugar residue from the molecule, thus the aglycone can be recovered. The Brazilian company »Quercegen« as the largest manufacturer of quercetin accredited the production process by the FDA (the Federal Drug Association, USA) and obtains GRAS (General Recognized As Safe) status (Figure 7).
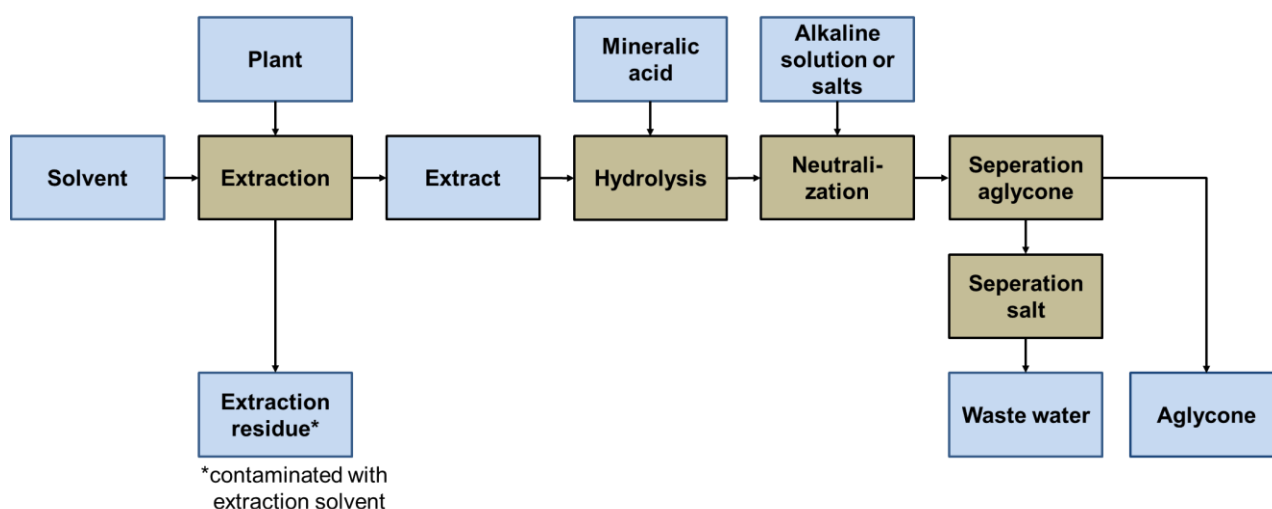
Figure 7: Conventional production process of quercetin – company »Quercegen©« (accreditation from FDA)

In the first production step, a rutin-containing extract is produced from a plant. This extract is hydrolyzed with a diluted mineral acid, in this case nitric acid, at 90 °C. Nitric acid and 90 °C is sufficient to split rutin to its sugar and aglycone. After the hydrolysis, neutralization by an alkaline solution follows. As an alkaline solution, various salts, e.g. sodium carbonate, but also dilute strong alkalis, e.g. sodium hydroxide solution or potassium hydroxide solution, can be used. The formed salts must be separated by a reverse osmosis before they enter the wastewater treatment in order to not exceed the maximum salt concentration in the effluent. The salts formed from the neutralization are nitrates, sulfates or chlorides, depending on the acid used. After neutralization, quercetin precipitates during cooling due to the lower solubility of the aglycone and is separated with a centrifuge.

The Chinese patents CN101985439B [92], CN104387357A [93], CN102659740B [94] and CN103965153 B [95] describe acid-catalyzed hydrolysis using mineral acids such as hydrochloric acid and sulfuric acid and thus, correspond to the state of the art (Table 2). China is the largest producer of quercetin and is therefore, predominant on the market.

Table 2: Patent survey - hydrolysis conditions

Patent	Acid	pH	Temperature [K]	Pressure [bar]
CN101985439B [92]	H_2SO_4	2	343.15 – 353.15	-
CN104387357A [93]	HCl, H_2SO_4	3	373.15	-
CN102659740B [94]	HCl, H_2SO_4, H_2PO_4	2	353.15 – 363.15	-
CN103965153 B [95]	mineral acid	3-5	423.15 – 473.15	5 – 7.5

1.5 Hydrolysis of glycosides

1.5.1 Acid hydrolysis

In general, glycosides consist of two parts, the glycosidic part – the glycosidic C-atom – is bonded via an O, N, S or Se atom to the second part, the aglycone. The aglycone can also be a carbohydrate or a random compound, which includes an alcoholic or phenolic hydroxyl group. In water the glycoside subverts during exposure to acid according to following scheme:

The acid hydrolysis of glycosides exists of three reaction steps (Figure 8):
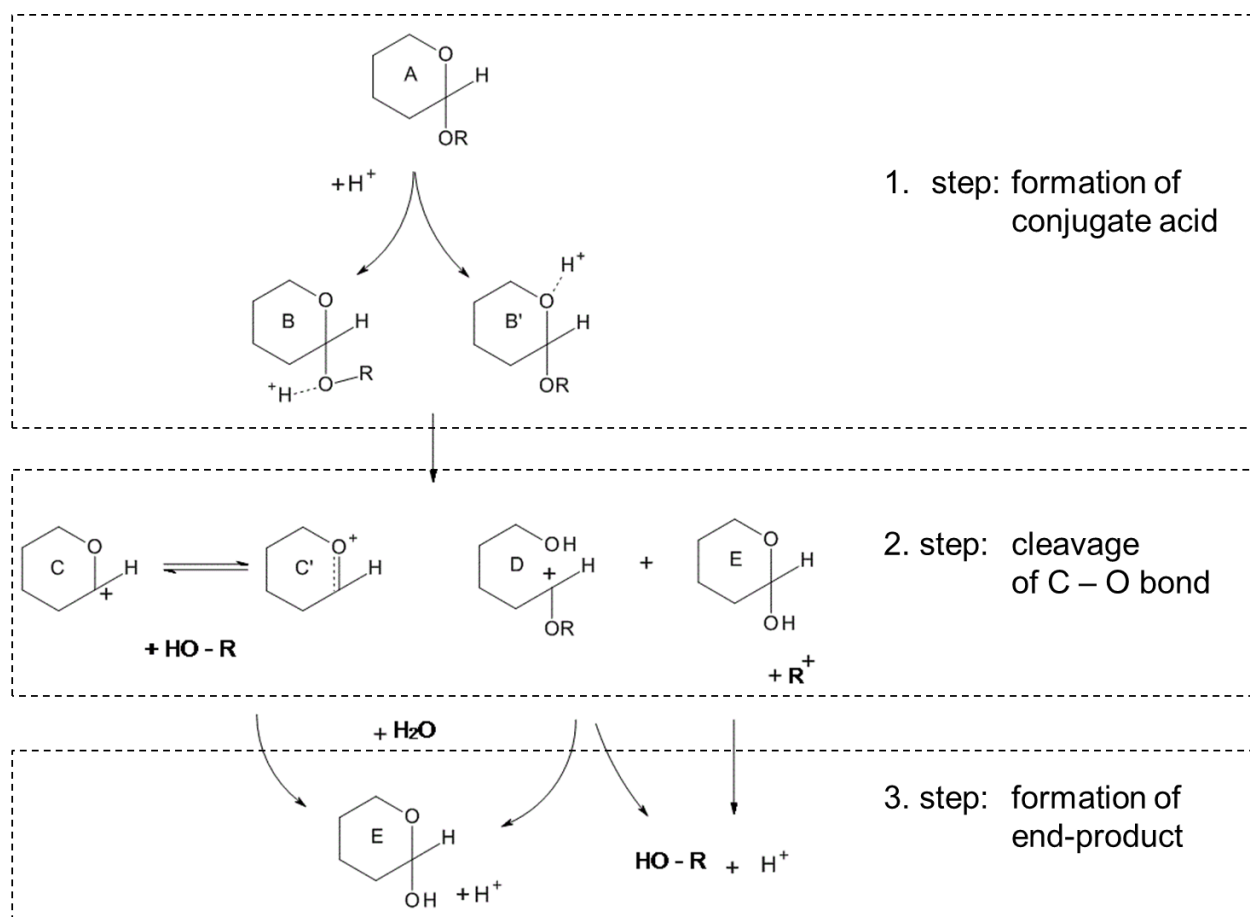
Figure 8: Hydrolysis reaction mechanism of glycosides [96–101]

- *1.step – formation of the conjugate acid:* The catalyst proton (H^+) interacts with the glycosidic oxygen (B) or the ring oxygen (B'). The reaction on the glycosidic oxygen is more likely. This reaction step is fast and ends up in an equilibrium. [99]
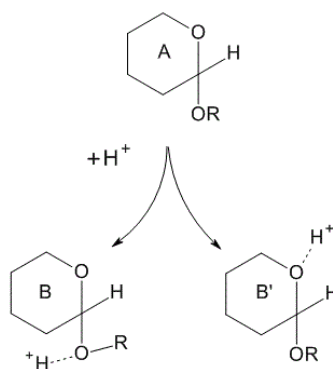
- *2.step – cleavage of C – O bond:* Due to the cleavage of this bond a carbenium cation (C,D or R^+) and oxonium cation (C') forms. This can occur in four different ways:

  a) **A → B → C**: according to this reaction pathway, a cyclic carbenium cation occurs and one of the end products that is the aglycone alcohol. The glycosidic bond cleaves already in the first step

  b) **A → B' → D**: formation of an open-chain cation, the glycoside is cleaving by an additional step **D → E**

  c) **A → B → E**: formation of an aglyconyl cation, the reaction is already finished in the mononuclear step, this can even be faster than a) or b)

  d) **A → B' → C'**: protonation of the ring oxygen, the ring is not cleaved, a cyclic oxonium ion is formed (carbenium cation)
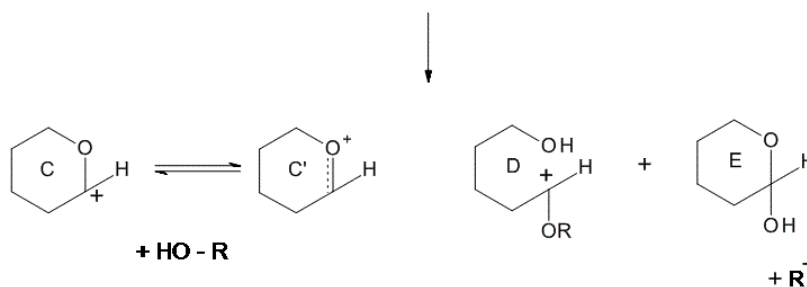
- *3.step – formation of end-product:* The carbenium cation causes heterolysis with the water molecule (H^+ + OH^-). From this information, it is not clear which step is the rate-limiting step, the second (monomolecular) or the third (bimolecular).
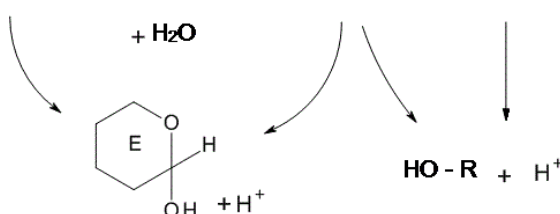
Hydrolysis is generally applied in organic-chemistry industry, food production and especially in the pharmaceutical industry to cleave glycosides to aglycones or carbohydrates. In most cases, a complete hydrolysis is targeted but for glycosidic mixtures a selective hydrolysis is important. Sample preparation for analysis requires an optimal set of conditions including temperature, acid / enzyme concentration and time. Hydrolysis depends on inner and outer factors. The inner factors are dependent on the structure and properties of the glycoside and the outer factors are determined by the hydrolysis conditions [102]:

- *Phase conditions*

The total hydrolysis effect (H_{eff}) in a diluted solution at a certain temperature can be expressed as:

$$H_{eff} = r \cdot i_a \cdot m \cdot \alpha \cdot c \cdot \gamma = r \cdot i_a \cdot m \cdot a_{H+}$$

Here r is a proportional factor, i_a is a measure of heterogeneity and is 1.00 in homogeneous solutions and 0.00 in an inner crystal. i_a is identical to the accessibility

factor for the hydrolysis of polysaccharides. The mobility factor of hydronium ions is described with m and is 1.00 for strong mineral acids with low relative molecular weights and for polymeric acids it is reverse proportional to the distance between ionized groups. The stiffer the polymeric acid, the smaller is m – e.g. for cation exchanger resin m ≤ 0.1. α describes the dissociation of the acid, γ the activity coefficient of hydronium ion and c is the normality of the expressed acid concentration. α, c, and γ can be expressed as activity a_{H+}. Because of the total hydrolysis effect (H_{eff}), two possible cases will be described for the hydrolysis:

1. *hydrolysis in a homogeneous phase*

2. *hydrolysis in a heterogeneous phase*

In homogeneous phase, the glycoside and the low molecular weight acid are in solution (i_a = m = 1.00). The reaction rate of the hydrolysis reaction is the highest and depends largely on the acid activity a_{H+}.

In the case of an insoluble glycoside – heterogeneous phase (m = 1.00, i_a = accessibility factor), the ratio between crystalline and amorphous amount, the specific surface area and the permeability are the rate limiting steps [103].

- *Acid and hydrolytic activity*

The hydrolysis reaction is influenced to a certain degree by the nature of different acids. In the 19th century, scientists already observed a different affinity for hydrolysis reaction caused by different acids. In the following, all catalyst activities were normalized with the acid activity of hydrochloric acid (Table 3).

Table 3: Catalyst activity related to HCl [104]

Acid	catalyst activity related to HCl
Hydrochloric acid	100 %
Sulfuric acid	50.5 %
Acetic acid	21.3 %
Oxalic acid	20.4 %
Sulfurous acid	4.8 %

The causes of these differences are due to the varying charging relationship between the ions and the electrostatic interaction. The differences can also be described by the HAMMETT acidity function (H_0) – activity coefficients γ are included in H_0. The activity coefficients of different acids vary with the acid concentration and the temperature.

- _Temperature_

Increasing temperature results in an enhancement of the reaction rate and a raise of the activation energy. The temperature dependence can be approximated by the law of Arrhenius:

$$k = A \cdot e^{-\frac{E_a}{R \cdot T}}$$

k is the reaction rate constant; A is the pre-exponential factor which is constant for each chemical reaction that defines the rate due to frequency of collisions in the correct orientation; E_a is the activation energy for the reaction in [J/mol]; T is the absolute temperature in [K] and R is the universal gas constant in [J/molK]. The activation energy and the reaction rate constant can be determined by the law of Arrhenius by

plotting the equation in linearized form. Different compounds (glycosides) result in different activation energies (Table 4):

Table 4: Activation energies of various compounds (degradation process)

Compound	Ea [kJ/mol]
cellulose	~ 170 [105]
starch	~ 70 [105]
amino acids from BSA	~ 235 [105]
rutin	~ 90 [106]
hesperidin	80 – 140 [31]

Complex molecules (e.g. BSA or cellulose) need higher activation energies than smaller molecules, e.g. starch, rutin or hesperidin, to overcome the energy barrier to start the reaction.

- *Concentration of glycoside*

An increase of the glycoside concentration can influence the reaction rate of hydrolysis reactions. The increase of glycoside concentration lowers the ratio of solvent to glycoside and enhances the effective acidity, which lowers the pH-value and accelerates the reaction rate for small molecules, e.g. flavonoid glycosides [96]. The reaction rate for saccharides hydrolysis increases with increasing concentrations

- *Solvent*

Besides water as a reaction solvent, mixtures of water and alcohol can enhance the hydrolysis reaction. A reason for choosing alcohol as a cosolvent is the limited solubility of the specific glycoside in water. Hydrolysis reaction in an alcoholic environment is also called alcoholysis. In alcoholic media, the reaction rate is a function of the solvent composition. The reaction rate decreases at an alcoholic concentration between 40 % and 60 % [107], however with the same amount of acid, the cleavage of glycosidic bonds can be faster in alcohol than in pure water (qualitative behavior in Figure 9).
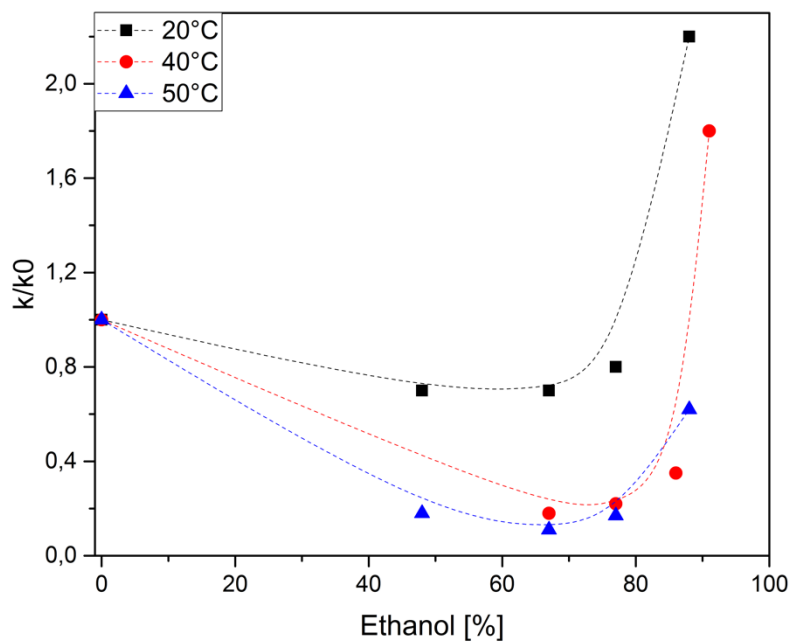
Figure 9: Alcoholysis of starch with 0.5 N HCl at 20 °C (86 d), 40 °C (120 h) and 0.1 N at 50 °C (24 h) [108]

- *Pressure*

At constant temperatures and increasing pressures, the reaction rate of hydrolysis reaction is practically constant, only at pressures above some 1000 bar the reaction rate increases (Figure 10 and Figure 11).
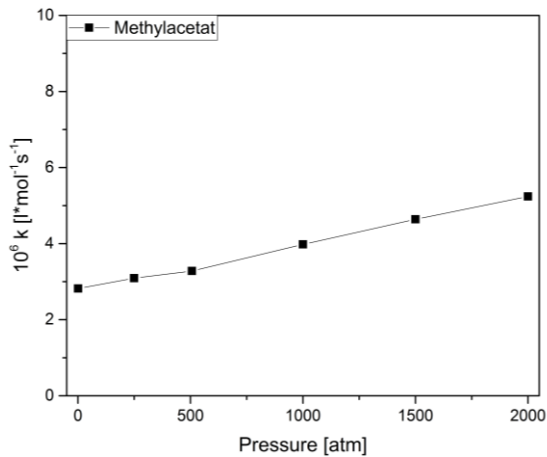
Figure 10: Pressure effect of hydrolysis reaction of methyl acetate between 1 and 2000 atm [109]
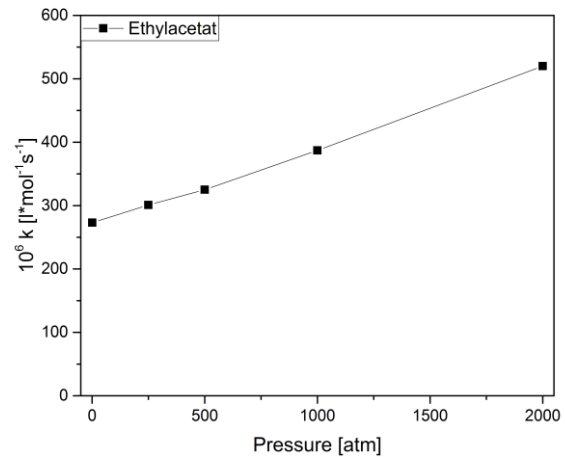
Figure 11: Pressure effect of ethyl acetate between 1 and 2000 atm [109]

1.5.2 **Enzymatic hydrolysis of glycosides**

For enzymatic hydrolysis, enzymes are used. Those hydrolytic enzymes, namely hydrolases, are able to hydrolyze glycosidic bonds and are common in nature. Hydrolases cleaving glycosides are also called glycosidases. Glycosidases can enzymatically hydrolyze oxygen-, nitrogen- and sulfur-glycosidic bonds. Enzymes act as a biological catalyst and lower the activation energy of hydrolysis reaction [110]. Following, the hydrolysis will be discussed in the example of an O-glycoside and the α glycosidase. Figure 12 shows the glycoside (sugar and R) in the middle and the carboxy (HA) and the carboxylate (B-) group of the glycosidase. The enzymatic hydrolysis with glycosidase is shown in three reaction steps [111]:
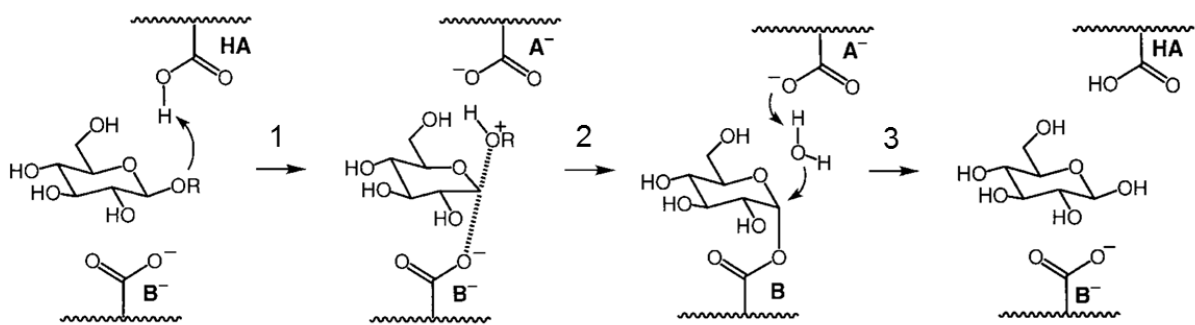
Figure 12: Enzymatic catalysis of O-glycosides with glycosidases [111]

- *1.step:* HA group donors an H+-ion to the glycoside and the oxygen of B- forms an ester with the glycoside

- *2.step:* R is separated from the sugar (which is bonded to B)

- *3.step:* R is replaced by an H+-ion and returns the H+-ion to the carboxy-group and the remaining OH- bonds on the sugar and cleaves the ester bond

In industrial hydrolysis processes, enzymes are usually bond on a carrier for re-use. Sheldon summarized in a review different types of enzyme immobilization [112]. In general, it is distinguished between:

1. _Support binding_ can be physical (such as hydrophobic and van der Waals interactions), ionic, or covalent in nature.

2. _Entrapment via inclusion_ of an enzyme in a polymer network (gel lattice) such as an organic polymer or a silica sol-gel, or a membrane device such as a hollow fiber or a microcapsule.

3. _Cross-linking_ of enzyme aggregates or crystals, using a bifunctional reagent, to prepare carrierless macroparticles.

1.6 CO_2- intensified hydrolysis

In the last few years, several researchers conducted studies referring to the effects of CO_2 in water and on the ion product of subcritical water. One of the first was Rogalinski et al. [105]. He investigated the hydrolysis of biopolymers in subcritical water at CO_2-pressures of 250 bar and temperatures between 513.15 K and 583.15 K. da Silva et al. [32] investigated the CO_2-assisted autohydrolysis (initial CO_2 pressure of 60 bar and temperatures between 453.15 K and 483.15 K) of wheat straw. In the same research group, Morais et al. [33] also studied the conversion of wheat straw in water with initial CO_2 pressures between 0 and 54 bar and temperatures between 403.15 K and 498.15 K. Moreover, Morais et al. [34] carried out experiments to study the influence of CO_2 in: 1) dehydration reaction of xylose into furfural (initial CO_2 pressures between 0 (without CO_2) and 50 bar, temperatures between 433.15 K and 473.15 K, holding time between 15 and 120 min); 2) dehydration of hemicellulose (initial CO_2 pressure at 50 bar, temperatures between 433.15 K and 453.15 K, holding time between 30 and 90 min). Furthermore, Toscan et al. [35] investigated the pre-treatment of sugarcane bagasse and elephant grass in water with constant initial CO_2 pressure of 50 bar and temperatures between 453.15 K and 493.15 K. Fan et. al [113] investigated at 70 bar static pressure and temperatures between 393.15 K and 453.15 K the mechanism of glycyrrhizic acid hydrolysis in subcritical water and described the reaction kinetics with an applied model. Glycyrrhizic acid was hydrolyzed to glycyrrhetinic acid and glycyrrhetinic acid 3-O-mono-β-D-glucuronide. Ruen-ngnam et. al [30, 31] hydrolyzed hesperidin (hesperetin-7-O-rutinoside) to hesperetin-ß-glycoside and hesperetin at constant CO_2-pressure of 250 bar and at temperatures between 383.15 K and 413.15 K up to 4 h. The author investigated the reaction kinetics and obtained conversion rates of hesperidin of 70 % and formation rates of hesperetin of around 95 %. The reactions rates increased with increasing temperature and were

determined for the reaction: »hesperidin to hesperetin-ß-glucoside« reaction rates between 0.05 s^{-1} (383.15 K) and 0.32 s^{-1} (413.15 K), »hesperetin-ß-glucoside to hesperetin« reaction rates between 0.126 s^{-1} (383.15 K) and 0.140 s^{-1} (413.15 K), »hesperidin to hesperetin« reaction rates between 0.005 s^{-1} (383.15 K) and 0.100 s^{-1} (413.15 K)

Recently, Ravber et al. [29] hydrolyzed 10 mL of rutin-water suspensions with concentrations of up to 5 mg/mL to quercetin in subcritical water at temperatures between 433.15 K and 493.15 K and pressures between 50 and 545 bar (CO_2 or N_2) for 30 min. The author investigated the decomposition of glucose and rhamnose above 448.15 K to 5-hydroxymethylfurfural and 5-methylfurfural, which showed a potential carcinogenicity in in-vitro tests [114]. The highest yields of quercetin were obtained at 215 bar CO_2-pressure, 478.15 K and concentrations between 0.01 and 2 mg/mL. Lower yields of quercetin were obtained with a N_2 atmosphere. Based on these studies, Ravber et al. [106] investigated the reaction kinetics of rutin to quercetin and decomposition products by varying the temperature between 393.15 K and 493.15 K and at constant N_2/CO_2-pressure of 215 bar. The resulting kinetic model was simplified to the direct reaction of rutin to quercetin. For the reaction »rutin to quercetin« the obtained reaction rates rose with increasing temperature: $2.2 \cdot 10^{-5}$ s^{-1} (CO_2, 393.15 K) and $6.3 \cdot 10^{-4}$ s^{-1} (CO_2, 433.15 K). All experiments with N_2-pressure resulted in lower reaction rates than experiments with CO_2-pressure.

1.7 System CO$_2$-water

1.7.1 Solubility of CO$_2$ in water

For CO$_2$-intensified hydrolysis, it is essential to understand the solubility behavior of CO$_2$ in water. Various studies have been conducted to investigate and model the solubility of CO$_2$ in water [115–124] at temperatures and pressures between 273.15 K to 533.15 K and 0 bar to 3500 bar. Duan et. al [119] applied a model of solubility of CO$_2$ in water out of these experimental solubility measurements. The solubility of CO$_2$ in water increases with increasing pressure and decreases with increasing temperature (Figure 13). The amount of dissolved CO$_2$ in water is needed to determine the dissociation equilibrium in order to obtain the possible reduction of pH-value.
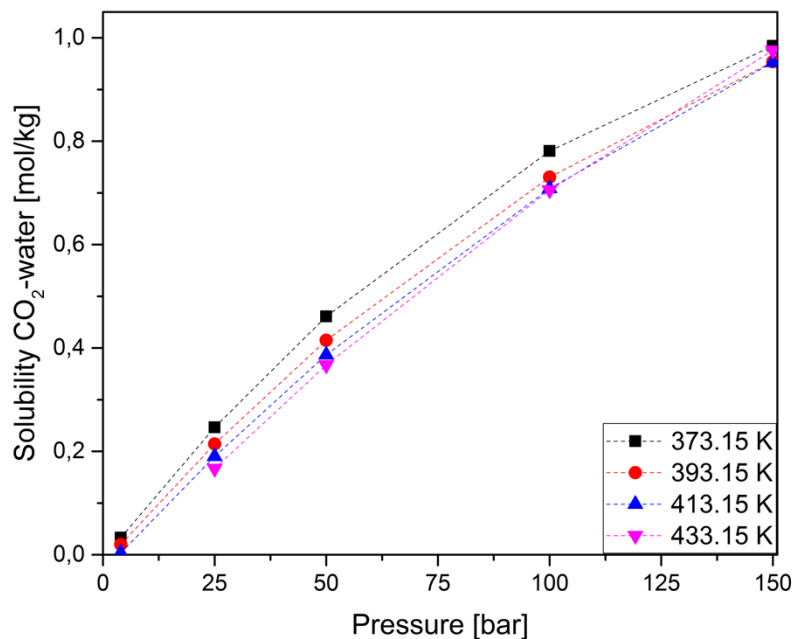
Figure 13: Solubility of CO$_2$ in water at 373.15 K, 393.15 K, 413.15 K and 433.15 K at pressures of 4 bar, 25 bar, 50 bar, 100 bar and 150 bar [119]

1.7.2 **Dissociation of the system CO₂ – water**

In order to understand the mechanism of CO_2-intensified hydrolysis, it is essential to discuss the dissociation of CO_2 in water. CO_2 can occur as free CO_2 (excess or related CO_2) or as bound CO_2 (half-bound (HCO_3^-) or totally bound (CO_3^{2-})). Therefore, organic carbon occurs in water as gaseous CO_2 or as HCO_3^- and CO_3^{2-} ions. [125]

Dissociation depends on the amount of dissolved CO_2 in water from the CO_2 phase. Once CO_2 dissolves in water, the dissolved CO_2 dissociates partially into H^+, HCO_3^- and CO_3^{2-}, water dissociates in H^+ and OH^-. The dissociation of CO_2 in water is extensively described in the literature in various chemistry textbooks [125–127].

1.Dissociation of CO₂/water:

$$H_2CO_3 \rightarrow CO_2 + H_2O \leftrightarrow H^+ + HCO_3^- \quad \text{(pK1 = 6.35)}$$

2.Dissociation of CO₂/water:

$$HCO_3^- \leftrightarrow H^+ + CO_3^{2-} \quad \text{(pK2 = 10.33)}$$
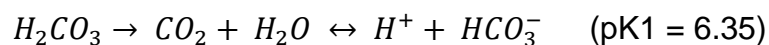
Dissociation of water:

$$H_2O \leftrightarrow H^+ + OH^- \quad \text{(pKw = 7)}$$

The amount of dissociated ion products depends on the different pH levels (Figure 14).
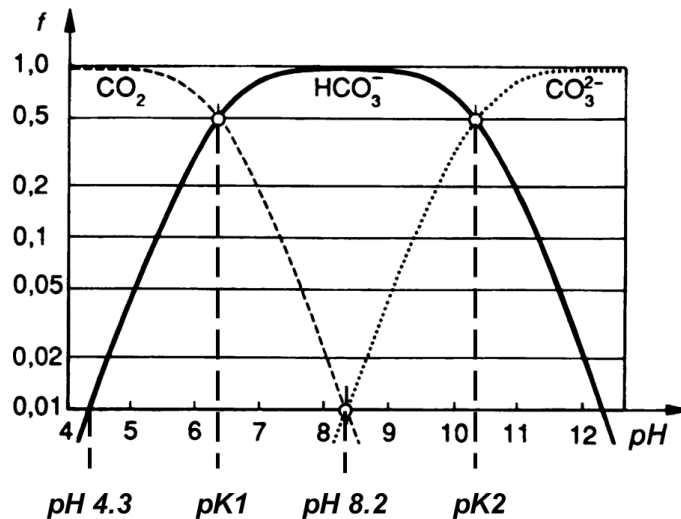
Figure 14: Carbonate equilibrium titrated with calcium hydroxide, f = ratio of concentrations [125]

In literature the general reaction of CO₂ in water is often described as $CO_2 + H_2O \leftrightarrow H_2CO_3$, however the equilibrium constant of carbonic acid is around 2 x 10⁻³ which means that only a very small amount of the dissolved CO₂ transfers to carbonic acid [125]. The formed carbonic acid immediately reacts into its ionization products HCO₃⁻ and CO₃²⁻:

The degree of dissociation depends on the pH value of the carbonated water. If the pH value is between 0 < pH < 4.3 the concentrations of CO₃²⁻, HCO₃⁻ and OH⁻ are negligible and only H⁺ ions of strong mineral acids exist. Above a pH value of 4.3, the formed carbonic acid immediately dissociates in its 1. dissociation step. Between a pH of 4.3 and 8.2 the HCO₃⁻ ions can act as an acid or base [126].

1.7.3 **Speciation equilibrium of CO_2 in water at high pressures**
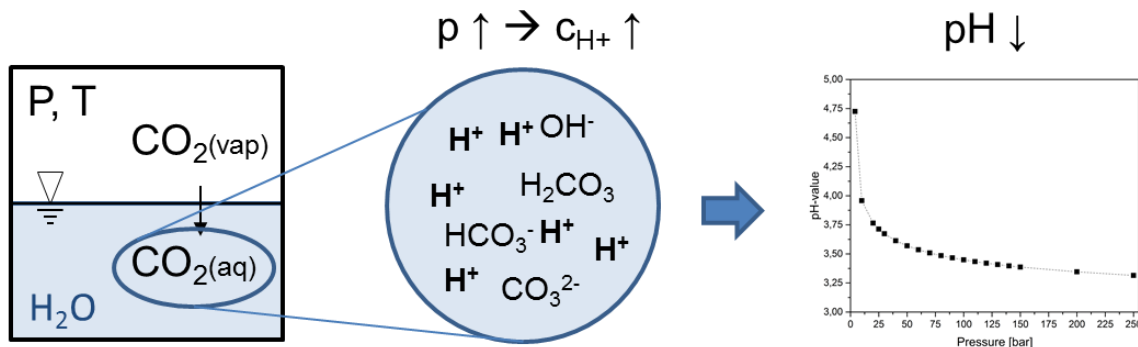
Figure 15: Dissociation of CO_2 in water and the pressure induced pH drop (cH+ qualitatively)

The speciation equilibrium highly depends on temperature and pressures. As described in chapter 1.7.1, the solubility of CO_2 in water can be influenced by increasing pressure. Water and CO_2 form carbonic acid, but more accurate, in the moment CO_2 dissolves in water, the dissolved CO_2 dissociates partially into H^+, HCO_3^- and CO_3^{2-}, water dissociates in H^+ and OH^- (Figure 15). There are several models available for determination of the carbonate equilibria in seawater at high pressures and low temperatures [128–133]. Li et al. [134] created a model for the speciation equilibrium coupled with phase equilibrium in the water-CO_2-sodium chloride system for temperatures between 273.15 K and 533.15 K, pressures between 0 and 1000 bar and sodium chloride concentration between 0 and 5 molality. The working group of Duan developed an online available model: http://models.kl-edi.ac.cn/models/h2o_co2/index.htm. With this model, it was possible to determine the speciation equilibrium and the concentration of H^+ at certain temperatures, pressures and dissolved CO_2 concentrations. With these calculated data fits for H+ concentration for different pressures and different temperatures were accomplished (Figure 16 and Figure 17).
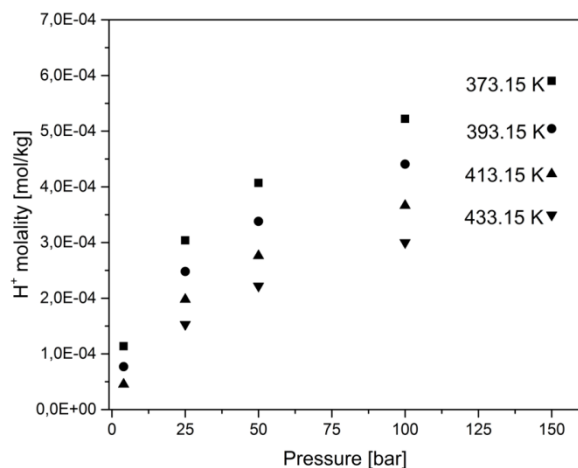
Figure 16: Hydrogen ion molality at 373.15 K, 393.15 K, 413.15 K and 433.15 K and at pressures from 4 to 150 bar [119, 134]
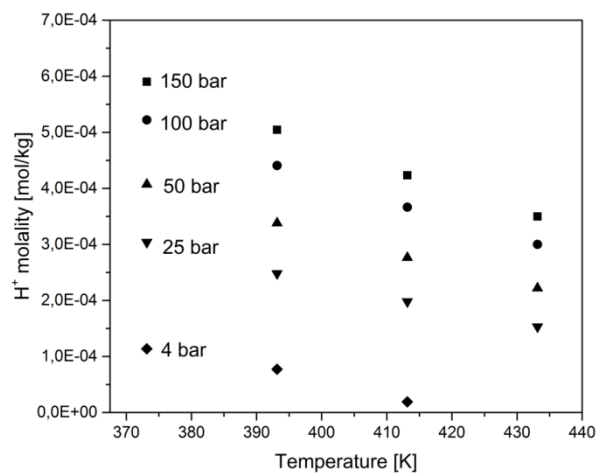
Figure 17: Hydrogen ion molality at 4 bar, 25 bar, 50 bar, 100 bar and 150 bar and temperatures from 373.1 to 433.15 K [119, 134]

2 Material and Methods

2.1 Materials

The used EMHSP are listed with their Latin name in Table 8 and were purchased from Kottas in Vienna. Deionized water was used from the in-house installed tap.

For RDM all reagents were analytical grade or the best grade available. Acetone, methanol, ascorbic acid, sodium hydroxide, agarose (type I), bovine serum albumin (fraction V), glacial acetic acid and Petri plates were obtained from VWR International. Tannic acid was obtained from Alfa aesar. Pentagallyolglucose (PGG) was purchased from Sigma Aldrich. Pyrogallol was purchased from Roth.

For hydrolysis with strong and weak acid all reagents were analytical grade or the best grade available. 37% hydrochloric acid, 100% acetic acid, sodium hydroxide (NaOH), sodium hydrogen carbonate ($NaHCO_3$), methanol, ethanol and acetonitrile were HPLC grade, ascorbic acid, agarose (type I), bovine serum albumin (fraction V) were purchased from VWR. Rutin was purchased from Roth as rutin trihydrate ≥ 95%. Quercetin dihydrate ≥97% was obtained from Alfa Aesar. Tannic acid was obtained from Alfa aesar. Pentagallyolglucose (PGG, Figure 3) was purchased from Sigma Aldrich. *Rubi fruticosus, Alchemilla vulgaris, Fragaria* and *Arctostaphylos uva-ursi* were used as plant material.

For the CO_2-intensified hydrolysis rutin, quercetin and tannic acid were used as model compounds. Methanol, ethanol, water, acetic acid and acetonitrile were used for HPLC analysis. Carbon dioxide was purchased from Yara with a purity of 99.5 % and had a permission for usage for food products.

2.2 Analytical methods

2.2.1 Radial diffusion method (RDM)

First, 340 mL deionized water plus 11,44 mL glacial acetic acid plus 4,2 mg ascorbic acid has to be adjusted with sodium hydroxide (5M) to a pH value of 5. In a separate flask, 400 mg bovine serum albumin (BSA) was dissolved in 40 mL deionized water. Second, 2 g of agarose (type I) was dissolved in a screw – mountable bottle with the solution prepared in the first step. This bottle was heated and boiled in a water bath until the agarose is dissolved. After that, the bottle was placed in another water bath with a temperature to assure that the agarose will not harden. When the agarose had a temperature of slightly above 45 °C the prepared BSA solution was poured in and the bottle was mixed for a few seconds to guarantee mixing homogeneity. Two aliquots of 10 mL of the prepared agarose – BSA solution were dispensed via a pipette into each Petri plates in order to obtain constant gel thickness. The finished Petri plates were stored on an even surface and after total hardening, the plates were stored in a refrigerator at 4 °C until usage. As an appropriate standard for this assay, tannic acid was found to be most suitable. Three calibration curves for the radial diffusion method with water, 50% methanol/ 50% water and 50% acetone/ 50% water as solvents for 20 ml agarose – BSA gel were prepared. 10 concentrations of tannic acid ranging from 5 mg/mL to 50 mg/mL were prepared and 20 µL of each solution was spiked in the agarose – BSA gel (Figure 18). According to their equilibrium time, the plates were stored for at least for 72 to 150 h in a room with a temperature of 30 °C. The area of the formed ring was calculated and listed with the according tannin content (solution concentration multiplied by the dispensed volume of 20 µL). All experiments were performed in triplicate. The diameters of the rings were measured with a caliper and image analysis software ImageJ© (Freeware).
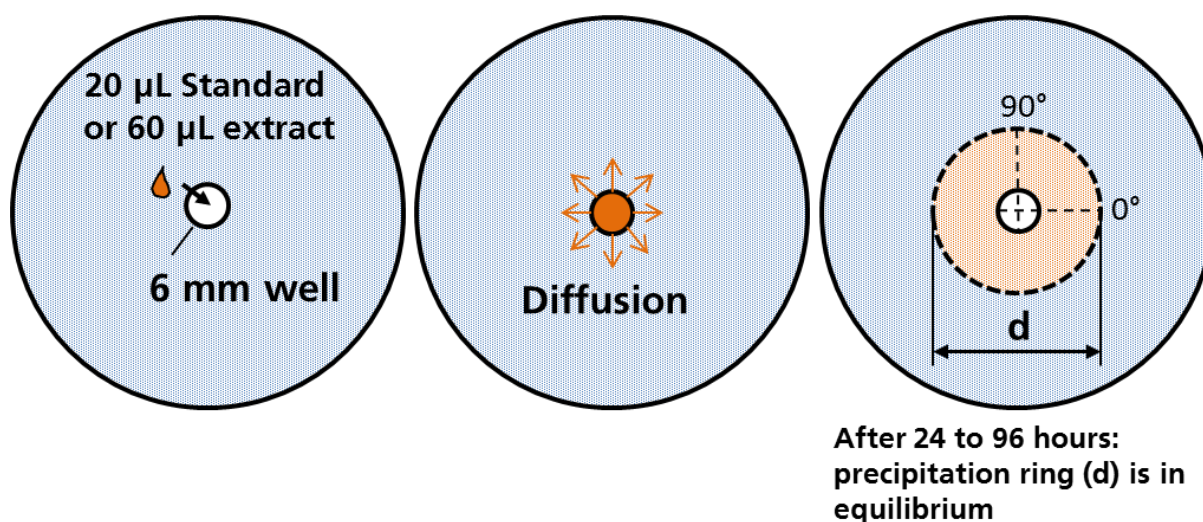
Figure 18: Radial diffusion method [13]

For the software, each plate is photocopied in a photo box with a fixed distance to the lens of the camera. Each photo was taken with a scale and the name. The series of pictures were imported to the image analysis software. The distance of one cm was measured in pixel to set the scale of the software. After that, the threshold was adjusted to measure the correct area of the formed precipitation rings. Each ring was measured and the data were imported into Excel to calculate the calibration curve. All three solvents (deionized water, methanol/water (50 v%/ 50 v%) and acetone/water (50 v%/ 50 v%)) had a good performance with an error squared around 0.99. This assay correlates linearly to the tannin content in the solution (Figure 20).

From all three calibration curves (water, water/methanol and water/acetone) concentrations of 5 and 45 mg/mL were investigated regarding their equilibrium time, where no diameter change was observed for RDM. After spiking the solutions into the wells, the diameter of the formed rings was measured at the first and second day every 2 hours, from the third day on every 4 hours until the rings were in equilibrium and the radial diffusion stopped (Figure 21).

To prove that this assay does not interact with not tannable polyphenols, such as gallic

acid, catechin, pyrogallol, a series of experiments with pyrogallol and tannic acid were performed. Five solutions of Pyrogallol (M = 126,11 g/mol) and tannic acid (M = 1701,2 g/mol) were prepared (0, 25, 50, 75, 100 % pyrogallol and vice versa for tannic acid). The precipitation ring areas were compared with those from the standard curve. All experiments were performed in triplicate. In Figure 19, a comparison is showed between experiments with Pyrogallol and without Pyrogallol. No significant difference was observed. That means, Pyrogallol does not interact with the assay and consequently also no polyphenols with small molecular weights, such as gallic acid, catechin, etc. interact with this assay.
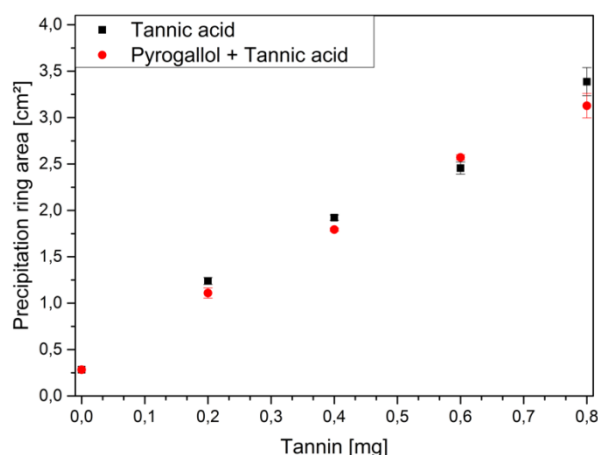
Figure 19: Interaction tannic acid / pyrogallol: Comparison with and without Pyrogallol
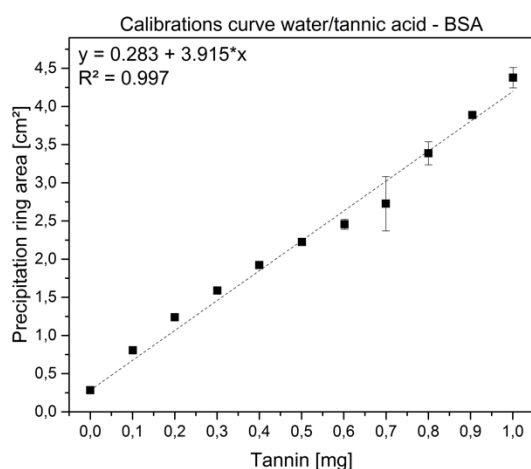
Figure 20: Calibration curve: water – tannic acid
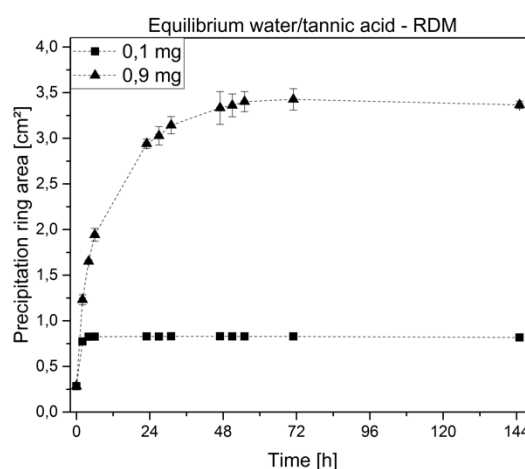
Figure 21: Equilibrium time of water/tannic acid - RDM

2.2.2 **Determination of tannin content**

The radial diffusion method (RDM), developed by Hagerman [90], was adapted for analyzing the tannin contents (TC) of the herbs and the herbal extracts. Commercially available tannic acid was used as a reference substance for tannins. The RDM was calibrated with a solution of tannic acid in demineralized water between 5 and 50 mg/mL. The obtained precipitation ring diameters correlated linearly with the amounts of tannic acid. Hagerman [135] showed that the RDM assay interacts with both, hydrolyzable and condensed tannins. In comparison to hydrolyzable tannins, condensed tannins may result in smaller precipitation rings at the same concentration of tannin solution. As in this work, calibration was conducted with hydrolyzable tannic acid plants containing condensed tannins could show underestimated tannin contents. Characterization of tannin and non-tannin of tannic acid was performed according to chapter 2.2.4. One aliquot of 60 µL crude extract (cooled down to room temperature) was spiked in each well of the RDM. Each extract was analyzed in triplicate on one plate. The agar plates were incubated at 30 °C for 72 hours. The precipitation rings were measured with a sliding caliper at 0 ° and 90 °and were arithmetically averaged (Figure 18). Tannic acid equivalent per 60 µL crude extract was obtained via calibration curve and adjusted with the factor 0.895 (obtained at the characterization of tannic acid by HPLC). For calculation of the TC per dried herb, the adjusted result was extrapolated to the weighed portions of the beginning of the respective extractions. All results of TCs refer to the adjusted tannic acid standard.

For the calculation of the TC per dried extract, the adjusted result was extrapolated to the mass of filtered and centrifuged dried extract. The dried extract was produced first by filtering the dispersion of plant tissue and liquid extract with filter paper (VWR Folded qualitative filter paper, 303) and additional centrifugation of the filtrate (HERMLE

Z300K) at 6000 rpm for one hour. 40 mL (2 x 20 mL) of each centrifuged extract was dried at 105°C ± 5 °C for at least 12 hours.

2.2.3 HPLC – rutin and quercetin

For quantitative analysis of quercetin and rutin, a high-performance liquid chromatography device connected with a diode array detector (Agilent Technologies HPLC 1200 Quat Pump) was used. The injection volume was 10 µL and the separation was performed in an Agilent Zorbax Eclipse XDB-C18 150 x 4.6 mm 5 µm column at 308.15 K. The samples were diluted 1:1 with the eluent. Isocratic elution was performed and consisted of methanol / acetonitrile / water (40/15/45) (v/v/v %) containing 1% acetic acid at a flow rate of 0.8 mL/min. Rutin and quercetin were detected at a wavelength of 368 nm. The calibration curves for rutin and quercetin were prepared to quantify its amounts in each sample. Both compounds were dissolved in ethanol. The solutions were then diluted with the eluent to generate the concentrations for the calibration curve. Isoquercetin was not calibrated

2.2.4 HPLC – tannic acid and pentagallyolglucose

Characterization of tannin and non-TC of tannic acid was performed at a high-performance liquid chromatography device connected with a diode array detector (Agilent Technologies HPLC 1200 Quat Pump) by comparison with pentagallyolglucose at the same HPLC-method. The injection volume was 10 µL and the separation was performed in an Agilent Zorbax Eclipse XDB-C18 150 x 4.6 mm 5 µm column at 35 °C. Tannic acid was dissolved in the eluent. Gradient elution was performed consisting of eluent A (water containing 0.3 % acetic acid) and eluent B

(ACN containing 0.3 % acetic acid) at a flow rate of 0.8 mL/min. The gradient of eluent B was 0 % at the beginning, increasing in 20 minutes to 50 % B and was held for 5 minutes. Tannic acid and PGG were detected at a wavelength of 280 nm. PGG was analyzed with the same HPLC method. All peaks occurring at retention times lower than this of PGG were classified as no tanning ability (non-tannin). All peaks occurring after the PGG peak were classified with tanning ability. Used Tannic acid showed a tanning content of 89.5 %.

2.3 Extractions

2.3.1 Extraction procedure I

Each plant (Table 8) was extracted in a mass ratio of 1:10 (one part dried plant tissue and ten parts demineralized water). 10 g plant tissue was used for each extraction. Extractions were performed in triplicate at 70 °C for one hour with a Heidolph ® HiTech magnetic stirrer (including a temperature sensor) and a magnetic stirring bar. The moisture content of the 47 herbs (before extraction) varied between 8.5 and 11 %. Each sample was milled with a commercial cutting mill before extraction. The extractions of the 47 herbs will be referred to as »screening« hereafter.

Additional extractions (method mentioned above) were performed with 16 of 47 EMHSP to obtain the TC not only per dried herb but also per dried extract. *Fragaria, Alchemilla vulgaris, Potentilla erecta* and *Arctostaphylos uva-ursi* came from different batches than for the screening.

2.3.2 Extraction procedure II

Fragaria and *Arctostaphylos uva-ursi* leaves were extracted in a 5 L round-bottom flask. The extraction solvent was demineralized water. 300 g of grinded plant material

was extracted with 3000 g of solvent for one hour. The 5 L round-bottom flask was heated with a Heidolph head on device for a Heidolph magnetic stirrer (MR- Heitech © + Pt 1000 temperature sensor). The extraction was assisted with an additional lab stirrer from Heidolph. After the extraction, one sample was taken and analyzed with RDM. The agar plates were put in an incubator at 30 °C for 72 hours. The dry matter of the extracts was determined in duplicate.

2.4 Hydrolysis

2.4.1 CO_2 – intensified hydrolysis of rutin - preliminary experiments

In preliminary experiments, it was tested if rutin hydrolyzes in an alcoholic mixture with demineralized water due to a higher solubility of rutin. A solution of 0.2 g/L rutin was prepared in a mixture of ethanol and demineralized water (50v%/50v%). 30 mL of this solution was transferred into a high pressure view cell with a syringe. The solution was heated to 413.15 K and after reaching the desired temperature a 1.5 mL sample was taken. Thereafter, a CO_2-pressure of 150 bar was applied. The next samples were taken after 4 h and 8 h. All samples were analyzed with a HPLC method (chapter 2.2.3)

2.4.2 CO_2 – intensified hydrolysis of rutin

<u>Experimental set up:</u> In Figure 22 the experimental set up for the CO_2-intensified hydrolysis is displayed. It consisted of a high pressure view cell (a) with a volume of 60 mL and three valves (valve b: CO_2-pressurization, valve c: CO_2-depressurization, valve d: sampling). 40 mL of the prepared rutin solution (50 mg/L) was injected at a t-

junction (e). The rutin concentration was below the maximum solubility (125 mg/L at 298.15 K [136]). The rutin solution was stirred inside the cell. The CO_2-pressure was adjusted with a hand valve (b) and the temperature was controlled with heating elements (h).
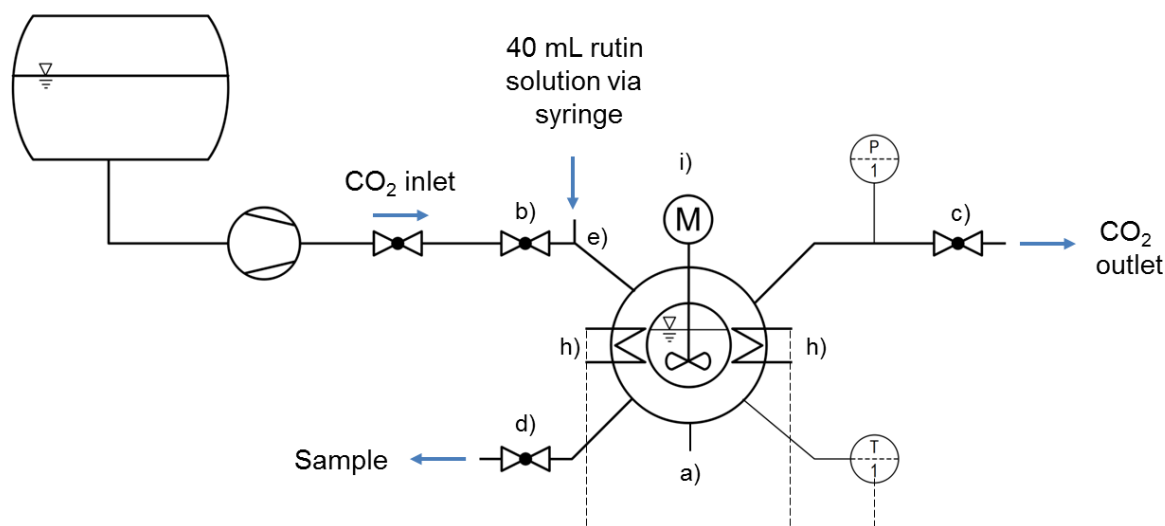
Figure 22: Experimental set up – high pressure view cell [137]

After injecting rutin solution, the cell was rendered inert and heated up to the desired temperature within one hour. During heating, the rutin solution was pressurized with 4 bar CO_2-pressure. Thereafter, the cell was pressurized with respective CO_2-pressure for eight hours. Six samples were taken for HPLC-analysis during each experiment (Table 5). Samples of 1.5 mL were withdrawn and the first 0.5 mL were discarded. The pressure drop during sampling was compensated by adjusting the pressure with hand valve.

Table 5: Sampling for HPLC analysis during hydrolysis – rutin and quercetin

Number of samples	1	2	3	4	5	6
characterization	From rutin stock solution, before injection	Out of the cell - after reaching desired hydrolysis temperature at 4 bar CO_2	Out of the cell - after 2 h under hydrolysis pressure	Out of the cell - after 4 h under hydrolysis pressure	Out of the cell - after 6 h under hydrolysis pressure	Out of the cell - after 8 h under hydrolysis pressure

<u>CO_2-intensified hydrolysis | temperature dependence:</u> In a first set of experiments, the temperature dependence of the CO_2-intensified hydrolysis was investigated. The pressure was set to 150 bar CO_2 pressure in each experiment. Experiments at each temperature (373.15 K, 393.15 K, 413.15 K, 433.15 K) were performed in triplicate.

<u>CO_2-intensified hydrolysis | pressure dependence:</u> As a result of »CO_2-intensified hydrolysis | temperature dependence« temperature was set to 413.15 K. Experiments at each CO_2-pressure (4 bar, 25 bar, 50 bar, 100 bar, 150 bar) were performed in triplicate.

2.4.3 **CO_2 – intensified hydrolysis of tannic acid**

For the CO_2-intensified hydrolysis of tannic acid, the same experimental setup as for the CO_2-intensified hydrolysis of rutin was used (Figure 22). 40 mL tannic acid solution of 5 g/L in purified water was used to investigate the hydrolysis behavior for hydrolyzable tannins. Eight samples were taken for RDM-analysis during each experiment (Table 6). Sampling of the hydrolyzed tannic acid solution was conducted by rejecting the first 0.5 mL and taking the additional 1 mL for RDM-analysis. The pressure drop during sampling was compensated by adjusting the pressure with hand

valve. The experiments were performed in triplicate and each sample was analyzed in triplicate.

Table 6: Sampling for RDM analysis during hydrolysis – tannic acid

Number of samples	1	2	3	4	5	6	7	8
character-ization	From tannic acid stock solut-ion before inject-tion	Out of the cell - after reaching desired hydrol. temp. at 4 bar CO_2	Out of the cell - after 1 h under hydrol. pressure	Out of the cell - after 2 h under hydrol. pressure	Out of the cell - after 3 h under hydrol. pressure	Out of the cell - after 4 h under hydrol. pressure	Out of the cell - after 6 h under hydrol. pressure	Out of the cell - after 8 h under hydrol. pressure

2.4.4 CO_2 – intensified hydrolysis of plant extracts

For the CO_2-intensified hydrolysis of plant extracts the same experimental setup as for the CO_2-intensified hydrolysis of rutin was used (Figure 22). 40 mL of plant extract was used to investigate the CO_2-intensified hydrolysis. Six samples were taken for RDM-analysis during each experiment (Table 7). Sampling of the hydrolyzed plant extract was conducted by rejecting the first 0.5 mL and taking the additional 1 mL for RDM-analysis. The pressure drop during sampling was compensated by adjusting the pressure with hand valve. The experiments were performed in triplicate and each sample was analyzed in triplicate.

Table 7: Sampling for HPLC analysis during hydrolysis – plant extracts

Number of samples	1	2	3	4	5	6
characterization	From prepared plant extract, before injection	Out of the cell - after reaching desired hydrolysis temperature at 4 bar CO_2	Out of the cell - after 2 h under hydrolysis pressure	Out of the cell - after 4 h under hydrolysis pressure	Out of the cell - after 6 h under hydrolysis pressure	Out of the cell - after 8 h under hydrolysis pressure

2.4.5 Hydrolysis of plant extracts- strong and weak acid

Strong acid hydrolysis: Three beakers with 150 mL rutin (50 mg/L) or tannic acid (5 g/L) solutions or plant extracts (*Fragaria* and *Arctostaphylos uva-ursi* prepared at 90 °C for 1 h and in a ratio of 20 g plant material and 200 g purified water, purified with a syringe attachment filter) were heated to 90 °C. After reaching the desired temperature, 2.5 mL of 37 % hydrochloric acid were added to get an acid concentration of 0.2 mol/L. Hydrochloric acid was used due to the linear behavior between H_0 (Hammett Acidity function) and the logarithmic rate constant [102]. At the beginning, a 0-sample was taken (without HCL), after adding HCl every hour one sample was taken up to 8 hours. The sample was neutralized with sodium hydroxide (NaOH). 500 µL sample were neutralized with 225 µL 0.44 mol/L NaOH and mixed with 275 µL methanol / acetonitrile with 1 % acetic acid for HPLC analysis (eluent: 45 % water/ 15 % acetonitrile/ 40 % methanol without water and 1 mL acetic acid). The hydrolyzed rutin solutions were analyzed with the HPLC method described in chapter 2.2.3. The hydrolyzed tannic acid solutions were analyzed with the RDM method described in chapter 2.2.1. The hydrolyzed plant extracts were analyzed with both, the RDM (2.2.1) and the HPLC method (2.2.3).

<u>Weak acid hydrolysis:</u> Three beakers with 150 mL of plant extracts (*Fragaria* and *Arctostaphylos uva-ursi* prepared at 363.15 K for 1 h and in a ratio of 20 g plant material and 200 g purified water, purified with a syringe attachment filter) were heated to 363.15 K. After reaching the desired temperature, 0.9 mL of 100 % acetic acid was added to get an acid concentration of 0.1 mol/L. At the beginning, a 0-sample was taken (without acetic acid). After adding acetic acid every hour one sample was taken up to 8 hours. The sample was neutralized with sodium carbonate (Na_2CO_3). 500 µL sample was neutralized with 225 µL 0.22 mol/L Na_2CO_3 and mixed with 275 µL methanol / acetonitrile with 1 % acetic acid for HPLC analysis (eluent: 45 % water/ 15 % acetonitrile/ 40 % methanol without water and 1 mL acetic acid). The hydrolyzed rutin solutions were analyzed with the method described in chapter 2.2.3. The hydrolyzed tannic acid solutions were analyzed with the method described in chapter 2.2.1. The hydrolyzed plant extracts were analyzed with both methods.

2.5 Used software

ImageJ was used to determine the exact precipitation area of RDM and the tannin content was calculated with Excel. Matlab and Excel were used to calculate modeled and empirical reaction kinetic rates and correlation coefficients. All figures were created with Origin.

3 Extraction of Tannins and Flavonoid Glycosides

A screening of EMHSP with adequate tannin contents was conducted. The best four plants with the highest tannin contents in the dried extract were further hydrolyzed with acid to determine their flavonoid- aglycone content, in particular, the quercetin content.

3.1 Screening of European medicinal herbs and spice plants on their tannin content

In Maier et al. [13] a screening of EMHSP on their tannin content (TC) was performed (Figure 23). First, a literature review was conducted to identify plants with promising tannin contents [12, 88, 138–141] (Table 8). 47 plants from the families *Rosaceae* (8), *Compositeae* (6), *Lamiaceae* (old name *Labiateae*) (16), *Ericaceae* (5)*, Boraginaceae, Umbellifeaera, Leguminaceae, Urticaceae, Malvaceae, Verbenaceae, Polygonaceae* and *Guttifeare* were found in literature with a TC between "present" and "up to 30 %". The 47 EMHSP were analyzed from selected plant parts. Those parts were leaves (22 plants), whole herbs (20 plants) and roots (8 plants). Plants stated with "present" are mostly analyzed qualitatively with metal salts (iron salts most of the cases). The quantitative analysis of TC is mostly performed by the gravimetric hide powder method [138, 142], the Folin-Ciocalteu assay [143], the HCl – vanillin assay [86] and similar methods. From literature, it is not clear which quantification method was used for each plant in particular. That was the reason for the performed screening of EMHSP to obtain comparable data of their TC by RDM.

	What?	Criteria	Result
1. Selection	**Identifying European medicinal herbs**	**Literature Tannin content Availability**	**47 herbs**
2. Selection	**Extraction of 47 herbs at 70°C, 1h, 1:10**	**Tannin content (RDM)**	**16 herbs**
3. Selection	**Limitation to 16 herbs**	**Tannin content and flavonoid content**	**4 herbs**
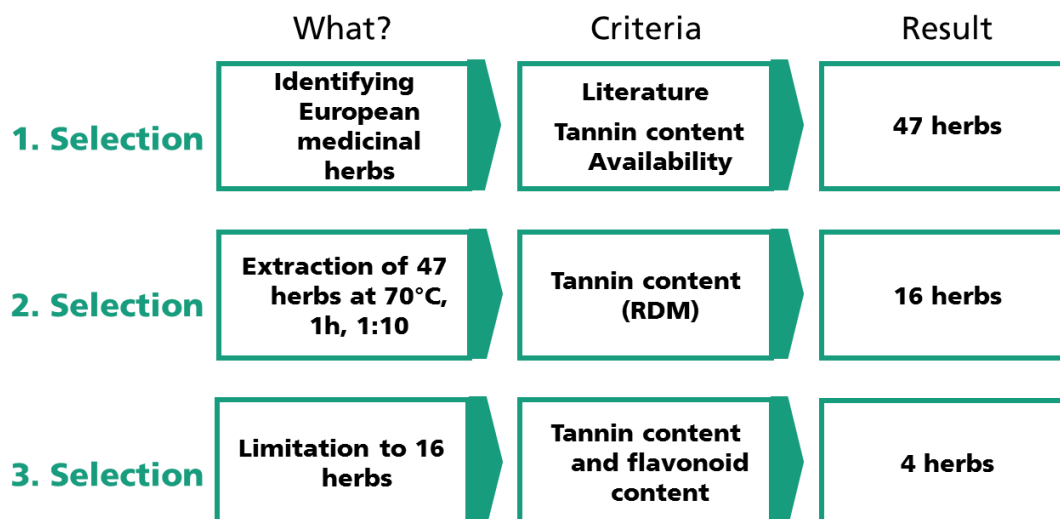
Figure 23: Graphical abstract of a screening of European medicinal herbs and spice plants (EMHSP) on their tannin content

Out of these 47 plants, 16 plants were identified with an appropriate TC to complex with BSA in the RDM. TCs between 0.8 w% and 16.0 w% were obtained. Three plants listed with tannin content "present" (*Rheum palmatum*, *Vaccinium myrtillus* and *Agrimonia eupatoria*) had TCs between 2.3 w% and 5.2 w%. Six plants (*Alchemilla vulgaris, Arctostaphylos uva-ursi, Fragaria, Potentilla anserine, Potentilla erecta* and *Rubi fruticosus*) confirmed the TC found in literature. Seven plants (*Geum urbanum, Melissa officinalis, Mentha piperita, Origanum vulgare, Rubi idaei, Salicis folium* and *Vaccinium vitis-idaea*) showed lower TC values than reported in literature. Especially, for Lamiaceae (*Melissa officinalis, Mentha piperita, Origanum vulgare)* TC values are of up to 12 w% are mentioned. RDM measurements of *Lamiaceae* provided TC between 0.8 w% and 2.2 w%, respectively. Although in literature TC of Lamiaceae were mentioned of up to 12 %, out of 16 analyzed 13 did not show a verifiable TC. This might be explained by the presence of "labiate tannins" in Lamiaceae. In literature, labiate tannins are described as pseudo tannins or tannin likely substances. It can be assumed that labiate tannins complex with iron salts and yield in a colour change [144]

due to their hydroxyl groups. According to definitions of Bate-Smith and Swain, tannins have a molecular weight between 500 and 3000 g/mol and the ability to interact with proteins, e.g. BSA, those mentioned caffeic acid derivates have lower molecular weights and did not interfere with RDM. Therefore, those 13 plants might contain labiate tannins with a molecular weight below 500 g/mol. Only extracts of *Melissa officinalis* (1.0 w%)*, Mentha piperita* (2.2 w%) and *Origanum vulgaris* (0.8 w%) had verifiable TC. TC was detected for all plants from Rosaceae and varied between 2.3 w% (Agrimonia eupatoria) and 16.0 w% (Potentilla erecta). TC from Ericaceae: 2.5 w% (Vaccinium myrtillus) up to 13.7 w% (Arctostaphylos uva-ursi) and plants from Polygonaceae (Rheum palmatum 5.2 w%) and Salicaceae (Salicis folium 1.4 w%). The last two plants will not be further discussed as their TC was too low. Nonetheless, 31 plants did not show a verifiable TC. Tannin concentration might be below the detection limit of RDM (detection limit of 0.0179 mg/20 µL tannic acid). From literature, it is not clear if there is an exact distinction between non-tannins (like labiate tannins) and tannins. Some tannin assays also show interaction of polyphenols with a molecular weight lower than 500 g/mol. Our investigations showed an exclusively interaction of BSA with tannins (molecular weight above 500 g/mol) and no interaction of non-tannins, e.g. pyrogallol. Hagerman showed also no interference between RDM, gallic acid and catechin [135]. Besides that, origin, harvest, storage and diversity between subspecies within a plant family could influence TC and yield lower TC than mentioned in literature. *Mentha piperitae* and *Menthae piperitae austriaca* proved this argument of subspecies, where *Mentha piperitae* yielded an extract with detectable TC and the subspecies *Menthae piperitae austriaca* not.

Table 8: Plant name (Latin and English), plant species, tannin content literature [w%] [12, 88, 138–141], used plant parts (H: whole herb, L: leaves and R: roots) and Tannin content RDM ± SD [w%]; SD: standard deviation

Plant (Latin name)	Plant (English name)	Plant species	Tannin content - literature	Used Plant part	Tannin content [w%] ± SD, RDM, Screening
Achillea millefolium	Milfoil	Compositae	up to 2.8%	H	-
Agrimonia eupatoria	Agrimony	Rosaceae	present	H	2.3 ± 0.1
Alchemilla vulgaris	Lady´s mantle	Rosaceae	6-8%	H	3.5 ± 0.2
Angelica archangelica	Angelica	Umbellifera	present	R	-
Arctostaphylos uva-ursi	Bearberry	Ericaceae	up to 20%	L	13.7 ± 0.8
Artemisia absinthium	Wormwood	Compositae	present	L	-
Borago officinalis	Pectoral flowers	Boraginace	up to 3%	H	-
Carlina acaulis	Stemless Carline	Compositae	present	R	-
Cichorium intybus	Succory	Compositae	present	R + L	-
Cnicus benedictus	Blessed thistle	Compositae	up to 8%	H	-
Erica vulgaris	Common health flower	Ericaceae	3-7%	H	-
Eryngium campestre	Eryngo	Umbellifera	present	H	-
Fragaria	Strawberry	Rosaceae	up to 10%	H	3.3 ± 0.2
Galega officinalis	Common goats rues herb	Leguminosa	present	H	-
Galeopsidis segetum	Hemp nettle	Labiatae	5-10%	H	-
Geum urbanum	Avens	Rosaceae	up to 30%	R + H	4.9 ± 0.4

Continuing Table 9: Plant name (Latin and English), plant species, tannin content literature [w%] [12, 88, 138–141], used plant parts (H: whole herb, L: leaves and R: roots) and Tannin content RDM ± SD [w%]; SD: standard deviation

Plant (Latin name)	Plant (English name)	Plant species	Tannin content - literature	Used Plant part	Tannin content [w%] ± SD, RDM, Screening
Glechoma hederacea	Ground ivy herb	Labiatae	up to 7%	H	-
Hypericum perforatum	St. John's Wort	Guttiferae	3,8-10%	H	-
Lamium album	White dead nettle flowers	Labiatae	up to 14%	H	-
Malva austriaca	Hollyhock	Malvaceae	present	L	-
Marrubium vulgare	White horehound wort	Labiatae	up to 7%	L	-
Melissa officinalis	Melissa	Labiatae	4-5%	L	1.0 ± 0.2
Mentha crispa	Curled mint	Labiatae	up to 12%	L	-
Mentha piperita	Peppermint	Labiatae	up to 12%	H	2.2 ± 0.1
Mentha piperita	Peppermint austria	Labiatae	up to 12%	L	-
Menyanthes trifoliata	Buckbean	Menyanthac	1-7%	L	-
Ocimum basilicum	Basil	Labiatae	up to 5%	H	-
Origanum marjorana	Marjoram austria	Labiatae	9-10%*	H	-
Origanum vulgare	Common majoram	Labiatae	up to 8%	H	0.8 ± 0.0
Plantago lanceolata	Plantain herb	Plantaginac	up to 6,5%	L	-
Potentilla anserina	Cinquefoil	Rosaceae	2-10%	H	3.5 ± 0.2
Potentilla erecta	Common tormentill	Rosaceae	15-25%	R	16.0 ± 0.4

Continuing Table 10: Plant name (Latin and English), plant species, tannin content literature [w%] [12, 88, 138–141], used plant parts (H: whole herb, L: leaves and R: roots) and Tannin content RDM ± SD [w%]; SD: standard deviation

Plant (Latin name)	Plant (English name)	Plant species	Tannin content - literature	Used Plant part	Tannin content [w%] ± SD, RDM, Screening
Rheum palmatum	Pieplant	Polygonace	present	R	5.2 ± 0.6
Rosmarinus officinalis	Rosemary	Labiatae	up to 8%	L	-
Rubi fruticosus	Blackberry	Rosaceae	5-15%	L	4.6 ± 0.2
Rubi idaei	Raspberry	Rosaceae	5-14%	L	3.2 ± 0.1
Salicis folium	Willow	Salicaceae	up to10%	L	1.4 ± 0.1
Salvia officinialis	Sage	Labiatae	3-8%	L	-
Satureja hortensis	Savory wort	Labiatae	4-8,5%	L	-
Stachys officinalis	Wood betony herb	Labiatae	up to 15%	L	-
Taraxacum officinale	Dandelion	Compositae	present	R + L	-
Urtica dioica	Neetle Wort	Urticaceae	up to 10%	R + L	-
Vaccinium myrtillus	Blueberry	Ericaceae	present	L	2.5 ± 0.1
Vaccinium vitis-idaea	Cowberry	Ericaceae	6-11%	L	3.7 ± 0.1
Verbena odovata	Lemon verbena	Verbenacea	up to 8%	L	-
Verbena officinalis	Vervain	Verbenacea	present	H	-

Determination of tannin content in dried plant extracts:

For the determination of tanning agents, the dry weight of all 16 plants was determined. Besides the dry weight, the TC was determined again due to different batches of 5 plants (*Rubi fruticosus*, *Fragaria*, *Alchemilla vulgaris, Potentilla erecta* and *Arctostaphylos uva-ursi*). TC differs for *Rubi fruticosus*, *Fragaria*, *Alchemilla vulgaris, Potentilla erecta* and *Arctostaphylos uva-ursi*. The TCs of the other 11 plants were similar (Table 11). With the TC and the dry weight, it was possible to calculate the TC of the dried extract. This resulted in TC of dried extracts between 3 w% and 38 w% (Figure 24).
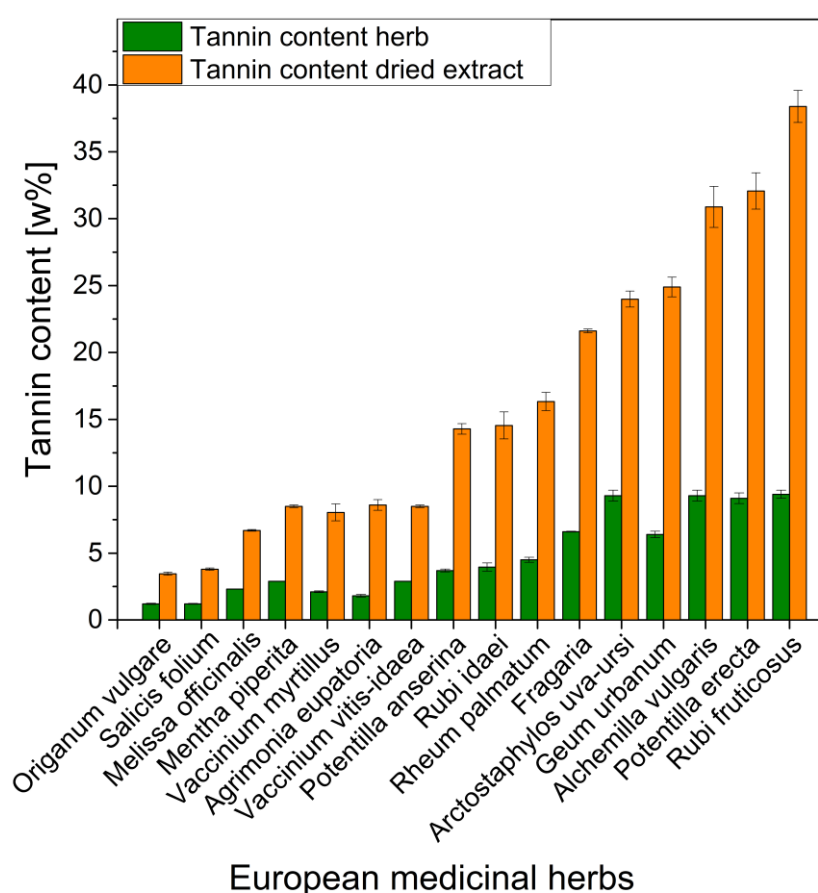
Figure 24: Screening results of 16 European medicinal herbs and spice plants - Tannin content of dried herb and dried extract ± SD in [w%], SD: standard deviation

Seven extracts showed TC below 10 w%, 4 extracts showed TC between 10 w% and 20 w% and 5 extracts showed TC above 20 w%. In general, plants from Rosaceae

showed the highest TC (between 8.6 w% (*Agrimonia eupatoria*) and 38.4 w% (*Rubi fruticosus*)) and plants from Ericaceae family yielded TC between 8.0 w% (*Vaccinium myrtillus*) and 24.0 w% (*Arctostaphylos uva-ursi*). Comparison of TC of the plant and the dried extract did not show a direct correlation. Extracts with a high dry weight tend to result in a higher ratio of non-tannins to tannins and therefore, in a lower TC, whereas extracts with low dry weights resulted in lower ratios of non-tannins to tannins and therefore higher TC. For instance, Arctostaphylos uva-ursi yielded the second highest TC of all dried plants. However, the dried extract resulted in the fifth highest TC of the dried extracts due to the high ratio of non-tannins to tannins [12]. *Arctostaphylos uva-ursi* (4.08 w%) and *Vaccinium vitis-idaea* (1.5 w%) differ from the average dry weight (2.5 ± 0.5 %) of herbs, leaves and roots (all resulted in similar dry weights; Table 11). Commercial vegetable tanning agents / extracts, e.g. chestnut, quebracho and mimosa, have higher TC than found in the dried herbal extracts analyzed in this work. Chestnut wood provides commercial tanning extracts with TC of about 70 % (analyzed with filter method) [145–148]. In industry, the filter method is the most applied analysis method for commercially tanning extracts. The principle of the filter method is based on a filled hide powder column, which is percolated with a tannin-containing extract. The amount of hide powder has to be sufficient to bind all the containing tannins. After the extract percolated the hide powder, the dry weight is determined and compared to the dry weight at the beginning. The fixed amount of tannins on the hide powder is determined by measuring the dry weight before and after soaking the extract in the column [149].

However, the results are not comparable due to different analysis methods – commercial extracts (filter method) versus screening (RDM). The results of the two methods did not show the same relation considering two extracts. For *Rubi fruticosus* (hydrolyzable) both methods showed similar results (RDM 38.4 w% and 33.1 w% (filter

method) per dried extract). In view of the fact that the filter method detects all phenolic compounds and RDM detects only tannins - similar results would indicate that the extract contains tannins but no phenolic compounds smaller than 500 g/mol. For *Potentilla erecta* (condensed & hydrolyzable) the filter method (48.3°w%) showed significantly higher results than RDM (23.9 w%). The two analyzed extracts were not equal to the extracts of the screening, which is explained by the different analysis method. The filter method detects also tannins with a molecular mass under 500 g/mol. RDM detects only tannins above 500 g/mol.

Table 11: Additional extractions: Tannin content dried herb ± SD [w%], Dry weight extract ± SD [w%] and Tannin content dried extract ± SD [w%]; Type of tannins – hydrolyzable (Hydr.), condensed (Cond.) or labiate tannins (Lab.); *Fragaria, Alchemilla vulgaris, Potentilla erecta* and *Arctostaphylos uva-ursi* came from different batches than for the screening, SD: standard deviation

Plant	Tannin content dried plant ± SD [w%], RDM, Additional extractions	Dry weight extract ± SD [w%]	Tannin content dried extract ± SD [w%], RDM / Additional extractions	Type of tannins
Agrimonia eupatoria	1.8 ± 0.1	1.94 ± 0.01	8.6 ± 0.4	Cond. [a]
Alchemilla vulgaris	9.3 ± 0.4	2.72 ± 0.01	30.9 ± 1.5	Cond. & Hydr. [a]
Arctostaphylos uva-ursi	10.5 ± 0.2	4.08 ± 0.20	24.0 ± 0.6	Hydr.[a]
Fragaria	6.6 ± 0.0	2.82 ± 0.20	21.6 ± 0.1	Cond. & Hydr. [a,b]
Geum urbanum	6.4 ± 0.2	2.32 ± 0.01	24.9 ± 0.7	Cond. & Hydr. [a,c]
Melissa officinalis	2.3 ± 0.0	3.10 ± 0.20	6.7 ± 0.1	Lab. [g]
Mentha piperita	2.9 ± 0.0	3.61 ± 0.01	8.5 ± 0.1	Lab. [g]
Origanum vulgare	1.2 ± 0.0	3.09 ± 0.01	3.5 ± 0.1	Lab. [g]
Potentilla anserina	3.7 ± 0.1	1.94 ± 0.01	14.3 ± 0.4	Hydr. [a]
Potentilla erecta	9.1 ± 0.5	2.54 ± 0.00	32.1 ± 1.4	Cond. & Hydr.[a]
Rheum palmatum	4.5 ± 0.2	2.51 ± 0.00	16.3 ± 0.7	Cond. & Hydr.[a]
Rubi fruticosus	9.4 ± 0.3	2.48 ± 0.01	38.4 ± 1.2	Hydr.[d]
Rubi idaei	4.0 ± 0.3	2.49 ± 0.10	14.5 ± 1.0	Hydr.[d]
Salix folium	1.2 ± 0.0	2.80 ± 0.02	3.8 ± 0.1	Cond.
Vaccinium myrtillus	2.1 ± 0.1	2.31 ± 0.22	8.0 ± 0.6	Cond. [e,f]
Vaccinium vitis-idaea	2.9 ± 0.1	1.50 ± 0.01	8.5 ± 0.1	Cond. [f]

[a] [12], [b] [150], [c] [151], [d] [152], [e] [153], [f] [154],   [g] [155]

Nevertheless, hide powder has its origin of animal hide, the method, in most of the cases, overestimates the TC of an extract [156]. Besides tannins, smaller phenolic compounds, e.g. flavonoids or phenolic acids, adsorb on the hide powder due to solubilizing effects of tannins on non-tannins [84],[157]. Another important difference between commercial extracts and the screening extracts are the optimized specific process parameter, which were applied for commercial extracts. Due to that fact, higher TC for the screening extracts may be obtained by optimizing the extraction parameters. Six plants with tannin contents in the dried extract higher than 20 % were identified: *Fragaria, Geum urbanum, Alchemilla vulgaris*, *Arctostaphylos uva-ursi, Potentilla erecta* and *Rubi fruticosus.* Even though Potentilla erecta and Geum urbanum have high tannin contents, no quercetin could be quantified. In the end, four plants with the potential for tannin and quercetin production were evaluated based on their availability and the calculated extract yield per hectare: *Fragaria, Alchemilla vulgaris*, *Arctostaphylos uva-ursi* and *Rubi fruticosus.* The evaluation was conducted based on data of existing cultivation area and the cultivation as a criterion, the harvest methods and the utilization for each used plant part (Table 12). The theoretical extract yields were based on calculations using literature data and data obtained from this work.

Table 12: Plant evaluation on: A – cultivation [c]/ wild collection [w], B - plant parts for commercial products, C – plant parts for tannin extraction, D - cuts / harvest per year, E - cultivation area in Germany [ha], F - plant tissue per hectare and G - quantity of theoretical tanning agent per hectare [kg]; [13]

Plant	A	B	C	D	E	F	G
Rubi fruticosus	w/c	berries and leaves	leaves and tendrils	anytime / > 1	~100[1]	~30	520
Arctostaphylos uva-ursi	w*	leaves	leaves	anytime / 1	n. a.	n. a.	n. a.
Alchemilla vulgaris	w/c	whole weed	whole weed	2[4] / 1	< 10	50[2]	950-1.900
Fragaria	c	berries	whole weed	up to 2 / up to 2	~15.400[3]	~20	395

*vulnerable in Germany, [1] [158], [2] [159], [3] [160], [4] [161]

n.a. = not available

Rubi fruticosus: *Rubi fruticosus* can occur in two forms, cultivated and wild growing, and is mainly used for its berries and leaves. A small part of the leaves is utilized for herbal teas. The tendrils and most of the leaves of *Rubi fruticosus* are not used and therefore, would be an ideal source for new products. Tendrils and leaves contain high amounts of tannins and could be a potential source for new tanning agents. *Rubi fruticosus* may grow several centimeters per day. Kirby [162] determined the total dried biomass per square meter obtained up to 300 g/(m²·a) biomass. Multiplied by the official cultivation area in Germany of 100 ha [158] this would result in 3 t/ha or 300 t of dried biomass in Germany (the total amount of *Rubi fruticosus* is even higher as this plant is able to grow on almost every soil). Those 3 t/ha of *Rubi fruticosus* plant material would result in a calculated potential of 520 kg/ha of tanning agent [13]. An extract obtained after one hour at 90 °C was hydrolyzed with 1 mol/L hydrochloric acid and analyzed with HPLC to determine the quercetin content. The dried extract of *Rubi fruticosus* resulted in a quercetin content of 0.08 w%.

Alchemilla vulgaris: *Alchemilla vulgaris* is mainly cultivated for medicinal purposes or is collected from wild stock. Normally, *Alchemilla vulgaris* when cultivated can be cut up to two times, as the growth rate is rather slow [163]. The first cut of the plants is used for herbal teas and other medicinal applications, whereas the second cut is not further processed and could be utilized for new tanning agents. The second cut does not compete with any other application and due to already existing mechanical harvesting method, it would be an ideal source. One hectare could yield 5 to 10 t/ha of dried weed [159, 161]. Out of this amount, about 950 kg/ha to 1.900 kg/ha of tanning agent could be produced. An extract, obtained after one hour at 90 °C, was hydrolyzed with 1 mol/L hydrochloric acid and analyzed with HPLC to determine the quercetin content. The dried extract of *Alchemilla vulgaris* resulted in a quercetin content of 0.15 w%.

Arctostaphylos uva-ursi: *Arctostaphylos uva-ursi* is mainly used as a decorative plant to cover the ground and has a relevance for medicinal purposes. A production of tanning agent out of *Arctostaphylos uva-ursi* would be competitive due to mainly medical uses. The plant is mainly collected from wild stocks in Eastern Europe and Spain, in Germany it is declared as vulnerable. The growth rate of *Arctostaphylos uva-ursi* is classified as medium [163]. In the last years, cultivation trials were accomplished but failed [164]. No commercial cultivation of *Arctostaphylos uva-ursi* is known. No estimation of availability could be made. An extract, obtained after one hour at 90 °C, was hydrolyzed with 0.2 mol/L hydrochloric acid for eight hours and analyzed with HPLC to determine the quercetin content. The dried extract of *Arctostaphylos uva-ursi* resulted in a quercetin content of 0.65 w% after four hours.

Fragaria: In Europe, *Fragaria* species are mainly cultivated for their fruits. *Fragaria* plants are growing fast [163] and the whole weed is suitable for tanning agent production. In outdoor plantations 35.000 plants could be cultivated per hectare [165]. The weed has to be cut after fruit harvesting in order to avoid fungi or bacteria caused diseases at long-term plants [165]. There is no utilization of the weed except plowing back it into the soil to act as a natural fertilizer, when not having substrate plantations. From literature, it is known that dry weights of weed between 56.6 g and 77.3 g could be obtained per plant [166]. Multiplied by the number of plants per hectare this would result in 2 t of *Fragaria* weed per hectare. In Germany, 15.400 ha of *Fragaria* were cultivated in 2014 [160]. This would result in a potential of 395 kg/ha tanning agent or 6100 t of tanning agent per year (assumption of no substrate plantation). An extract, obtained after one hour at 90 °C, was hydrolyzed with 0.2 mol/L hydrochloric acid for 8 hours and analyzed with HPLC to determine the quercetin content. The dried extract of *Fragaria* resulted in a quercetin content of 0.42 w% after four hours.

Out of this screening study, four potential plants with TCs between 21.6 w% and 38.4 w% and quercetin contents between 0.08 w% and 0.65 w% in the dried extract were identified. In order to obtain dried extracts containing quercetin and tannins, the extract has to be hydrolyzed. In the following, the CO_2-intensified hydrolysis of two model substances (rutin and tannic acid) will be evaluated with respect to the temperature and pressure influence. Hydrolysis with weak and strong acid, as well as CO_2-intensified hydrolysis will be further applied on *Fragaria* and *Arctostaphylos uva-ursi* extracts to compare different methods of hydrolysis.

4 Hydrolysis of Flavonoids and Tannins

4.1 Reaction kinetics of CO_2-intensified hydrolysis of rutin to quercetin

The following reaction mechanism of degradation of rutin to isoquercetin and quercetin, the degradation of isoquercetin to quercetin and the formation of quercetin can be described as a reaction of first-order. First-order reactions are expressed as a product of reaction rate constant and concentration of certain compounds at a certain time. Figure 25 illustrates the considered reaction pathways. Following assumption were made: rutin (A) degrades either directly to quercetin (C) or to isoquercetin (B); isoquercetin (B) is formed via degradation of rutin (A) and is further degraded to quercetin (C); quercetin (C) is either generated by direct degradation of rutin (A) or degradation of isoquercetin (B). To simplify the reaction mechanism, no byproducts or degradation products and associated pathways were taken into account. In Figure 26 the appointed first-order homogeneous differential equations (FOHDE) for the reaction rate of rutin degradation (FOHDE A), of quercetin formation (FOHDE C) and of isoquercetin formation / degradation (FOHDE B) are summarized.
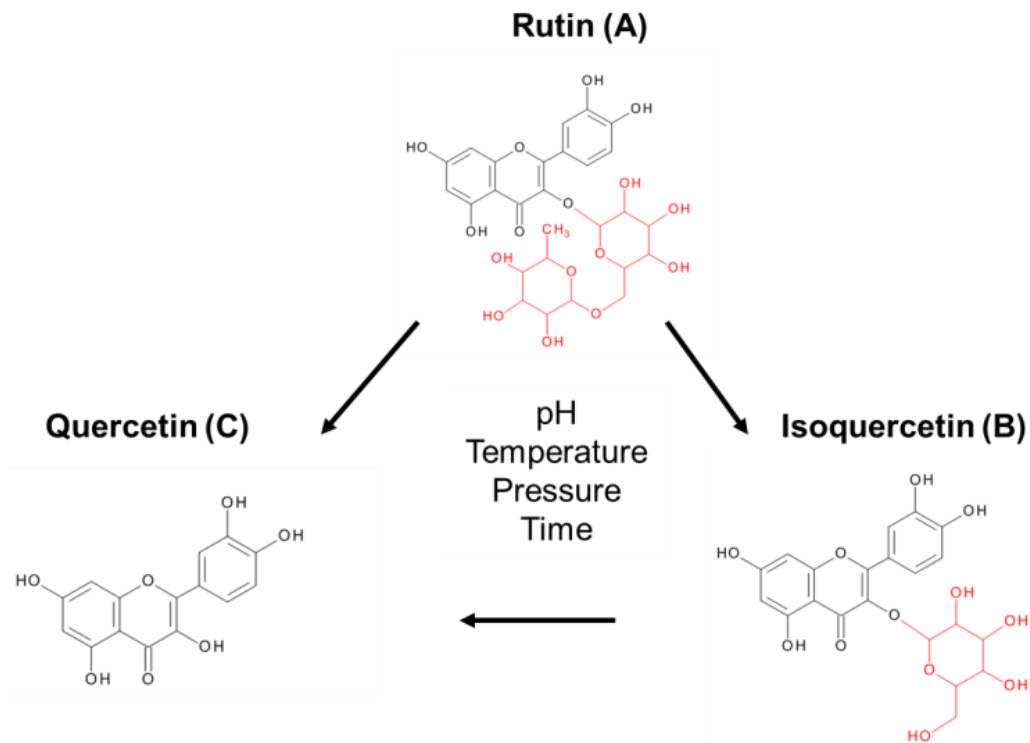
Figure 25: Hydrolysis pathway of rutin (A) to isoquercetin (B) and quercetin (C) [137]

$$-r_A = -\frac{dc_A}{dt} = \underbrace{(k_1 + k_2) \cdot c_A}_{\text{Degradation A}}$$

$$-r_B = -\frac{dc_B}{dt} = (\underbrace{k_3 \cdot c_B}_{\text{Degradation B}} - \underbrace{k_2 \cdot c_A}_{\text{Formation B}})$$

$$r_C = \frac{dc_C}{dt} = (\underbrace{k_1 \cdot c_A}_{\text{Formation C}} + \underbrace{k_3 \cdot c_B}_{\text{Formation C}})$$

Figure 26: First-order homogeneous differential equation to describe reaction kinetics of rutin (A, FOHDE A), isoquercetin (B, FOHDE B) and quercetin (C, FOHDE C) [137]

In order to determine the reaction rate constants k_1, k_2 and k_3, each FOHDE (A, B and C) has to be solved. To obtain all three solutions of the equations, FOHDE (dc_A/dt) was solved first (Equation 1). The solution of FOHDE A was inserted in FOHDE B (dc_B/dt) and resulted in a first-order inhomogeneous differential equation and was thereafter solved and expressed as c_B (Equation 2).

Equation 1: Degradation of rutin [137] **Equation 2: Formation and degradation of isoquercetin [137]**

$$c_A = c_{A,0} \cdot e^{-(k_1 + k_2) \cdot t}$$

$$c_B = c_{A,0} \cdot \frac{k_2}{k_3 - (k_1 + k_2)} \cdot \left(e^{-(k_1 + k_2) \cdot t} - e^{-k_3 \cdot t} \right)$$

An assumption of constant number of moles and no formation of byproducts due to degradation of isoquercetin and quercetin during the whole hydrolysis reaction was made: the initial amount of A (c_{A0}) has always to be the sum of A (c_A), B (c_B) and C (c_C) at a given time (Equation 3).

Equation 3: Molar balance of rutin, isoquercetin and quercetin [137]

$$c_{A,0} = c_A + c_B + c_C \rightarrow c_C = c_{A,0} - c_A - c_B$$

The combination of Equation 1, Equation 2 and Equation 3 resulted in Equation 4.

Equation 4: Formation of quercetin [137]

$$c_C = c_{A,0} \cdot \left[1 - e^{-(k_1+k_2)\cdot t} - \frac{k_2}{k_3-(k_1+k_2)} \cdot \left(e^{-(k_1+k_2)\cdot t} - e^{-k_3 \cdot t}\right)\right]$$

Equation 1 and Equation 4 were applied to calculate the reaction rate constants for temperature dependence and pressure dependence. One model is based on the variation of temperature and one model based on the variation of CO_2-pressure (Figure 27). MATLAB® (function: LsqCurveFit / least squares fit function) was used for determination of rate constants (k_1, k_2, k_3) by varying the starting values, lower and upper limits. Isoquercetin was analyzed qualitatively and was not considered in the two models.
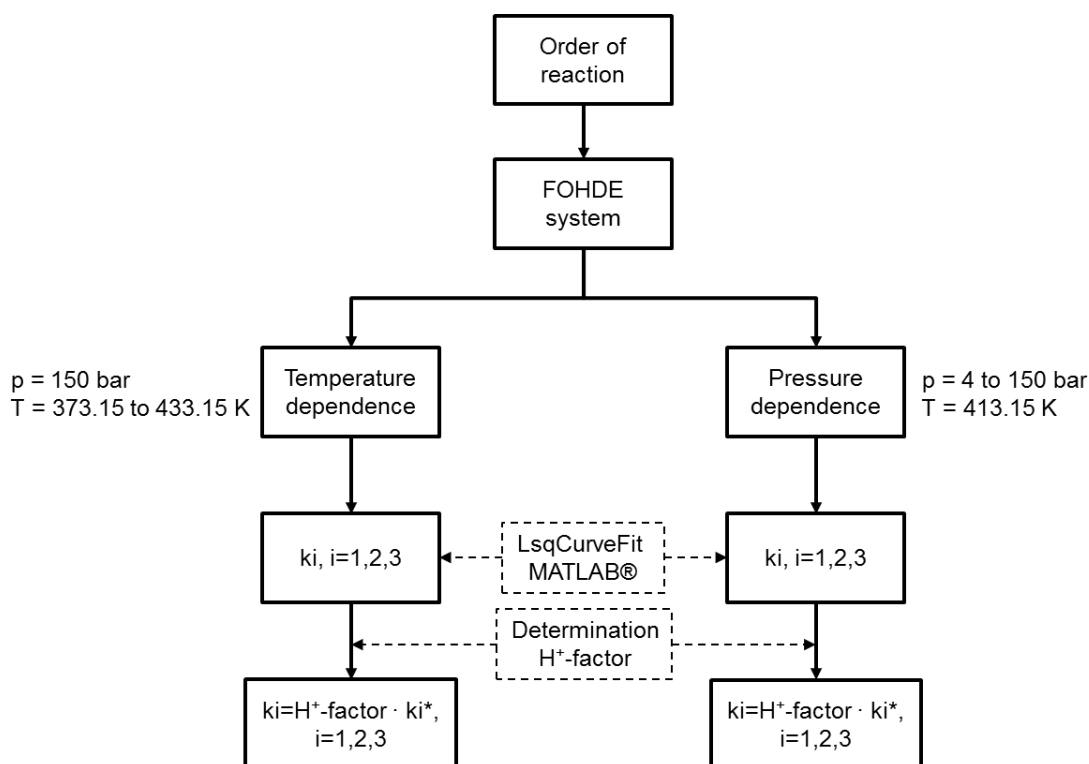
Figure 27: Flow diagram of the procedure to determine k1, k2 and k3, k1*, k2* and k3* [137]

The results of k_1, k_2 and k_3 had to be equal for both formation and degradation reaction (Equation 1 and Equation 4) for each respective parameter combination (variation of

temperature at constant pressure and variation of CO_2-pressure at constant temperature). The »H^+-factor« is described in more detail in chapter 4.1.1. Correlation coefficients (R^2) for c_A and c_C were calculated via Microsoft EXCEL® (Equation 5).

Equation 5: Coefficient of determination (R^2) [137]

$$R^2 = 1 - \frac{\sum_{t=0h}^{8h}\left(cC_{exp} - cC_{calc}\right)^2}{\sum_{t=0h}^{8h}\left(cC_{exp} - \overline{cC_{exp,mean}}\right)^2}$$

Activation energies ($E_{a,i}$) of all three hydrolysis reactions were determined with the law of Arrhenius (Equation 6) and were expressed as linear equations (Equation 7). The natural logarithm of the reaction rate constant was displayed against 1/T to assess activation energies graphically.

Equation 6: Arrhenius equation for activation energy

$$k_i = k_0 \cdot e^{-\frac{E_{a,i}}{R \cdot T}}$$

Equation 7: Linear equation form of Arrhenius

$$\ln k_i = \ln k_0 + \frac{1}{T} \cdot \left(-\frac{E_{a,i}}{R}\right)$$

Activation energies were determined by multiplying the slope with the universal gas constant (8.314 J/molK). The ln(k)- intercept is the pre-exponential factor k_0.

4.1.1 **Determination of »H^+-factor«**

CO_2 dissolves in a limited amount in water. CO_2 and H_2O dissociate to H^+, OH^-, HCO_3^- and CO_3^{2-} [167]. Pressure and temperature affects the solubility of CO_2 in water. With increasing pressure, the amount of dissolved CO_2 in water increases, whereas at

increasing temperature the solubility of CO_2 in water is decreasing. This effect leads to in- or decrease of H^+-ions concentrations [119, 134]. At constant temperature and increasing pressure the amount of dissociated H^+ increases, since the higher amount of CO_2 pushes the equilibrium of dissociation on the side of the H^+ ions ($CO_2 + H_2O \leftrightarrow H^+ + HCO_3^-$). Due to increasing the H^+ ion concentration in water the pH can achieve values around 3 under CO_2-pressure [167, 168]. pH values around 3 are responsible for dissociation of HCO_3^- to CO_3^{2-} to a small extend, this can be seen by the slightly higher concentrations for H^+ than for HCO_3^-. This effect is confirmed by Li et al. [134] and is shown in Table 13.

Table 13:Concentrations of CO_2, H^+, HCO_3^- and CO_3^{2-} at pressures between 4 bar and 150 bar at 413.15 K [119, 134]

Pressure [bar]	CO_2 [mol/kg]	H^+ [mol/kg]	HCO_3^- [mol/kg]	CO_3^{2-} [mol/kg]
4	0.0017	1.90E-05	1.89E-05	5.35E-11
25	0.1901	1.98E-04	1.98E-04	5.36E-11
50	0.3867	2.76E-04	2.76E-04	5.21E-11
100	0.7085	3.66E-04	3.66E-04	5.09E-11
150	0.9526	4.23E-04	4.23E-04	5.14E-11

The performed experiments indicated a significant influence of the CO_2-pressure. Therefore, it was assumed that not only increasing pressure itself is responsible for the increasing yields of the hydrolysis reaction, but also the increasing H^+ ion concentration due to pushing the dissociation on the side of H^+ and HCO_3^- in water. To show the H^+ ion molality in the model, a new factor »H^+-factor« was introduced. This factor describes the ratio of molality of H^+ ions and the initial molar concentration of rutin (c_{A0}). The H^+ ion molality is a function of pressure and temperature. The »H^+-factor« was

used to describe k_1, k_2 and k_3 (k_i = H+-factor $\cdot$ k_i^*) and to illustrate the CO_2-pressure dependency of CO_2-intensified hydrolysis.

Calculations of speciation equilibrium and H^+-concentration at certain temperatures, pressures and CO_2-solubilities were conducted with the abovementioned model (see chapter 1.7.3). The generated data allowed the calculation of the »H^+-factor« (c_{H+} / c_{A0}) for each parameter combination (Table 14 and Table 15).

Table 14: »H^+-factor« for each parameter combination - at 150 bar between 393.15 K and 433.15 K (T: temperature, cH^+: molality of H^+ in water) [137]

T	cH^+	H^+-factor
[K]	[mol/kg]	[mol H^+/ mol Rutin]
373.15	5.90E-04	7.19
393.15	5.05E-04	6.15
413.15	4.23E-04	5.16
433.15	3.50E-04	4.26

Table 15: »H^+-factor« for each parameter combination - at 413.15 K between 4 bar and 150 bar (p: pressure, cH^+: molality of H^+ in water) [137]

p	cH^+	H^+-factor
[bar]	[mol/kg]	[mol H^+/mol Rutin]
4	2.76E-05	0.34
25	1.98E-04	2.41
50	2.76E-04	3.37
100	3.66E-04	4.47
150	4.23E-04	5.16

4.1.2 CO_2-intensified hydrolysis | temperature dependence

Temperature has the highest influence on CO_2-intensified hydrolysis. At 373.15 K (the lowest temperature) and after 8 h, the lowest yield of quercetin (5 %) was observed (Figure 28). Increasing temperature enhances the yield of quercetin. 393.15 K yielded 30 % quercetin after 8 h. At 413.15 K the CO_2-intensified hydrolysis showed the best performance (100 % degradation of rutin and an equimolar formation of quercetin

(100 %). Exceeding 413.15 K resulted in a lower concentration of quercetin. At that temperature (433.15 K) rutin degraded totally after 4 hours, the yield of quercetin did not result in an equimolar formation, which indicates a formation of by-products or a destruction of the flavonoid structure (rutin, isoquercetin or quercetin). In Figure 28 and Figure 29 the yields of quercetin and rutin at four different temperatures (373.15 K, 393.15 K, 413.15 K and 433.15 K) are shown.
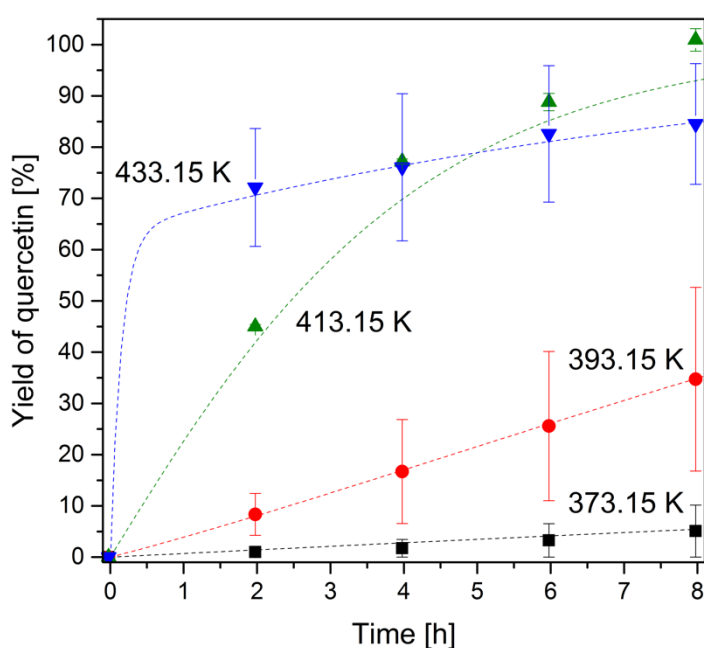
Figure 28: Yield of quercetin over 8 hours at different hydrolysis temperatures between 373.15 K and 433.15 K at 150 bar, modeled data (dotted line) versus experimental data (■ 373.15 K, ● 393.15 K, ▲ 413.15 K, ▼ 433.15 K) [137]
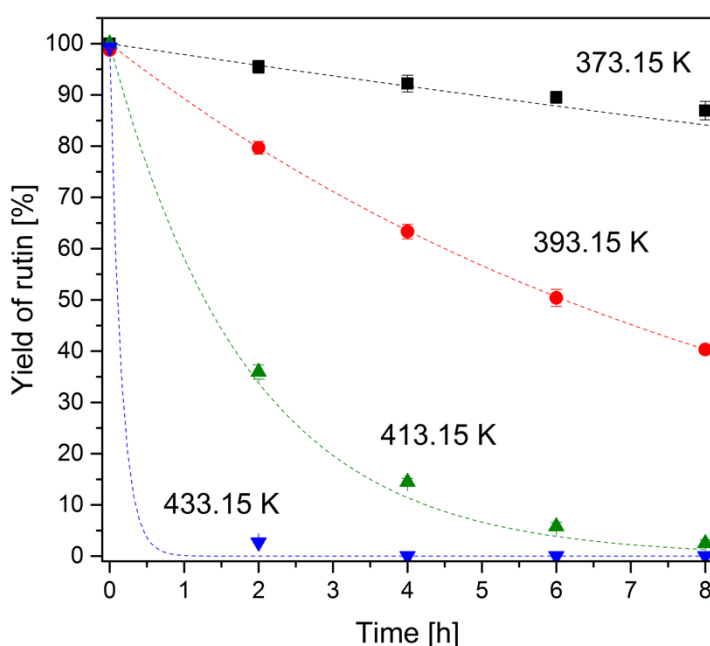
Figure 29: Yield of rutin over 8 hours at different hydrolysis temperatures between 373.15 K to 433.15 K at 150 bar, modeled data (dotted line) versus experimental data (■ 373.15 K, ● 393.15 K, ▲ 413.15 K, ▼ 433.15 K) [137]

The calculated kinetic model agreed with the experimentally obtained yields of quercetin and rutin and yielded high correlation coefficients. Except at 373.15 K, the obtained correlation coefficients exceeded values above 0.99 and therefore, a good accordance with the empirically obtained yields (Table 16). At 373.15 K the model showed an accuracy of $R^2 \geq 0.86$ (rutin (0.89); quercetin (0.86)).

Table 16: Reaction rate constants k_1, k_2 and k_3 for temperatures between 373.15 K and 433.15 K at 150 bar [137]

Temperature	k_1	k_2	k_3	R² rutin	R² quercetin
[K]	[1/h]	[1/h]	[1/h]	[-]	[-]
373.15	0.007	0.014	0.004	0.895	0.859
393.15	0.037	0.076	0.113	0.999	0.999
413.15	0.217	0.310	0.413	0.998	0.996
433.15	4.246	2.386	0.110	0.999	0.999

The activation energies (E_a) and pre-exponential factors (k_0) of all three reactions were calculated from the linear functions (obtained from logarithmized results and displayed in Figure 30) are summarized in Table 17.
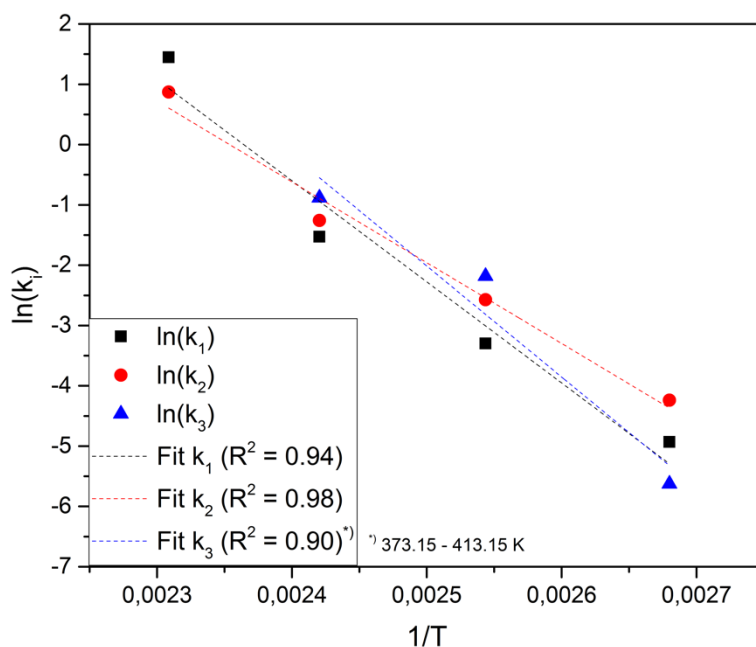
Figure 30: Linearization of Arrhenius Equation – determination of activation energy (E_a) and pre-exponential factor (k_0) via linear fit (dotted line) of ln(k). [137]

Table 17: Activation energy (E$_a$) of each assumed hydrolysis reaction with confidence interval (±) and pre-exponential factor (k$_0$) between 373.15 K and 433.15 K [137]

Reaction	E$_{ai}$ [kJ/mol]	k$_0$ [1/h]
1 (A → C)	139.4 ± 19.3	1.65E+17
2 (A → B)	111.4 ± 10.0	4.96E+13
3 (B → C)*	153.0 ± 35.2	1.28E+19

* 373.15 K to 413.15 K: Hydrolysis reaction above 413.15 K showed a bend at the reaction rate for reaction B to C (k$_3$) (Table 16) (from 0.413 1/h at 413.15 K to 0.110 1/h at 433.15 K). The bend of the reaction rate constant (k$_3$) resulted in a bend of activation energy. The activation energy of reaction 3 (B to C) was therefore calculated up to 413.15 K. Above this temperature it cannot be stated clearly which degradation or side reaction occurred.

Activation energies of reaction 1 »A to C« (E$_{a1}$) and reaction 2 »A to B« (E$_{a2}$) varied between 112 and 140 kJ/mol. Szejtli [96] investigated the acid-catalyzed hydrolysis of different glycosides and obtained activation energies in a similar range (106 to 145 kJ/mol). Ravber et al. [106] and Ruen-ngam et al. [31] calculated activation energies for hydrolysis reactions of rutin to quercetin (87 kJ/mol) and hesperidin to hesperetin (143 kJ/mol) in a comparable range. Reaction 3 »A to C« requires a higher activation energy for separating the glycosidic bond between aglycone and glucose than reaction 1 »A to B« for separating rhamnose from glucose.

The possibility of reactions is quantified by the pre-exponential factor. The higher k$_0$ the more probable is the reaction. Although reaction 3 »B to C« has the highest k$_0$ value, reaction 1 »A to C« is the most probable reaction. Before B can further be hydrolyzed to C, B has to be formed by reaction 2 »A to B«. It is assumed that B immediately after its formation is hydrolyzed to C. HPLC results confirmed the rapid

degradation of isoquercetin to quercetin. The content of isoquercetin was analyzed qualitatively and showed only small peaks in the chromatograms for all investigated parameter combinations (Figure 31).

Quercetin decomposes into various compounds via cleavage of the ring structure or an oxidation with a further addition of nucleophiles to quercetin-quinone. Ravber et al. [106] quantified a quercetin degradation of about 14 % at 433.15 K. At a retention time (RT) of 4.29 min, the HPLC chromatograms (Figure 31) showed one peak after two hours of hydrolysis at 433.15 K. An additional peak appeared at a RT of 4.87 min in samples that were hydrolyzed at 433.15 K for 6 hours. These peaks might indicate decomposition or side reactions of quercetin as rutin and isoquercetin were already decomposed. At 393.15 K and 413.15 K no additional peaks were observed, except for isoquercetin.
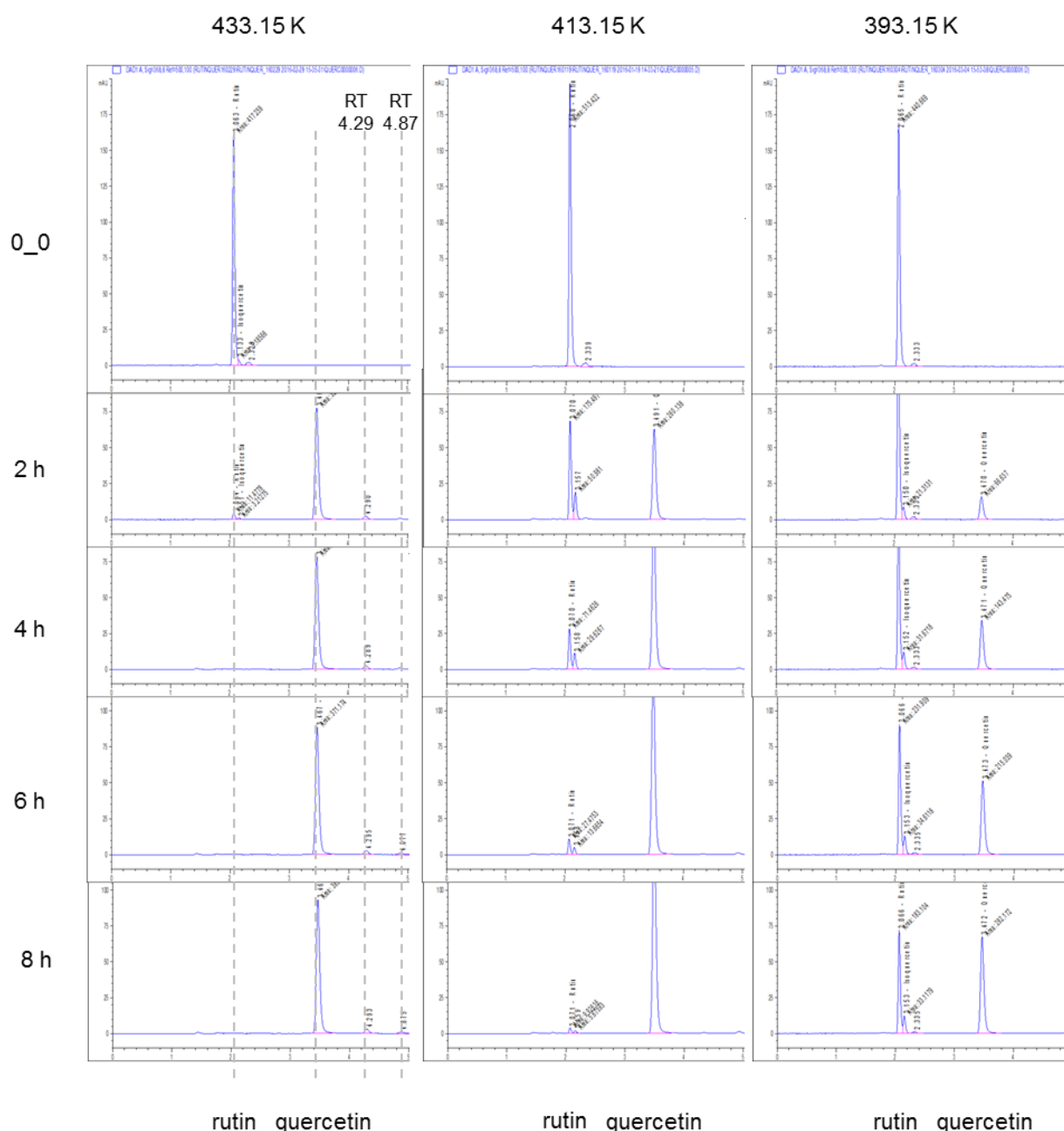
Figure 31: Examples of HPLC chromatograms for hydrolysis over 8 hours at 393.15 K, 413.15 K and 433.15 K and 150 bar (0_0: chromatogram of rutin-solution before hydrolysis - stock solution; RT: retention time) [137]

The experiments at temperatures between 373.15 K and 433.15 K, showed the high impact of temperature on the reaction rates (increasing temperature resulted in increasing reaction rates). The »H+-factor« was applied to the reaction kinetic model for temperature dependence (Table 18) and no significant change of the fitted functions

for the reaction rates between k_i and k_i^* was detected (comparison of Table 16 and Table 18). This clearly shows that the H^+-ion concentration was superimposed by the effect of temperature. The probability of hydrolysis reactions increased with increasing pH value, or the H^+-ion concentration, which refers to the »H^+-factor«. The highest »H^+-factor« was observed at 373.15 K (Table 14), but due to increasing temperature, the solubility of CO_2 decreases and the speciation equilibrium translocated to the side of CO_2 and lower H^+-ion concentrations were observed – the »H^+-factor« decreased. The highest »H^+-factor« at 373.15 K was too weak to initiate the hydrolysis reaction. The hydrolysis reaction needs both, an adequate temperature and a certain »H^+-factor«.

Table 18: Adjusted reaction rate constants with »H^+-factor«, temperature varied between 373.15 K and 433.15 K at 150 bar [137]

Temperature [K]	k_1^* [mol H+ /mol rutin·h^{-1}]	k_2^* [mol H+ /mol rutin·h^{-1}]	k_3^* [mol H+ /mol rutin·h^{-1}]
373.15	0.001	0.002	0.001
393.15	0.006	0.012	0.018
413.15	0.045	0.060	0.080
433.15	0.996	0.560	0.026

The parity plot (Figure 32) shows the comparison between the calculated normalized concentrations and experimental normalized concentrations. For temperatures above 393.15 K, the parity plot showed an accuracy of ± 25 %. The highest deviation (> 25 %) was observed for quercetin at 393.15 K due to a high deviation between each experiment. At 373.15 K and 413.15 K, the highest accuracies (< 25 %) for rutin and

quercetin were observed. At 433.15 K the variation was higher than for 373.15 K and

413.15 K but was within the ± 25 % range.
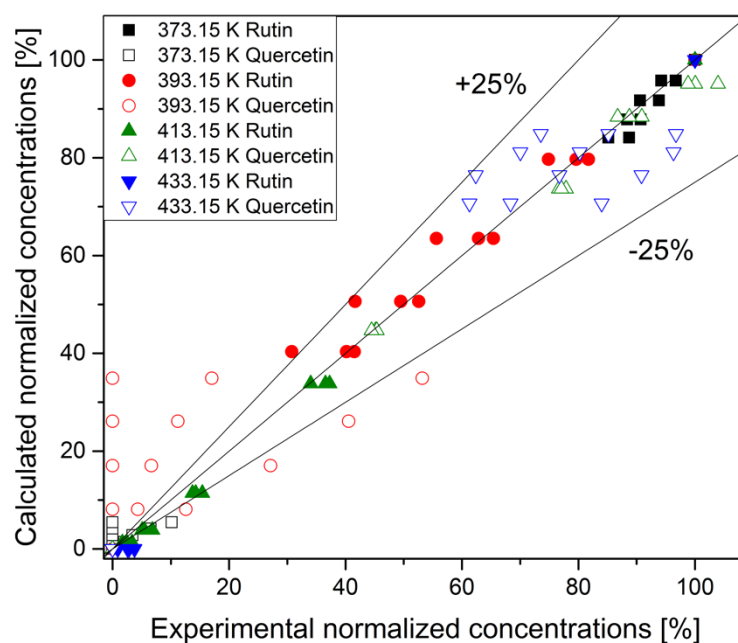
Figure 32: Parity plot of normalized rutin and quercetin concentrations at 150 bar and 373.15 K, 393.15 K, 413.15 K and 433.15 K [137]

Out of these results, the temperature for the pressure dependence experiments was

set to 413.15 K.

4.1.3 **CO₂-intensified hydrolysis | pressure dependence**

Experiments at 413.15 K and pressures between 4 bar and 150 bar showed a rutin degradation between 25 % (4 bar) and 97 % (150 bar) – summarized in Figure 33. Increasing pressure on the system resulted in lower rutin concentrations or higher rutin degradation, respectively. At 25 bar (25 %), a three times lower normalized rutin concentration was observed in comparison to experiments at 4 bar (75 %) after 8 h. Exceeding pressures of 25 bar (50 bar, 100 bar and 150 bar), the relative decrease of rutin was lower than for experiments between 4 and 25 bar. Already at 50 bar, a normalized rutin concentration of almost 10 % was observed. Increasing the pressure to 100 bar resulted in a normalized rutin concentration of 5 % and at 150 bar a normalized rutin concentration of 3 % was observed.
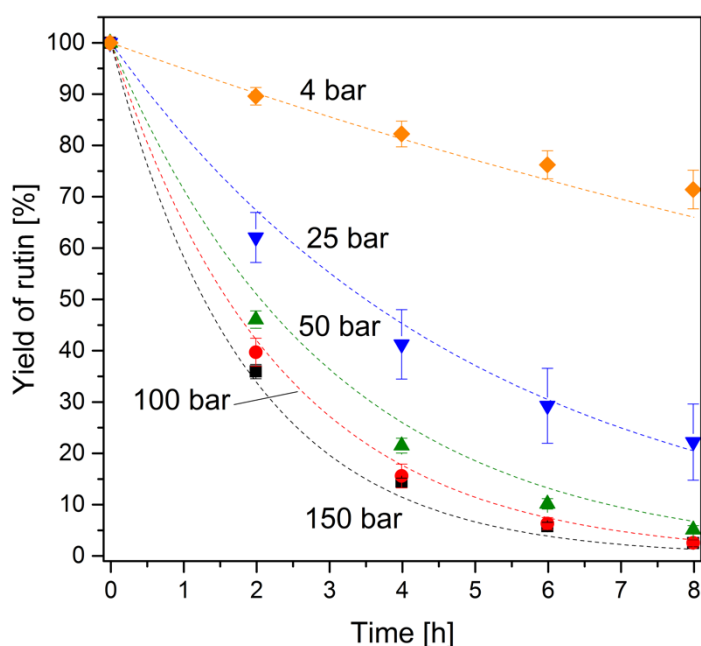
Figure 33: Normalized concentration of rutin over 8 hours at 413.15 K and pressures between 4 bar to 150 bar, modeled data (dotted line) versus experimental data (■ 150 bar, ● 100 bar, ▲ 50 bar, ▼ 25 bar, ♦ 4 bar) [137]

Experiments at 413.15 K and pressures between 4 bar and 150 bar showed a quercetin formation between 21 % (4 bar) and 100 % (150 bar) – summarized in Figure 34. Increasing pressure on the system resulted in higher quercetin yields. At 25 bar (45 %), a two times higher yield of quercetin was observed in comparison to experiments at 4 bar (21 %) after 8 h. Already at 50 bar, a yield of quercetin of almost 80 % was observed. Increasing the pressure to 100 bar resulted in a yield of quercetin of 85 % and at 150 bar a total conversion of rutin to quercetin (100 %) was observed.
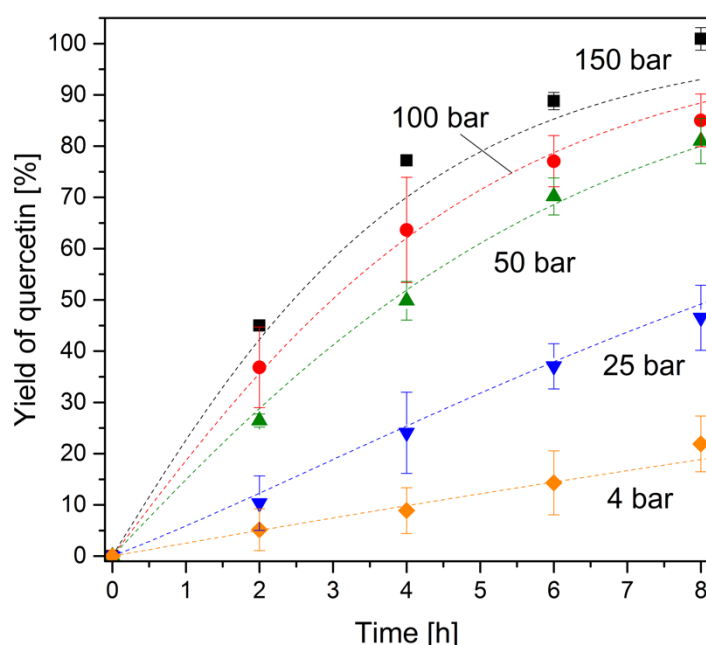
Figure 34: Yield of quercetin over 8 hours at 413.15 K and pressures between 4 bar to 150 bar, modeled data (dotted line) versus experimental data (■ 150 bar, ● 100 bar, ▲ 50 bar, ▼ 25 bar, ◆ 4 bar) [137]

The developed reaction kinetic model »pressure dependence« showed a good applicability. Correlation coefficients (R^2) for 25, 50, 100 and 150 bar were above 0.96 (Table 19). Except at 4 bar, the model showed a $R^2 \geq 0.92$. According to the increasing yields of quercetin, the reaction rate constants increased with increasing pressure (Table 19). Increasing the pressure, the reaction rate constants (k_1, k_2 and k_3) followed

an exponential growth function with correlation coefficients between 0.95 and 0.99 (Figure 35).

Table 19: Reaction rate constants between 4 and 150 bar at 413.15 K [137]

Pressure [bar]	k_1 [1/h]	k_2 [1/h]	k_3 [1/h]	R^2 rutin [-]	R^2 quercetin [-]
4	0.026	0.026	0.031	0.922	0.964
25	0.055	0.142	0.135	0.987	0.994
50	0.152	0.186	0.270	0.991	0.997
100	0.188	0.246	0.358	0.998	0.996
150	0.233	0.310	0.413	0.997	0.966
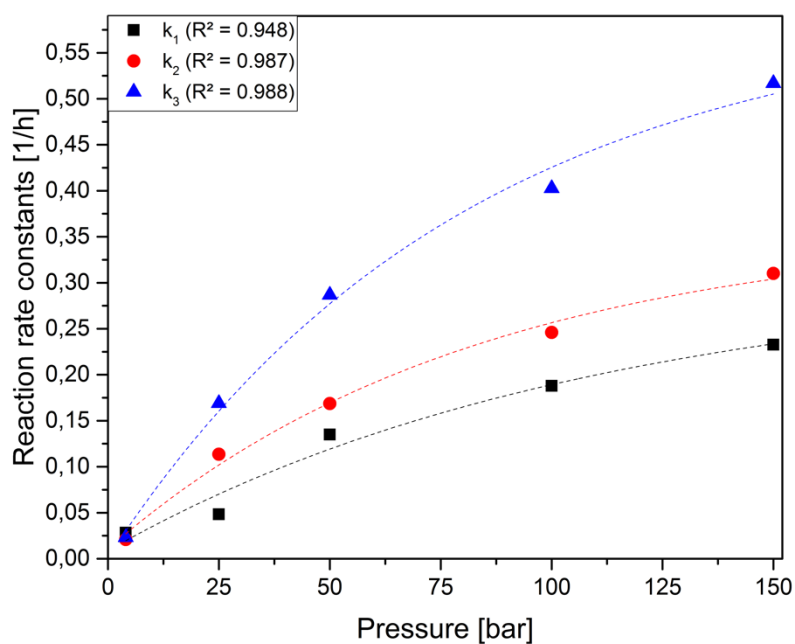
Figure 35: Reaction rate constants at pressures of 4, 25, 50, 100 and 150 bar and at 413.15 K [137]

The obtained results showed a clear correlation with CO_2-pressure at hydrolysis reaction of flavonoid glycosides.

Whitey and Whalley [169] investigated the acid-catalyzed racemization of sec-butanol at 373.15 °K and observed an increase of reaction rate constants of around 5 % between 1 to 1000 bar (static pressure). Taking this into account, the influence of static pressure is marginal. In comparison to acid-catalyzed racemization, the performed CO_2-intensified hydrolysis experiments »pressure dependence« showed a 10-fold increase of reaction rates for all three reactions (A→B, B→C and A→C) between 4 bar and 150 bar at 413.15 K. This increase of reaction rate constants shows an additional correlation on the CO_2-intensified hydrolysis reaction besides the static pressure and leads to a different perspective of reaction rate constants. The reaction rate constants were divided into an adjusted reaction rate constant (k_i^*) and a new dependence for CO_2-intensified hydrolysis, the »H^+-factor«. The adapted reaction rate constants k_i^* are summarized in Table 20. The correlation of »H^+-factor« and CO_2-intensified hydrolysis is described by the excess of H^+-ions in comparison to the initial amount of rutin in mole H^+-ions per mole rutin. The introduced »H^+-factor« increases with increasing pressure (Table 15). In Figure 36 a comparison was made between the calculated k-values and k*-values (Table 20). The elimination of »H^+-factor« out of the reaction rates resulted into almost constant k_i^*-values and proofed the influence of the excess of H^+-ions on the CO_2-intensified hydrolysis.

Table 20: k_i^* between 4 bar and 150 bar at 413.15 K [137]

Pressure [bar]	k_1^* [mol H+ /mol rutin·h^{-1}]	k_2^* [mol H+ /mol rutin·h^{-1}]	k_3^* [mol H+ /mol rutin·h^{-1}]
4	0.076	0.078	0.092
25	0.023	0.059	0.056
50	0.045	0.055	0.080
100	0.042	0.055	0.080
150	0.045	0.060	0.080
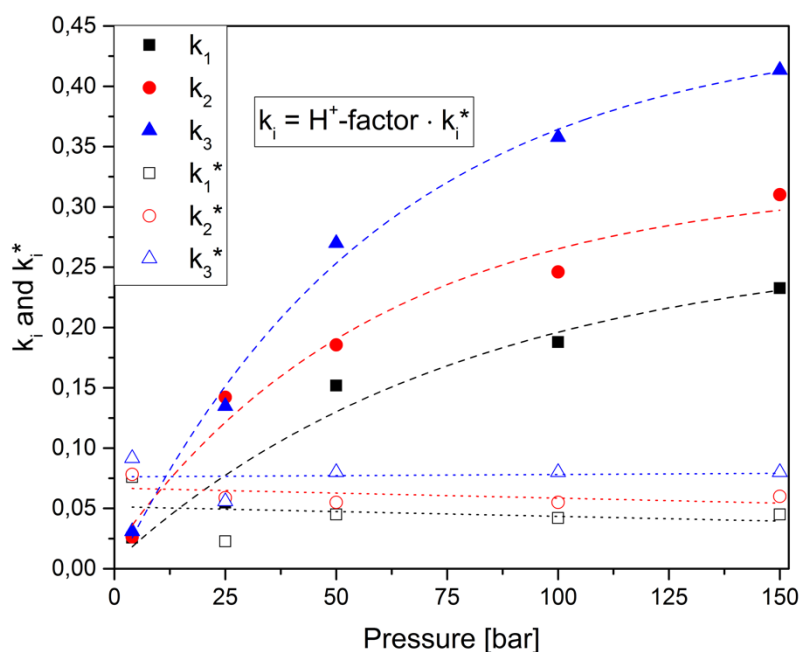
Figure 36: Comparison between k and k* at 413.15 K and pressures between 4 bar and 150 bar; k = H+-factor xk*, (■ k1, ● k2, ▲ k3; □ k1*, ○ k2*, △ k3*) [137]

The parity plot of CO_2-intensified hydrolysis »pressure dependence« (Figure 37)

shows the comparison between the calculated normalized concentrations and

experimental normalized concentrations. For pressures between 4 and 150 bar, the parity plot showed an accuracy of ± 25 %. The highest deviations (> 25 %) were observed for quercetin at 4 bar, 25 bar and 100 bar. At 150 bar the highest accuracy (< 25 %) for rutin and quercetin was observed.
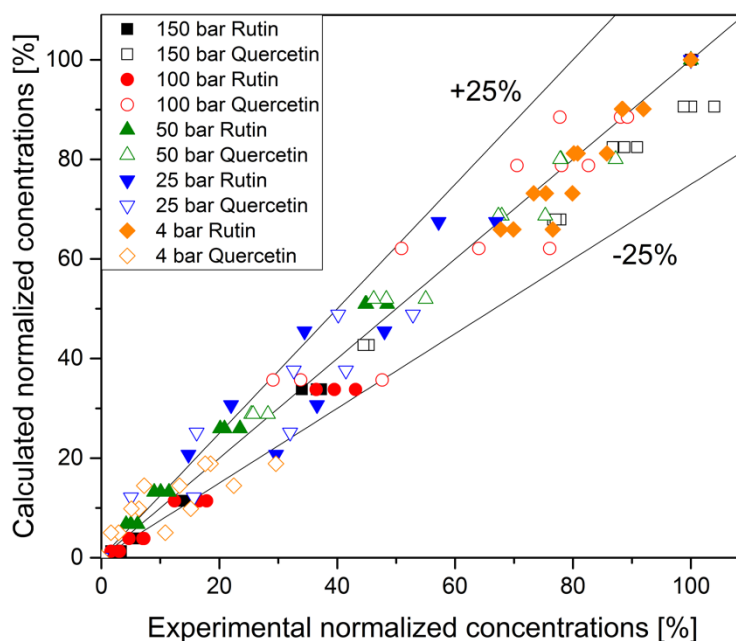
Figure 37: Parity plot of normalized rutin and quercetin concentrations at 413.15 K and 4 bar, 25 bar, 50 bar, 100 bar and 150 bar [137]

4.2 CO$_2$–intensified hydrolysis of tannic acid

In medicinal herbs, tannins and flavonoids often occur together. Flavonoids gain more and more interest as they are well known for their beneficial health properties to the human body. Flavonoids occur mainly as glycosides. Tannins occur as condensed or hydrolyzable tannins (gallyol linked with a glycosidic bond) and can be used for vegetable tanning agents or as an ingredient in food, cosmetics or pharmaceutical industries. In times of bio-economy and conservation of resources, it is important to obtain as many products out of a process as possible. One way could be a combined

process of obtaining flavonoids as aglycones for food and cosmetics and tannins as a vegetable tanning agent for leather tanning. For evaluation of this possible process, it is important to know the hydrolysis behavior of hydrolyzable tannins. Tannic acid will be used as a model substance for hydrolysis experiments with and without CO_2. The idea is to hydrolyze hydrolyzable tannins with the aid of pressure, temperature and carbon dioxide. An aqueous solution of tannic acid will be prepared to investigate the carbon dioxide intensified hydrolysis. Furthermore, tannic acid will be hydrolyzed with strong and weak acid to investigate the role of pH value and hydrolysis rate.

The CO_2-intensified hydrolysis will be described by a process model for a selected pressure and will be compared with conventional hydrolysis via strong and weak acid.

4.2.1 Reaction kinetic of CO_2-intensified hydrolysis – hydrolyzable tannins

After determination of the tannin content, the reaction rates for degradation were calculated. The reaction kinetics of the hydrolysis reaction of tannic acid was simplified to calculate the reaction rate constant of the degradation of tannic acid.

In Figure 38 the proof of concept of CO_2-intensified hydrolysis at 413.15 K and 150 bar is shown. After six hours, tannic acid was completely degraded to non-tannable molecules, i.e. gallic acid, digallic acid,…, and its sugars.
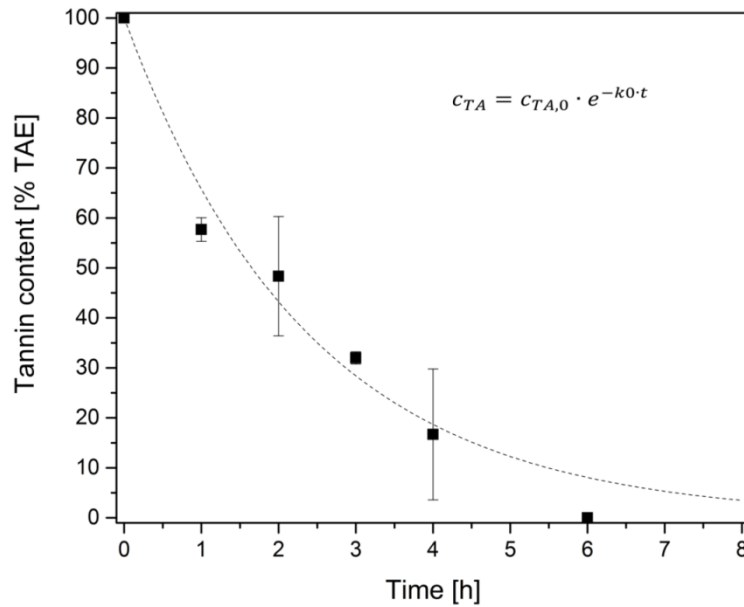
Figure 38: Experimental versus model - CO_2-hydrolysis – tannic acid

The decrease of tannin content at 413.15 K and 150 bar followed a first-order reaction $-\frac{dc_{TA}}{dt} = k \cdot c_{TA}$. The reaction rate constant was calculated for each data point to prove the reaction rate follows a first-order reaction. The reaction rate balance has to be integrated to $\ln\frac{c_{TA}}{c_{TA\_0}} = -k_0 \cdot t$. With the obtained experimental data of CO_2-intensified hydrolysis, the reaction rate was determined. In Figure 39 the natural logarithm of c/c_0 was drawn over time. A linear equation can be fitted and is therefore the proof of a 1st order reaction. The slope of the linear curve indicates the reaction rate constant.
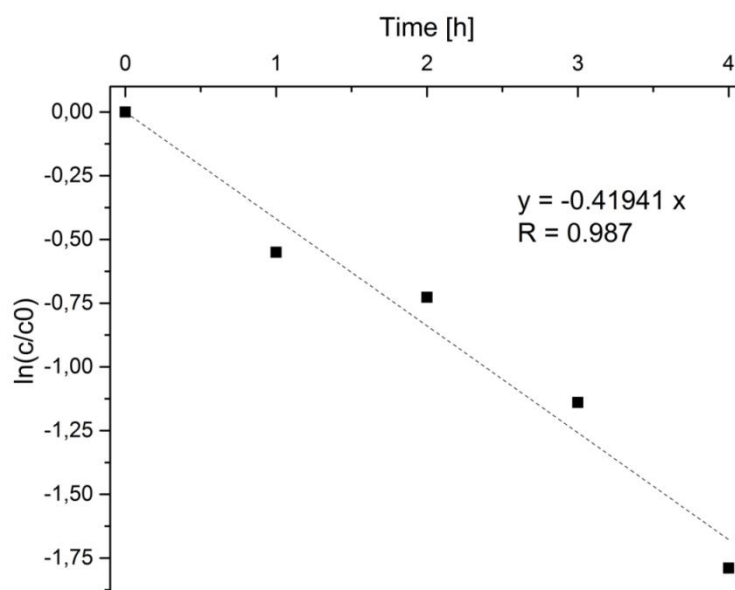
Figure 39: Reaction of TA hydrolysis at 140°C and 150 bar

After fitting the linear curve, a reaction rate constant k_0 of 0.4194 [1/h] was obtained. With k_0 it is possible to model the reaction progress of degradation reaction of tannic acid. In Figure 38 the experimental data points were compared with the calculated theoretical values. For determination of the theoretical values the reaction rate balance has to be expressed in concentration (in this case percentage) tannic acid.

The correlation coefficient of the model was calculated and resulted in an $R^2 = 0.989$.

5 Utilization Concepts of Tannins and Flavonoids
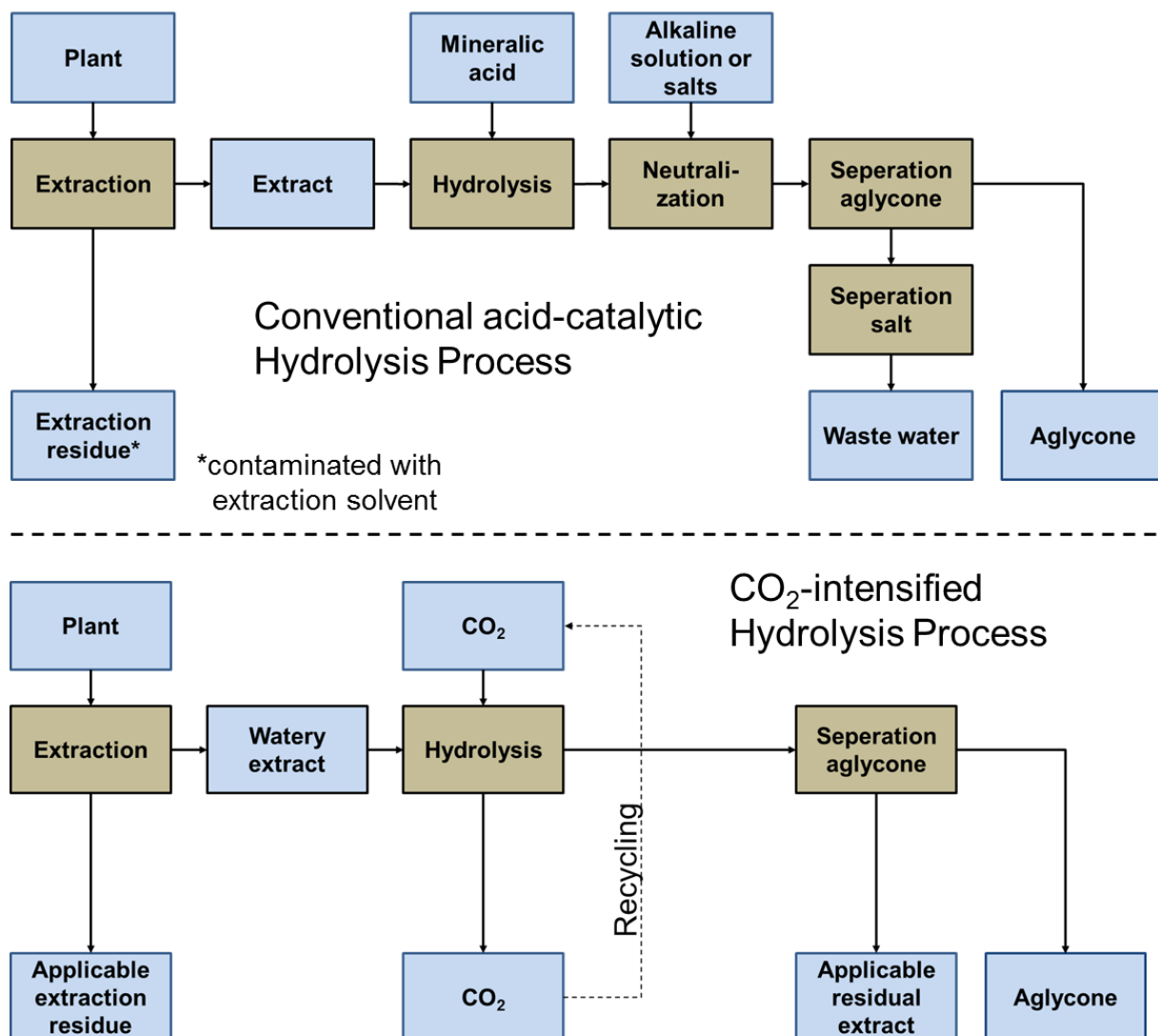
Figure 40: Comparison between conventional acid-catalytic Hydrolysis process and CO2-intensified hydrolysis process

The utilization concept of a conventional quercetin production (Figure 40) depends highly on the raw material and the extraction solvent. Usually, the raw material is grinded prior usage and then extracted with the solvent. The choice of solvents depends on the target compound and the polarity of the extraction solvent. In general,

flavonoids are better soluble in organic solvents than in purified water [170, 171]. After extraction, the residue will be squeezed to minimize the solvent losses. The extraction residue with low rest moisture could be contaminated with the extraction solvent (acetone, methanol, ethanol, methyl-acetate…) and should be dried to evaporate the residual solvent. Depending on the decomposition level of the residue (fiber length or residue compounds) the residue could be used as fibers in the pulp industry or as raw material for bio-polymers composites. If there are residual compounds, which are sparingly soluble, the extraction residue could be further leached with a different extraction solvent and the residue could be composted and used as natural fertilizer. As last option, the extraction residue could be used in thermal combustion.

The obtained extract will further be hydrolyzed with mineral acids (hydrochloric, nitric or sulfuric acid). After hydrolysis, the acidic extract will be neutralized with alkaline solutions or salts (depending on the used acid for hydrolysis). After neutralization, the aglycone rich extract will be cooled down. The solubility of aglycones rapidly decreases with decreasing temperature. This decrease of solubility is used to separate the aglycones from the extract. The aglycones crystallize and are separated by a filter. The aglycones have to be further cleaned for commercial use by re-crystallization.

After separation of the aglycones from the extract, the salt containing residual extract has to be treated with reverse osmosis to purify the wastewater from the formed neutralization salts. Depending on the used acid and the used neutralization salt/alkaline, several salts can be formed. Assuming Na_2CO_3 is used for neutralization of HCl, H_2SO_4 or HNO_3 the following salts can be formed: NaCl, Na_2SO_4, $NaNO_3$. Those salts are applied in several industrial processes and usages, e.g. $NaNO_3$ as a fertilizer for agriculture [172], Na_2SO_4 as a filler material in detergents, as a compound

in the pulp and paper industry [173] and NaCl as deicing salt in winter, etc… . The salt-free wastewater can be passed further to a municipal wastewater treatment plant.

5.1 Balance of the conventional hydrolysis process

Commercial sources for quercetin production have their origin mostly in Asia or South America (*Styphnolobium japonicum* with up to 30 w% (in the blossoms) [12], *Dimorphandra mollis* with up to 8 w% [91]). In Europe, the only source with high amounts of quercetin-glycosides is common or tartaric buckwheat (*Fagopyrum esculentum* or *tataricum*). European buckwheat has high rutin contents and is used already for commercial production of rutin as medication for venous disorders. According to literature, up to 5 % of rutin could be contained in the whole aerial part of buckwheat [12]. In order to produce one ton of quercetin, 20.000 kg of buckwheat is needed, assuming that the whole amount of rutin will be hydrolyzed into quercetin. This would subsequently mean that 200.000 kg of water is needed as well. (Assumptions are summarized in Table 21)

Table 21: Assumptions for conventional hydrolysis to produce one ton of quercetin

Assumptions for quercetin production	
Plant of choice	Buckwheat (common or tartaric)
Rutin content	5%
Extraction ratio	1:10
Amount of extraction material	20.000 kg
Extraction solvent	Water
Amount of extraction solvent	200.000 kg
Acid of choice	HCl, H_2SO_4, HNO_3
Neutralization salt	Na_2CO_3

According to a patent survey (Table 2), 0.2 mol/L acid (HCl, HNO_3) or 0.1 mol/L (H_2SO_4) is necessary to hydrolyze rutin into quercetin (pH ~ 1). 200.000 kg of water needs an acid strength of 0.2 mol/L (HCl and HNO_3) or 0.1 mol/L (H_2SO_4). This results in 40.000 mol of HCl and HNO_3 or 20.000 mol of H_2SO_4 (Table 22). In the following three chemical equations, the neutralization of each acid with Na_2CO_3 is described:

1) $H_2SO_4 + Na_2CO_3 \rightarrow Na_2SO_4 + H_2O + CO_2$

2) $2 HNO_3 + Na_2CO_3 \rightarrow 2 NaNO_3 + H_2O + CO_2$

3) $2 HCl + Na_2CO_3 \rightarrow 2 NaCl + H_2O + CO_2$.
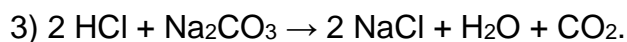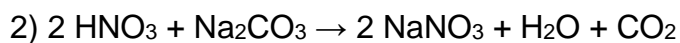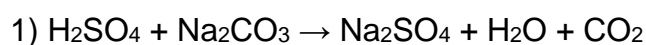
The amounts of formed salts are summarized in Table 22.

Table 22: Amount of acid needed for 20.000 kg of buckwheat to obtain 1.000 kg of quercetin and amount of formed salt

Acid	n_{acid} [mol]	n_{Na2CO3} [mol]	M_{salt} [g/mol]	m_{salt} [kg]
H_2SO_4	20.000	20.000	142.04 [1)]	2840[1)]
HNO_3	40.000	20.000	84.9947 [2)]	1700[2)]
HCl	40.000	20.000	58.44 [3)]	1170[3)]

[1)] Na_2SO_4 [2)] $NaNO_3$ [3)] NaCl

The desired CO_2-intensified hydrolysis process (Figure 40) would overcome the addition of mineral acids, neutralization of those acids and wastewater treatment from the conventional acid-catalyzed hydrolysis process. In order to obtain good results for the CO_2-intensified hydrolysis, it is necessary to work with watery extracts because even minimal amounts of other solvents (such as alcohols) would hinder the CO_2-intensified hydrolysis [31]. Consequently, the extraction is performed with water as extraction solvent. Out of this process, the extraction residue is not contaminated with organic solvents and is therefore, applicable for further usage without a purification step. The pure watery extract can further be hydrolyzed with carbonic acid, formed by dissolving pressurized CO_2 and temperature. The CO_2-intensified hydrolysis only works in combination with higher temperatures. The activation energy of those glycosidic cleavage reactions requires temperatures above 373.15 K to break the bond. The optimum temperature was found to be 413.15 K [137]. After the hydrolysis, the CO_2 evaporates and the pH-value increases back to the initial level. There are concepts stating that the released CO_2 can be reused within the process. The hydrolyzed residual extract (aglycones are already separated) can further be processed by drying (spray drying or vacuum belt dryer) to generate a fine powder, which could contain valuable compounds, depending on the used plant for quercetin

production. This all can be achieved when no mineral acids were added, and consequently, no neutralization has to be performed.

In the following chapter, hydrolysis was performed with *Fragaria* and *Arctstaphylus uva-ursi* extracts, besides conventional sources of quercetin production, to evaluate the potential for a combined production of an extract powder rich in more than one compound (e.g. flavonoids and tannins). For that purpose, hydrolysis was performed with acids (strong and weak acid) and CO_2 and water to compare different acid strengths on obtaining secondary phytochemicals and show a possible application of CO_2-intensified hydrolysis.

5.2 Hydrolysis of *Fragaria* and *Arctostaphylos uva-ursi* extracts
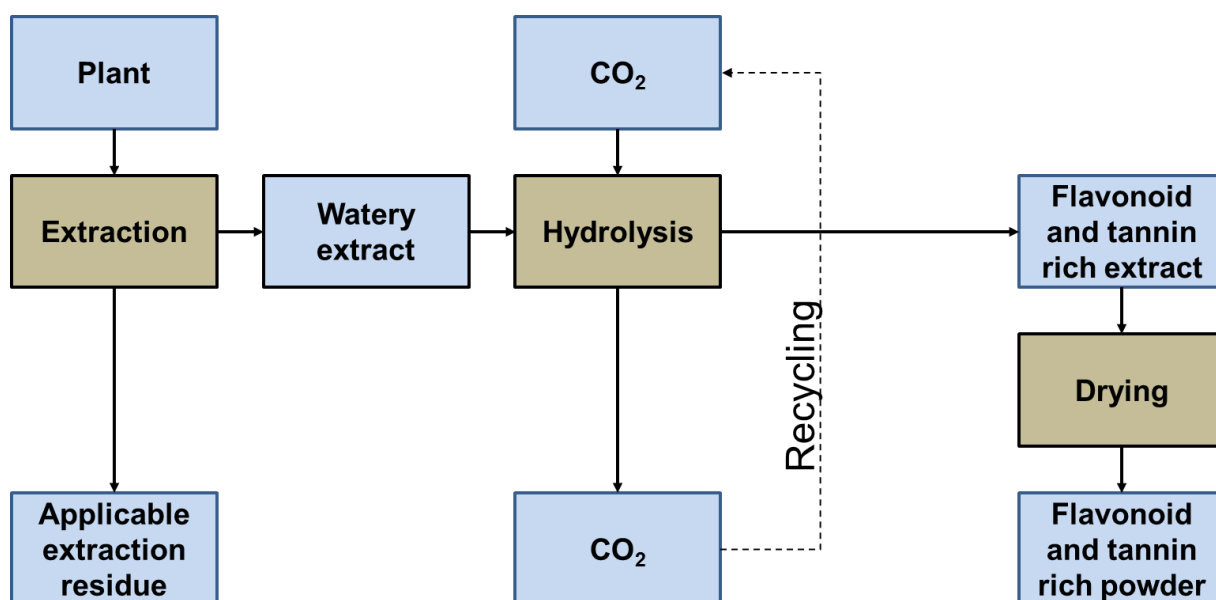
Figure 41: Combined CO₂-intensified hydrolysis process for obtaining a flavonoid and tannin-rich powder

In the next step, two EMHSP (*Fragaria* and *Arctostaphylos uva-ursi*) out of the screening study [13] were selected to test the suitability for a combined production of

flavonoids and tannins by hydrolyzing them with strong/weak acid and CO_2-intensified hydrolysis (Figure 41). To provide for all contingencies, it is important to discuss the characteristics of each plant.

Fragaria belongs to the family of *Rosaceae*. It is common in Europe and well known for its tannin content, as *Fragaria* still is used in the folk medicine as an astringence. In the leaves, tannin contents (hydrolyzable and condensed [12, 150]) of up to 10% were detected. Further ingredients, such as quercitrin, quercetin, kaempferol and leucoanthocyanidins, were verified. [12]

Arctostaphylos uva-ursi belongs to the plant family of *Ericaceae.* The plant is common in many parts of Europe and West Asia (Russia). The leaves are used against diseases in the urinary tract and the renal pelvis, especially against chronical urethritis and cystitis. Furthermore, the leaves are admixed in tea blends against bladder trouble, at gallstones and rheumatism. For technical purpose, the leaves are used in the leather and textile industry as tanning agent and dye. Arctostaphylos uva-ursi leaves contain high concentrations of arbutin (6 to 17%) and methylarbutin. Moreover, hydrochinon, hydrolyzable tannins (15-20%), up to 6% of gallic acid, ellagic acid, quinic acid, ursolic acid, isoquercitrin, quercitrin, myricitrin and its aglycones quercetin and myricetin, hyperin and essential oil. [12]

Both plants, *Fragaria* and *Arctostaphylos uva-ursi*, were extracted in a ratio of 1:10 with water (initial quercetin and tannin contents as well as dry matter see Table 23) and were afterwards hydrolyzed with HCl (strong acid), CH_3COOH (weak acid) and CO_2 (CO_2-intensified hydrolysis). For all experiments, the extracts were taken from the same extraction batch (see chapter 2.3.2.). It was assumed that all compounds in the extract were homogeneously dissolved.

Table 23: Initial extracts of Fragaria and Arctostaphylos uva-ursi

	Fragaria	*Arctostaphylos uva-ursi*
Quercetin concentration	1.5 ± 0.2 mg/L	1.7 ± 0.0 mg/L
Tannin content	6.3 ± 0.1%	12.8 ± 0.0%
Dry matter	2.9%	4.0%

Hydrolysis with HCl was performed at pH ~1 (0.2 mol/L) at 383.15 K and ambient pressure, hydrolysis with CH_3COOH was performed at pH 3 (0.1 mol/L) and CO_2-intensified hydrolysis was performed at pH 3, 413.15 K and 150 bar. All three hydrolysis reactions were conducted for eight hours. The hydrolysis with HCl was inspired by the conventional hydrolysis process to obtain quercetin, whereas the hydrolysis with CH_3COOH was performed at pH 3, comparable with CO_2-intensified hydrolysis (Table 24).

Table 24: Process conditions of HCL, CH_3COOH and CO_2-intensified hydrolysis of plant extracts

Hydrolysis	pH [-]	Temperature [K]	Pressure [bar]	Time [h]
Strong acid – HCl	1	383.15	Ambient pressure	8
Weak acid – CH_3COOH	3	383.15	Ambient pressure	8
CO_2-intensified hydrolysis	3	413.15	150	8

5.2.1 **Hydrolysis of plant extracts with HCl**
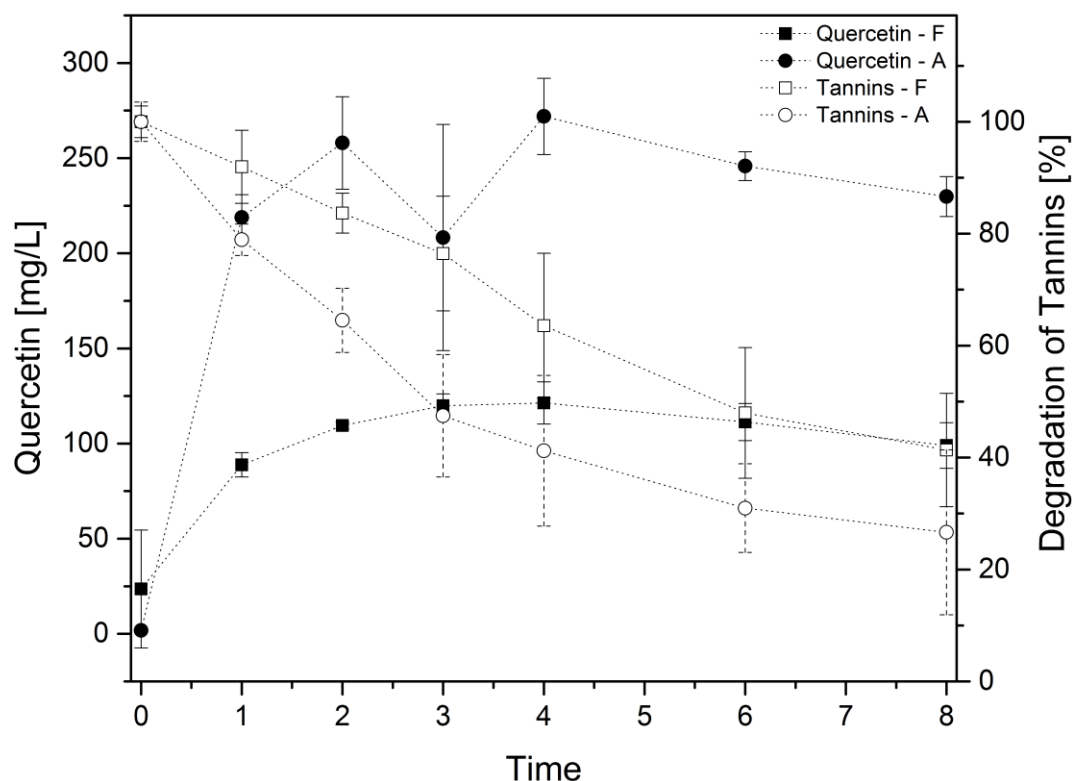
Figure 42: HCl hydrolysis of *Fragaria* (F) and *Arctostaphylos uva-ursi* (A) at 363.15 K and 0.2 mol/L HCl for 8 hours

Extracts of Fragaria and Arctostaphylos uva-ursi were hydrolyzed with 0.2 mol/L HCl and were analyzed on their quercetin and tannin content (Figure 42).

The quercetin concentration of Fragaria extract showed already a quercetin concentration of 24 mg/L at the beginning, after heating the extract up to 363.15 K and before adding 0.2 mol/L HCl to the extract, which probably is caused by thermal cleavage due to a temperature increase (from room temperature to 363.15 K). The quercetin concentration increased with increasing reaction time and after four hours a maximum of 121 mg/L was observed. With further increasing reaction time the

quercetin concentration started to decrease to 99 mg/L (after eight hours). This could be explained by degradation of quercetin caused by the low pH and the influence of temperature [29].

The tannin content at the beginning, after heating to 363.15 K and before adding 0.2 mol/L HCl, was higher than the initial tannin content at room temperature. Hydrolyzable tannins are not thermostable and start degrading by applying thermal energy. The tannin content at the beginning of the experiment at 363.15 K was normalized to 100% to investigate the degradation of tannins. After four hours (highest quercetin concentration), a tannin content of 63.6 ± 12.9% was observed. In general, after adding 0.2 mol/L HCl, the tannin content decreased constantly to 41.3 ± 10% after eight hours. Assuming that the dry matter of the extract did not change and is identical with the initial dry matter of the untreated extract, after four hours a dried *Fragaria* extract (maximum of quercetin concentration) with 15.7w% tannins and 0.42w% quercetin could be obtained.

The quercetin concentration of an extract *of Arctostaphylos uva-ursi* showed at the beginning, after heating to 363.15 K and before adding 0.2 mol/L HCl, a quercetin concentration of 1.3 mg/L. The quercetin concentration increased with increasing reaction time. After four hours, a maximum of 271.9 ± 20 mg/L was observed. With increasing reaction time, the quercetin started to decrease thereafter to 229.8 ± 10.5 mg/L (after eight hours).

In contrast to *Fragaria* extract, the tannin content of *Arctostaphylos uva-ursi* did not decrease while heating the extract to 363.15 K. However, the tannin content decreased faster when adding 0.2 mol/L HCl than for *Fragaria* extract. After four hours (maximum of quercetin concentration), the tannin content decreased to 41.2% ± 13.5% and decreased further to 26.6% ± 14.7% after eight hours. The faster decrease of the tannin

content in comparison to *Fragaria* extract is explained by the majority of hydrolyzable tannins in the *Arctostaphylos uva-ursi* extract, which are not stable against heat. Assuming that the dry matter of the extract did not change and is identical to the initial dry matter of the untreated extract, a dried extract of *Arctostaphylos uva-ursi* after two hours of 18.6% tannins and 0.65% quercetin could be obtained.

5.2.2 Hydrolysis of plant extracts with CH₃COOH
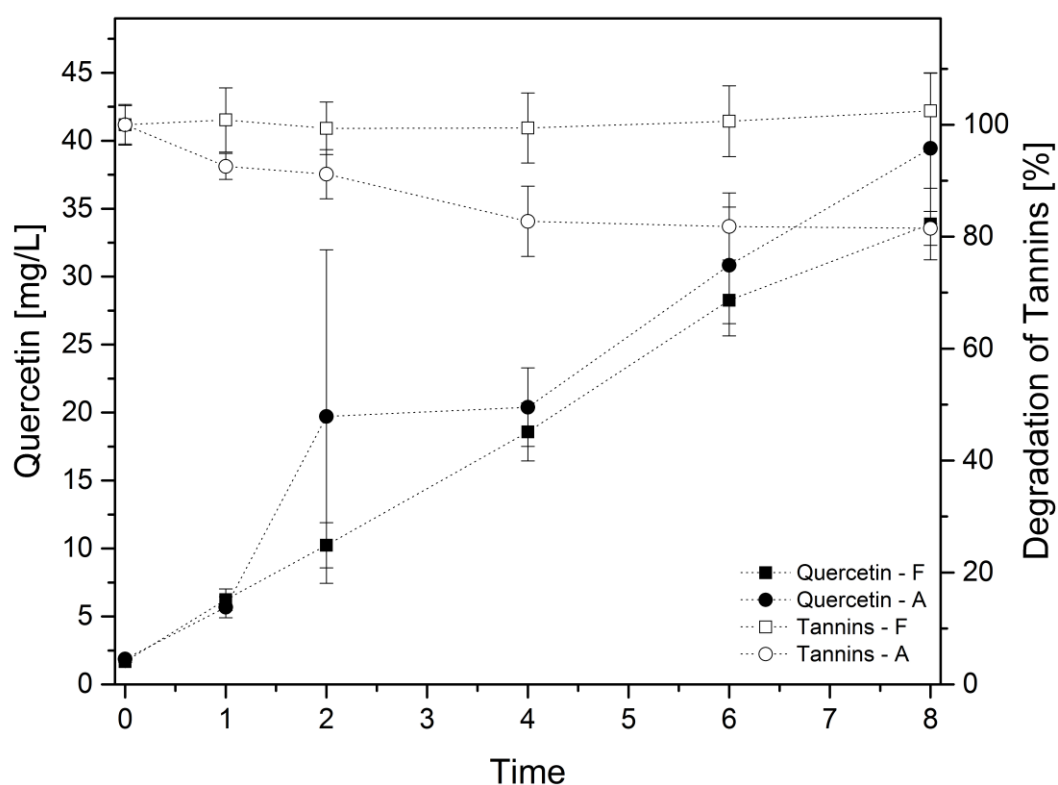
Figure 43: CH₃COOH hydrolysis of *Fragaria* (F) and *Arctostaphylos uva-ursi* (A) at 363.15 K and 0.1 mol/L CH₃COOH

Hydrolysis with weak acid (CH₃COOH) was inspired by the CO₂-intensified hydrolysis. With CO₂-intensified hydrolysis, a minimum pH value of 3 could be reached. Extracts

of *Fragaria* and *Arctostaphylos uva-ursi* were hydrolyzed with 0.1 mol/L CH_3COOH (pH 3) and were analyzed for their quercetin and tannin content (Figure 43).

The quercetin concentration of *Fragaria* extract, after heating the extract up to 363.15 K and before adding 0.1 mol/L CH_3COOH to the extract, had a quercetin concentration of 1.7 ± 0.1 mg/L. The quercetin concentration increased constantly with increasing reaction time. After eight hours a maximum of 33.9 ± 2.6 mg/L was detected. The tannin content of *Fragaria* increased during heating the extract to 363.15 K. However, the tannin content stayed constant when adding 0.1 mol/L CH_3COOH. After eight hours (maximum of quercetin concentration), the tannin content increased to $102.5 \pm 6.7\%$. This experiment shows that weak acid (CH_3COOH) at pH 3 is not strong enough to cleave condensed tannins and quercetin. Assuming that the dry matter of the extract did not change and is identical to the initial dry matter of the untreated extract, a dried extract of *Fragaria*, after eight hours, with 19.6w% tannins and 0.12w% quercetin could be obtained.

The quercetin concentration of *Arctostaphylos uva-ursi* extract after heating the extract to 363.15 K and before adding 0.1 mol/L CH_3COOH, had a quercetin concentration of 1.9 mg/L. The quercetin concentration increased constantly with increasing reaction time. After eight hours a maximum of 39.4 ± 5.5 mg/L was detected. The tannin content of *Arctostaphylos uva-ursi* increased during heating the extract to 363.15 K. When adding 0.1 mol/L CH_3COOH the tannin content started to decrease constantly. After eight hours (maximum of quercetin concentration), the tannin content decreased to $81.5 \pm 3.0\%$. In contrast to condensed tannins rich *Fragaria* extracts, hydrolyzable tannins of *Arctostaphylos uva-ursi* are not stable against acid hydrolysis. Assuming that the dry matter of the extract did not change and is identical to the initial dry matter

of the untreated extract, a dried extract of *Arctostaphylos uva-ursi*, after eight hours, with 25.9w% tannins and 0.1w% quercetin could be obtained.

5.2.3 CO_2-intensified hydrolysis of plant extracts
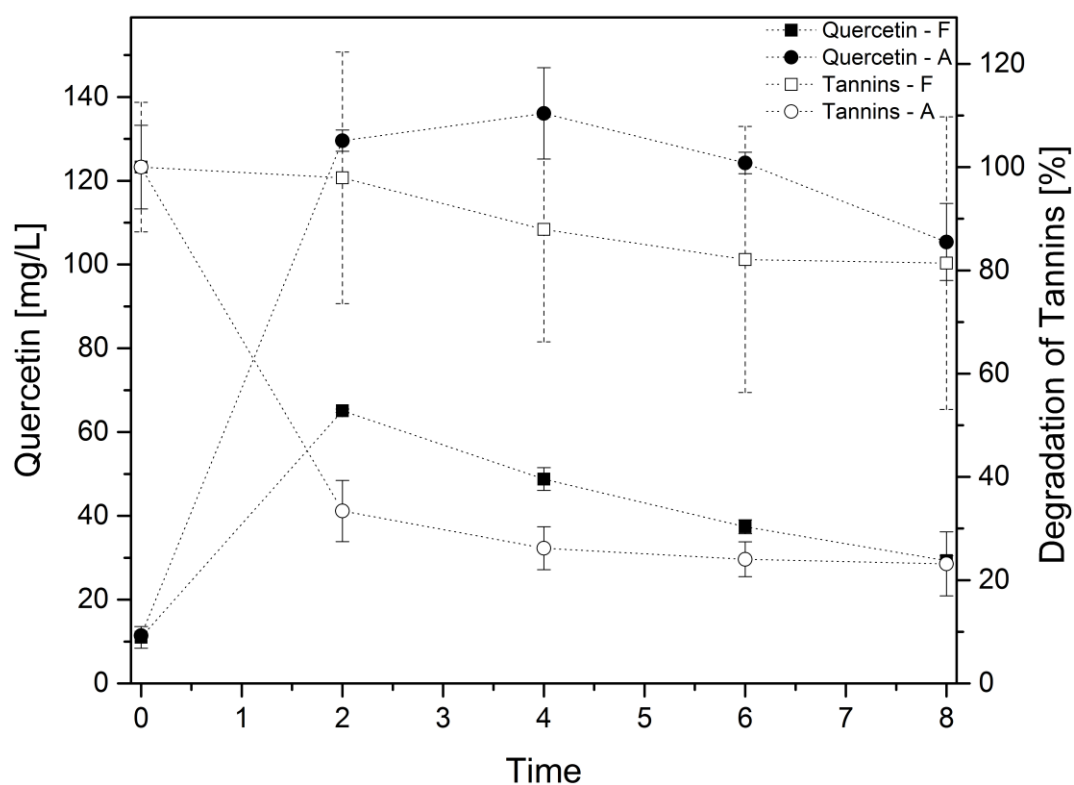
Figure 44: CO_2-intensified Hydrolysis of *Fragaria* (F) and *Arctostaphylos uva-ursi* (A) at 413.15 K and 150 bar up to eight hours

CO_2-intensified hydrolysis of *Fragaria* and *Arctostaphylos uva-ursi* extracts is based on the model experiments with rutin to obtain quercetin. With CO_2-intensified hydrolysis, a minimum pH value of 3 can be reached. Extracts of *Fragaria* and *Arctostaphylos uva-ursi* were hydrolyzed at 413.15 K and 150 bar CO_2-pressure

(optimum parameters of the pressure and temperature study, see chapter 4) and were analyzed on their quercetin and tannin content (Figure 44).

The quercetin concentration of *Fragaria* extract, after heating the extract to 413.15 K and before applying the pressure of 150 bar to the extract, had a quercetin concentration of 11.0 ± 2.6 mg/L. The quercetin concentration increased within the first two hours to its maximum of 65.1 ± 0.4 mg/L. After two hours of reaction time, the quercetin concentration decreased constantly to 29.3 ± 1.2 mg/L after eight hours. The tannin content of *Fragaria* increased to 102 ± 12.6% during heating the extract to 413.15 K. However, the tannin content started to decrease when applying 150 bar of CO_2-pressure. At the maximum quercetin concentration (two hours of reaction time) the tannin content decreased to 100 ± 24.4%. After eight hours, the tannin content decreased to 83.0 ± 28.3%. Assuming that the dry matter of the extract did not change and is identical to the initial dry matter of the untreated extract, a dried extract of *Fragaria*, after two hours, with 19.6w% tannins and 0.23w% quercetin could be obtained.

The quercetin concentration of *Arctostaphylos uva-ursi*, after heating the extract to 413.15 K and before applying 150 bar CO_2-pressure to the extract, had a quercetin concentration of 11.4 ± 0.3 mg/L. The quercetin concentration increased constantly with increasing reaction time. At four hours a maximum of 136.1 ± 10.9 mg/L was detected. After four hours the quercetin concentration started to decrease to 105.4 ± 9.2 mg/L (after eight hours) The tannin content of *Arctostaphylos uva-ursi* decreased to 82.0 ± 8.1% during heating the extract to 413.15 K. When applying 150 bar CO_2-pressure to the extract, the tannin content started to decrease rapidly. After four hours (maximum of quercetin concentration), the tannin content decreased to 21.5 ± 4.2%. After eight hours the tannin content decreased to 19.0 ± 6.2%. Assuming that the dry

matter of the extract did not change and is identical to the initial dry matter of the untreated extract, a dried extract of *Arctostaphylos uva-ursi*, after four hours, with 5.8w% tannins and 0.34w% quercetin could be obtained.

6 Conclusion and Outlook

Conventional acid hydrolysis is a major methodology for obtaining aglycones of secondary phytochemicals (e.g. quercetin, hespertin). This process needs additions of acid to initiate the hydrolysis step and salts for neutralization. Wastewaters with a high load of salts (depending on the used acids and neutralization salts) were produced and have to be removed in the wastewater treatment. The CO_2-intensified hydrolysis would overcome this issue and would have important benefits in comparison to conventional acid hydrolysis:

- no use of mineral acids (e.g. HCl, HNO_3, H_2SO_4)

- the hydrolyzed residual extracts can be used for further applications without purifications

- the neutralization step can be excluded due to reversible pH switches (dissolved amount of CO_2 decreases by releasing the pressure)

- released CO_2 can be recycled

- no separation of salts from the residual extract (e.g. Na_2SO_4, $NaNO_3$, $NaCl$)

- the product has no process induced impurities, e.g. salts or acid

The abandonment of mineral acids and salts for neutralization in the CO_2-intensified hydrolysis, in comparison to the conventional production process of quercetin, could result in a conservation of 1960 kg H_2SO_4, 1460 kg HCl or 2520 kg HNO_3 for a production of 1.000 kg of quercetin. Due to the abandonment of acids, a conservation of 2120 kg of Na_2CO_3 for the neutralization step could be reached. Further, this would result in wastewaters without a salt load and would thus, replace the salt separation step. In this work, it was shown that CO_2-intensified hydrolysis of rutin can be

performed at moderate temperatures and pressures. 100% cleavage of rutin and 100% formation of quercetin occurred already at 150 bar CO_2 pressure, which is considerably lower than pressures that are commonly used for the hydrolysis of secondary phytochemicals. The generated models for CO_2-intensified hydrolysis can be applied to estimate the rutin and quercetin yields between temperatures of 373.15 K and 433.15 K at 150 bar and pressures between 4 bar and 150 bar at 413.15 K. The »H^+-factor« can be used to describe the influence of CO_2 pressure on the CO_2-intensified hydrolysis process in more detail. Furthermore, with water as an extraction solvent, it was possible to extract both, tannins and flavonoid glycosides. Although alcoholic aqueous solvents would be a better extraction solvent than water, the CO_2- intensified hydrolysis of glycosides works only with 100% water and therefore no solvent recovery has to be considered. Additions of a few percent of alcohol (methanol, ethanol, etc.) would hinder the hydrolysis reaction and yield lower concentrations of quercetin. By applying CO_2-intensified hydrolysis on two plant extracts (identified out of the performed screening of EMHSP: *Arctostaphylos uva-ursi* and *Fragaria*), it was shown that this process could be applied for a combined production of flavonoids and condensed tannins. Condensed tannins usually do not hydrolyze to their aglycones, as they are bound via a C-C bonding. However, condensed tannins tend to form insoluble complexes due to the influence of the acidic pH value, the so-called phlobaphenes [174]. Tanners also call them "tanners red" and this complex is responsible for the mud, which precipitates during the tanning process with commercial tanning agents made of condensed tannins. It was shown that with CO_2-intensified hydrolysis no degradation of condensed tannins in plant extracts after two hours was observed in comparison to conventional acid hydrolysis.

In the future, the optimization of the extraction process and improved herb quality could lead to higher yields of secondary phytochemicals in the EMHSP-extracts. Calibration

of the RDM-assay with condensed tannin standard/s (standard/s are not commercially available) may lead to higher TCs of extracts, which contain condensed tannins. Isolated phytochemicals or extracts of promising EMHSP could show a higher added value in other applications. Further investigations should be performed on the chemical composition and mechanisms of actions for a better evaluation of the application in food, drugs or adhesives. Extraction of EMHSP phytochemicals could be implemented in bio-refinery-concepts as phytochemicals can be extracted from vegetable waste streams (e.g. skin of onions, citrus fruits, weed of strawberries…). For optimization of the models, the formation of byproducts and degradation products should be considered and included in one global model. The principle of this CO_2-intensified hydrolysis process could also be applied in bio-refinery-concepts and could replace conventional acid hydrolysis processes for obtaining secondary phytochemicals in respect of reducing process-induced waste streams.

7 References

[1] Lillo, C., Lea, U. S., and Ruoff, P. 2008. Nutrient depletion as a key factor for manipulating gene expression and product formation in different branches of the flavonoid pathway. *Plant, cell & environment* 31, 5, 587–601.

[2] Boyer, J. and Liu, R. H. Apple phytochemicals and their health benefits. *BioMed central*.

[3] Sudha, M. L., Baskaran, V., and Leelavathi, K. 2007. Apple pomace as a source of dietary fiber and polyphenols and its effect on the rheological characteristics and cake making. *Food Chemistry* 104, 2, 686–692.

[4] Diñeiro García, Y., Valles, B. S., and Picinelli Lobo, A. 2009. Phenolic and antioxidant composition of by-products from the cider industry. Apple pomace. *Food Chemistry* 117, 4, 731–738.

[5] YAO, L. H., Jiang, Y. M., SHI, J., Tomas-Barberan, F. A., DATTA, N., SINGANUSONG, R., and CHEN, S. S. 2004. Flavonoids in Food and Their Health Benefits. *Plant Foods Hum Nutr* 59, 3, 113–122.

[6] Palombo, E. A. 2006. Phytochemicals from traditional medicinal plants used in the treatment of diarrhoea. Modes of action and effects on intestinal function. *Phytotherapy research : PTR* 20, 9, 717–724.

[7] Garcia-Lafuente, A., Guillamon, E., Villares, A., Rostagno, M. A., and Martinez, J. A. 2009. Flavonoids as anti-inflammatory agents. Implications in cancer and cardiovascular disease. *Inflammation research : official journal of the European Histamine Research Society … [et al.]* 58, 9, 537–552.

[8] Ajazuddin, Alexander, A., Qureshi, A., Kumari, L., Vaishnav, P., Sharma, M., Saraf, S., and Saraf, S. 2014. Role of herbal bioactives as a potential bioavailability enhancer for Active Pharmaceutical Ingredients. *Fitoterapia* 97, 1–14.

[9] Chuarienthong, P., Lourith, N., and Leelapornpisid, P. 2010. Clinical efficacy comparison of anti-wrinkle cosmetics containing herbal flavonoids. *International journal of cosmetic science* 32, 2, 99–106.

[10] Arct, J. and Pytkowska, K. 2008. Flavonoids as components of biologically active cosmeceuticals. *Clinics in Dermatology* 26, 4, 347–357.

[11] Andersen, Ø. M. and Markham, K. R., Eds. 2006. *Flavonoids. Chemistry, biochemistry, and applications*. CRC, Taylor & Francis, Boca Raton, FL.

[12] Hoppe, H. A., Ed. 1975. *Drogenkunde. Angiospermen* 1. de Gruyter.

[13] Maier, M., Oelbermann, A.-L., Renner, M., and Weidner, E. 2017. Screening of European medicinal herbs on their tannin content—New potential tanning agents for the leather industry. *Industrial Crops and Products* 99, 19–26.

[14] Belitz, H.-D., Grosch, W., and Schieberle, P., Eds. 2008. *Lehrbuch der Lebensmittelchemie. Mit 634 Tabellen*. Springer-Lehrbuch. Springer, Berlin, Heidelberg.

[15] Lai, H. M. and Lin, T.-C. 2006. Bakery Products. In *Handbook of food science, technology, and engineering. Volume 4*, Y. H. Hui, Ed. Food science and technology 149. CRC/Taylor & Francis, Boca Raton [u.a.], 148-1 - 148-48.

[16] Bustos, G., Ramirez, J. A., Garrote, G., and Vazquez, M. 2003. Modeling of the Hydrolysis of Sugar Cane Bagasse with Hydrochloric Acid. *ABAB* 104, 1, 51–68.

[17] Aguilar, R., Ramírez, J.A., Garrote, G., and Vázquez, M. 2002. Kinetic study of the acid hydrolysis of sugar cane bagasse. *Journal of Food Engineering* 55, 4, 309–318.

[18] Rodríguez-Chong, A., Alberto Ramírez, J., Garrote, G., and Vázquez, M. 2004. Hydrolysis of sugar cane bagasse using nitric acid. A kinetic assessment. *Journal of Food Engineering* 61, 2, 143–152.

[19] Gámez, S., González-Cabriales, J. J., Ramírez, J. A., Garrote, G., and Vázquez, M. 2006. Study of the hydrolysis of sugar cane bagasse using phosphoric acid. *Journal of Food Engineering* 74, 1, 78–88.

[20] van der Maarel, Marc J.E.C, van der Veen, B., Uitdehaag, J. C.M., Leemhuis, H., and Dijkhuizen, L. 2002. Properties and applications of starch-converting enzymes of the α-amylase family. *Journal of biotechnology* 94, 2, 137–155.

[21] Adel, A. M., Abd El-Wahab, Z. H., Ibrahim, A. A., and Al-Shemy, M. T. 2010. Characterization of microcrystalline cellulose prepared from lignocellulosic materials. Part I. Acid catalyzed hydrolysis. *Bioresource Technology* 101, 12, 4446–4455.

[22] Girisuta, B., Janssen, L. P. B. M., and Heeres, H. J. 2007. Kinetic Study on the Acid-Catalyzed Hydrolysis of Cellulose to Levulinic Acid. *Ind. Eng. Chem. Res.* 46, 6, 1696–1708.

[23] Karimi, K., Kheradmandinia, S., and Taherzadeh, M. J. 2006. Conversion of rice straw to sugars by dilute-acid hydrolysis. *Biomass and Bioenergy* 30, 3, 247–253.

[24] Lavarack, B. P., Griffin, G. J., and Rodman, D. 2002. The acid hydrolysis of sugarcane bagasse hemicellulose to produce xylose, arabinose, glucose and other products. *Biomass and Bioenergy* 23, 5, 367–380.

[25] Bobleter, O. 1994. Hydrothermal degradation of polymers derived from plants. *Progress in Polymer Science* 19, 5, 797–841.

[26] Wahyudiono, Kanetake, T., SASAKI, M., and GOTO, M. 2007. Decomposition of a Lignin Model Compound under Hydrothermal Conditions. *Chem. Eng. Technol.* 30, 8, 1113–1122.

[27] Bühler, W., Dinjus, E., Ederer, H. J., Kruse, A., and Mas, C. 2002. Ionic reactions and pyrolysis of glycerol as competing reaction pathways in near- and supercritical water. *The Journal of Supercritical Fluids* 22, 1, 37–53.

[28] Qadariyah, L., Mahfud, Sumarno, Machmudah, S., Wahyudiono, Sasaki, M., and Goto, M. 2011. Degradation of glycerol using hydrothermal process. *Bioresource Technology* 102, 19, 9267–9271.

[29] Ravber, M., Knez, Ž., and Škerget, M. 2015. Optimization of hydrolysis of rutin in subcritical water using response surface methodology. *The Journal of Supercritical Fluids* 104, 145–152.

[30] Ruen-ngam, D., Quitain, A. T., Sasaki, M., and Goto, M. 2012. Hydrothermal Hydrolysis of Hesperidin Into More Valuable Compounds Under Supercritical Carbon Dioxide Condition. *Ind. Eng. Chem. Res.* 51, 42, 13545–13551.

[31] Ruen-ngam, D., Quitain, A. T., Tanaka, M., Sasaki, M., and Goto, M. 2012. Reaction kinetics of hydrothermal hydrolysis of hesperidin into more valuable compounds under supercritical carbon dioxide conditions. *The Journal of Supercritical Fluids* 66, 215–220.

[32] Magalhães da Silva, S. P., Morais, A. R. C., and Bogel-Łukasik, R. 2014. The CO 2 -assisted autohydrolysis of wheat straw. *Green Chem* 16, 1, 238–246.

[33] Morais, A. R. C., Mata, A. C., and Bogel-Lukasik, R. 2014. Integrated conversion of agroindustrial residue with high pressure CO 2 within the biorefinery concept. *Green Chem.* 16, 9, 4312.

[34] Morais, A. R. C., Matuchaki, M. D. D. J., Andreaus, J., and Bogel-Lukasik, R. 2016. A green and efficient approach to selective conversion of xylose and biomass hemicellulose into furfural in aqueous media using high-pressure CO 2 as a sustainable catalyst. *Green Chem* 18, 10, 2985–2994.

[35] Toscan, A., Morais, A. R. C., Paixao, S. M., Alves, L., Andreaus, J., Camassola, M., Dillon, A. J. P., and Lukasik, R. M. 2017. High-pressure carbon dioxide/water pre-treatment of sugarcane bagasse and elephant grass. Assessment of the effect

of biomass composition on process efficiency. *Bioresource Technology* 224, 639–647.

[36] Kew - Royal Botanic Gardens. *State of the Worlds's Plants 2017*.

[37] Adam, L. and Hoppe, B., Eds. 2009. *Grundlagen des Arznei- und Gewürzpflanzenbaus I*. Handbuch des Arznei- und Gewürzpflanzenbaus / Autoren Rolf Fritzsche … ; 1. Selbstverl. d. Vereins für Arznei- und Gewürzpflanzen SALUPLANTA, Bernburg.

[38] Bundesamt, S. Bodennutzung der Betriebe (Landwirtschaftlich genutzte Flächen) - Fachserie 3 Reihe 3.1.2 - 2016.

[39] Bernd Hoppe. Abschlussbericht. Studie zum Stand des Anbaus von Arznei- und Gewürzpflanzen in Deutschland (2003) und Abschätzung der Entwicklungstrends in den Folgejahren 2005.

[40] Makkar, H. P. S., Siddhuraju, P., and Becker, K., Eds. 2007. *Plant secondary metabolites*. Methods in molecular biology 393. Humana Press, Totowa, N.J.

[41] Thieme RÖMPP. *Sekundärmetabolite*. https://roempp.thieme.de/roempp4.0/do/data/RD-19-01743.

[42] Dräger, B. and Stinzting, F. C. 2011. *Flavonoide*. https://roempp.thieme.de/roempp4.0/do/data/RD-06-01067. Accessed 28 December 2016 11:58Uhr.

[43] Rice-evans, C. A., Miller, N. J., Bolwell, P. G., Bramley, P. M., and Pridham, J. B. 2009. The Relative Antioxidant Activities of Plant-Derived Polyphenolic Flavonoids. *Free Radical Research* 22, 4, 375–383.

[44] Torel, J., Cillard, J., and Cillard, P. 1986. Antioxidant activity of flavonoids and reactivity with peroxy radical. *Phytochemistry* 25, 2, 383–385.

[45] Cushnie, T. P. T. and Lamb, A. J. 2011. Recent advances in understanding the antibacterial properties of flavonoids. *International journal of antimicrobial agents* 38, 2, 99–107.

[46] Cushnie, T. T. and Lamb, A. J. 2005. Antimicrobial activity of flavonoids. *International journal of antimicrobial agents* 26, 5, 343–356.

[47] Weidenbörner, M., Hindorf, H., Jha, H. C., and Tsotsonos, P. 1990. Antifungal activity of flavonoids against storage fungi of the genus Aspergillus. *Phytochemistry* 29, 4, 1103–1105.

[48] Orhan, D. D., Ozcelik, B., Ozgen, S., and Ergun, F. 2010. Antibacterial, antifungal, and antiviral activities of some flavonoids. *Microbiological Research* 165, 6, 496–504.

[49] Kaul, T. N., Middleton, E., and Ogra, P. L. 1985. Antiviral effect of flavonoids on human viruses. *J. Med. Virol.* 15, 1, 71–79.

[50] Sánchez, I., Gómez-Garibay, F., Taboada, J., and Ruiz, B. H. 2000. Antiviral effect of flavonoids on the Dengue virus. *Phytother. Res.* 14, 2, 89–92.

[51] Hertog, M. G. L., Hollman, P. C. H., and Katan, M. B. 1992. Content of potentially anticarcinogenic flavonoids of 28 vegetables and 9 fruits commonly consumed in the Netherlands. *J. Agric. Food Chem.* 40, 12, 2379–2383.

[52] Seelinger, G., Merfort, I., Wolfle, U., and Schempp, C. M. 2008. Anti-carcinogenic effects of the flavonoid luteolin. *Molecules (Basel, Switzerland)* 13, 10, 2628–2651.

[53] Galluzzo, P., Martini, C., Bulzomi, P., Leone, S., Bolli, A., Pallottini, V., and Marino, M. 2009. Quercetin-induced apoptotic cascade in cancer cells: antioxidant versus estrogen receptor alpha-dependent mechanisms. *Molecular Nutrition & Food Research* 53, 6, 699–708.

[54] Askari, G., Ghiasvand, R., Feizi, A., Ghanadian, S. M., and Karimian, J. 2012. The effect of quercetin supplementation on selected markers of inflammation and oxidative stress. *Journal of Research in Medical Sciences : The Official Journal of Isfahan University of Medical Sciences* 17, 7, 637–641.

[55] de Boer, Vincent C J, Dihal, A. A., van der Woude, H., Arts, I. C. W., Wolffram, S., Alink, G. M., Rietjens, Ivonne M C M, Keijer, J., and Hollman, P. C. H. 2005. Tissue distribution of quercetin in rats and pigs. *The Journal of nutrition* 135, 7, 1718–1725.

[56] Ishizawa, K., Izawa-Ishizawa, Y., Ohnishi, S., Motobayashi, Y., Kawazoe, K., Hamano, S., Tsuchiya, K., Tomita, S., Minakuchi, K., and Tamaki, T. 2009. Quercetin Glucuronide Inhibits Cell Migration and Proliferation by Platelet-Derived Growth Factor in Vascular Smooth Muscle Cells. *J Pharmacol Sci* 109, 2, 257–264.

[57] Edwards, R. L., Lyon, T., Litwin, S. E., Rabovsky, A., Symons, J. D., and Jalili, T. 2007. Quercetin reduces blood pressure in hypertensive subjects. *Journal of Nutrition* 137, 11, 2405–2411.

[58] Quideau, S., Deffieux, D., Douat-Casassus, C., and Pouysegu, L. 2011. Plant polyphenols: chemical properties, biological activities, and synthesis. *Angewandte Chemie (International ed. in English)* 50, 3, 586–621.

[59] Ferreira, D., Slade, D., and Marais, J. P. J. 2006. Flavans and Proanthocyanidins. In *Flavonoids. Chemistry, biochemistry, and applications*, Ø. M. Andersen and K. R. Markham, Eds. CRC, Taylor & Francis, Boca Raton, FL, S. 553 – 616.

[60] Yoshida, A., Yoshino, F., Tsubata, M., Ikeguchi, M., Nakamura, T., and Lee, M.-C.-I. 2011. Direct assessment by electron spin resonance spectroscopy of the antioxidant effects of French maritime pine bark extract in the maxillofacial region of hairless mice.

[61] Haslam, E. and Cai, Y. 1994. Plant polyphenols (vegetable tannins). Gallic acid metabolism. *Nat. Prod. Rep.* 11, 41.

[62] Ma, H., Liu, W., Frost, L., Wang, L., Kong, L., Dain, J. A., and Seeram, N. P. 2015. The hydrolyzable gallotannin, penta-O-galloyl-β-D-glucopyranoside, inhibits the

formation of advanced glycation endproducts by protecting protein structure. *Molecular bioSystems* 11, 5, 1338–1347.

[63] Wang, Y., Xu, Z., Bach, S. J., and McAllister, T. A. 2008. Effects of phlorotannins from Ascophyllum nodosum (brown seaweed) on in vitro ruminal digestion of mixed forage or barley grain. *Animal Feed Science and Technology* 145, 1-4, 375–395.

[64] Bate-Smith, E. C. and Swain, T. 1962. Flavonoid compounds. *Comparative biochemistry* 3, 705–809.

[65] Harborne, J. B. and Dye, P. M., Eds. 1989. *Methods in Plant Biochemistry. Volume 1 Plant Phenolics.* Academic Press Limited.

[66] Lawrence J. Porter. 1989. 11 Tannins. In *Methods in Plant Biochemistry. Volume 1 Plant Phenolics*, J. B. Harborne and P. M. Dye, Eds. Academic Press Limited, 389–418.

[67] Pizzi, A. 2008. Tannins: Major Sources, Properties and Applications. In *Monomers, Polymers and Composites from Renewable Resources*, Mohamed Naceur Belgacem and Alessandro Gandini, Ed. Elsevier, 179–199.

[68] Ballerini, A., Despres, A., and Pizzi, A. 2005. Non-toxic, zero emission tannin-glyoxal adhesives for wood panels. *Holz Roh Werkst* 63, 6, 477–478.

[69] Pizzi, A. 2007. Tannin-Based Adhesives. *Journal of Macromolecular Science, Part C* 18, 2, 247–315.

[70] Roffael, E., Dix, B., and Okum, J. 2000. Use of spruce tannin as a binder in particleboards and medium density fiberboards (MDF). *Holz als Roh- und Werkstoff* 58, 5, 301–305.

[71] Kim, S. 2009. Environment-friendly adhesives for surface bonding of wood-based flooring using natural tannin to reduce formaldehyde and TVOC emission. *Bioresource Technology* 100, 2, 744–748.

[72] Aires, A., Carvalho, R., and Saavedra, M. J. 2016. Valorization of solid wastes from chestnut industry processing: Extraction and optimization of polyphenols, tannins and ellagitannins and its potential for adhesives, cosmetic and pharmaceutical industry. *Waste management (New York, N.Y.)* 48, 457–464.

[73] Kaspar, H. R. E. and Pizzi, A. 1996. Industrial plasticizing/dispersion aids for cement based on polyflavonoid tannins. *J. Appl. Polym. Sci.* 59, 7, 1181–1190.

[74] Sanchez-Martin, J., Beltran-Heredia, J., and Solera-Hernandez, C. 2010. Surface water and wastewater treatment using a new tannin-based coagulant. Pilot plant trials. *Journal of environmental management* 91, 10, 2051–2058.

[75] Beltrán-Heredia, J. and Sánchez-Martín, J. 2009. Municipal wastewater treatment by modified tannin flocculant agent. *Desalination* 249, 1, 353–358.

[76] Beltrán-Heredia, J., Sánchez-Martín, J., and Gómez-Muñoz, M. C. 2010. New coagulant agents from tannin extracts. Preliminary optimisation studies. *Chemical Engineering Journal* 162, 3, 1019–1025.

[77] Kolodziej, H., Kayser, O., Latte, K. P., and Kiderlen, A. F. 2000. ENHANCEMENT OF ANTIMICROBIAL ACTIVITY OF TANNINS AND RELATED COMPOUNDS BY IMMUNE MODULATORY EFFECTS. In *Plant Polyphenols 2: Chemistry, Biology, Pharmacology*, Herbert L. Hergert (auth.), Georg G. Gross, Richard W. Hemingway, Takashi Yoshida and Susan J. Branham (eds.), Eds., 575–594.

[78] Hagerman, A. E., Riedl, K. M., and Rice Robyn E. 2000. TANNINS AS BIOLOGICAL ANTIOXIDANTS. In *Plant Polyphenols 2: Chemistry, Biology, Pharmacology*, Herbert L. Hergert (auth.), Georg G. Gross, Richard W. Hemingway, Takashi Yoshida and Susan J. Branham (eds.), Eds., 495–505.

[79] Mitsunaga, T. 2000. ANTI-CARIES ACTIVITY OF BARK PROANTHOCYANIDINS. In *Plant Polyphenols 2: Chemistry, Biology,*

Pharmacology, Herbert L. Hergert (auth.), Georg G. Gross, Richard W. Hemingway, Takashi Yoshida and Susan J. Branham (eds.), Eds., 555–573.

[80] Sakagamia, H., Satoh, K., Ida, Y., Koyama, N., Premanathan, M., Arakaki, R., Nakashima, H., Hatano, T., Okuda, T., and Yoshida, T. 2000. INDUCTION OF APOPTOSIS AND ANTI-HIV ACTIVITY BY TANNIN- AND LIGNIN-RELATED SUBSTANCES. In *Plant Polyphenols 2: Chemistry, Biology, Pharmacology*, Herbert L. Hergert (auth.), Georg G. Gross, Richard W. Hemingway, Takashi Yoshida and Susan J. Branham (eds.), Eds., 595–611.

[81] Yang, L.-L., Wang, C.-C., Yen, K.-Y., Yoshida, T., Ratano, T., and Okuda, T. 2000. ANTITUMOR ACTIVITIES OF ELLAGITANNINS ON TUMOR CELL LINES. In *Plant Polyphenols 2: Chemistry, Biology, Pharmacology*, Herbert L. Hergert (auth.), Georg G. Gross, Richard W. Hemingway, Takashi Yoshida and Susan J. Branham (eds.), Eds., 615–628.

[82] Krenn, L., Steitz, M., Schlicht, C., Kurth, H., and Gaedcke, F. 2007. Anthocyanin- and proanthocyanidin-rich extracts of berries in food supplements – analysis with problems. *Pharmazie,* 62, 803–812.

[83] Martin, K. R. and Appel, C. L. 2010. Polyphenols as dietary supplements: A double-edged sword. *Nutrition and Dietary Supplements,* 2, 1–12.

[84] Scalbert, A. 1992. Quantitative Methods for the Estimation of Tannins in Plant tissue. In *Plant Polyphenols. Synthesis, Properties, Significance*, R. W. Hemingway and P. E. Laks, Eds. 1992, 259–280.

[85] Budini, R., Tonelli, D., and Girotti, S. 1980. Analysis of total phenols using the Prussian Blue method. *J. Agric. Food Chem.* 28, 6, 1236–1238.

[86] Broadhurst, R. B. and Jones, W. T. 1978. Analysis of condensed tannins using acidified vanillin. *J. Sci. Food Agric.* 29, 9, 788–794.

[87] Pizzi, A. 2008. Tannins: Major Sources, Properties and Applications. In *Monomers, polymers and composites from renewable resources*, M. N. Belgacem and A. Gandini, Eds. Elsevier, Amsterdam, Boston, 179–199.

[88] Kern, W., Ed. 1958. *Hagers Handbuch der Pharmazeutischen Praxis. Zweiter Ergänzungsband I Allgemeiner Teil Spezieller Teil A - H.* Springer Berlin Heidelberg, Berlin, Heidelberg.

[89] Hagerman, A. E. and Butler, L. G. 1978. Protein precipitation method for the quantitative determination of tannins. *J. Agric. Food Chem.* 26, 4, 809–812.

[90] Hagerman, A. E. 1987. Radial diffusion method for determining tannin in plant extracts. *Journal of Chemical Ecology* 13, 3, 437–449.

[91] Lucci, N. and Mazzafera, P. 2009. Distribution of rutin in fava d'anta (Dimorphandra mollis) seedlings under stress. *Journal of Plant Interactions* 4, 3, 203–208.

[92] Diping, Z., Xinfang, J., and Genggui, L. 2010. *Process for separating and extracting 98% quercetin from aboveground part of pubescent holly root,* CN101985439 B. Accessed 5 April 2017.

[93] Zhao, Z. 2011. *Quercetin production technology,* CN104387357 A. Accessed 5 April 2017.

[94] Jing, H., Zhao, H., and Shaojing, L. 2012. *Method for extracting quercetin from eucommia leaves,* CN102659740 B. Accessed 5 April 2017.

[95] Xu, D. 2014. *The use of rutin and quercetin rhamnose preparation method,* CN103965153 B. Accessed 4 April 2017.

[96] Szejtli, J. 1976. *Säurehydrolyse glykosidischer Bindungen. Einfluß von Struktur und Reaktionsbedingungen auf die Säurespaltung von Glykosiden, Disacchariden, Oligo- und Polysacchariden.* Akadémiai Kiadó, Budapest.

[97] Armour, C., Bunton, C. A., Patai, S., Selman, L. H., and Vernon, C. A. 1961. Mechanisms of Reactions in the Sugar Series. Part III. The Acid-catalysed Hydrolysis of t - Butyl beta-D - Glucopyranoside and Other Glycosides. *J. Chem. Soc.,* 73, 412–416.

[98] Banks, B. E. C., Meinwald, Y., Rhind-Tutt, A. J., Sheft, I., and Vernon, C. A. Mechanism of Reactions in the Sugar Series. Part IV. The Structure of the Carbonium Ions fromed in the Acid-catalysed Solvolysis of Glucopyranosides. *J. Chem. Soc.* 1961, 3240–3246.

[99] Bunton, C. A., Lewis, T. A., Llewellyn, D. R., and Vernon, C. A. 1955. Mechanisms of reactions in the sugar series. Part I. The acid-catalysed hydrolysis of α- and β-methyl and α- and β-phenyl D -glucopyranosides. *J. Chem. Soc.*, 4419–4423.

[100] Rhind-Tutt, A. J. and Vernon, C. A. 1960. 896. Mechanisms of reactions in the sugar series. Part II. Nucleophilic substitution in 2,3,4,6-tetra-O-methylglycopyranosyl chlorides. *J. Chem. Soc.*, 4637–4644.

[101] Overend, W. G., Rees, C. W., and Sequeira, J. S. 1962. 675. Reactions at position 1 of carbohydrates. Part III. The acid-catalysed hydrolysis of glycosides. *J. Chem. Soc.*, 3429.

[102] Szejtli, J. Allgemeine Gesetzmäßigkeiten der Hydrolyse glykosidischer Bindungen. *Die Stärke* 1967, Nr.5 / 19.Jahrg., 145–152.

[103] Hartler, N. and Hyllengren, K. 1962. Heterogeneous hydrolysis of cellulose with high polymer acids. Part 3. The acid hydrolysis of cellulose with finely divided cation-exchange resin in the hydrogen form. *J. Polym. Sci.* 56, 164, 425–434.

[104] Rolfe, G. W. and Defren, G. 1896. AN ANALYTICAL INVESTIGATION OF THE HYDROLYSIS OF STARCH BY ACIDS. *J. Am. Chem. Soc.* 18, 10, 869–900.

[105]   Rogalinski, T., Liu, K., Albrecht, T., and Brunner, G. 2008. Hydrolysis kinetics of biopolymers in subcritical water. *The Journal of Supercritical Fluids* 46, 3, 335–341.

[106]   Ravber, M., Pečar, D., Goršek, A., Iskra, J., Knez, Ž., and Škerget, M. 2016. Hydrothermal Degradation of Rutin. Identification of Degradation Products and Kinetics Study. *J. Agric. Food Chem.* 64, 48, 9196–9202.

[107]   Laidler, K. J. and Landskroener, P. A. 1956. The influence of the solvent on reaction rates. *Trans. Faraday Soc.* 52, 200.

[108]   Korol'Kov, I. I., Sarkov, V. I., and Levanova, V. P. 1956. *Sammelbd. Arb. Allunions-Forschungsinst. Hydrolyse- u. Sulfit-Spiritusind.*

[109]   A. R. Osborn and E. Whalley. PRESSURE EFFECT AND MECHANISM IN ACID CATALYSIS: VII. HYDROLYSIS OF METHYL, ETHYL, AND t-BUTYL ACETATES.

[110]   Meyer, A. H. and Hartmann-Schreier, J. 2010. *Enzyme.* https://roempp.thieme.de/roempp4.0/do/data/RD-05-01304. Accessed 26 December 2016 12:49Uhr.

[111]   Heightman, T. D. and Vasella, A. T. 1999. Neue Erkenntnisse über Hemmung, Struktur und Mechnismus konfigurationserhaltender Glycosdiasen. *Angew. Chem.,* 111, 794–815.

[112]   Sheldon, R. A. 2007. Enzyme Immobilization. The Quest for Optimum Performance. *Adv. Synth. Catal.* 349, 8-9, 1289–1307.

[113]   Fan, R., Li, N., Xu, H., Xiang, J., Wang, L., and Gao, Y. 2016. The mechanism of hydrothermal hydrolysis for glycyrrhizic acid into glycyrrhetinic acid and glycyrrhetinic acid 3-O-mono-beta-D-glucuronide in subcritical water. *Food Chemistry* 190, 912–921.

[114] Capuano, E. and Fogliano, V. 2011. Acrylamide and 5-hydroxymethylfurfural (HMF). A review on metabolism, toxicity, occurrence in food and mitigation strategies. *LWT - Food Science and Technology* 44, 4, 793–810.

[115] Carroll J. J., Slupsky J. D., and Mather A.E. 1991. The Solubility of Carbon Dioxide in Water at Low Pressures. *J. Phys. Chem. Ref. Data,* Vol. 20; No. 6, 1201–1209.

[116] Portier, S. and Rochelle, C. 2005. Modelling CO2 solubility in pure water and NaCl-type waters from 0 to 300 °C and from 1 to 300 bar. *Chemical Geology* 217, 3-4, 187–199.

[117] Wiebe, R. and Gaddy, V. L. 1940. The Solubility of Carbon Dioxide in Water at Various Temperatures from 12 to 40° and at Pressures to 500 Atmospheres. Critical Phenomena *. *J. Am. Chem. Soc.* 62, 4, 815–817.

[118] Coan C. R. and King A. D. 1971. Solubility of Water in Compressed Carbon Dioxide, Nitrous Oxide and Ethane. Evidence for Hydration of Carbon Dioxide and Nitrous Oxide in the Gas Phase. *Journal of the American Chemical Society*.

[119] Duan, Z. and Sun, R. 2003. An improved model calculating CO2 solubility in pure water and aqueous NaCl solutions from 273 to 533 K and from 0 to 2000 bar. *Chemical Geology* 193, 3-4, 257–271.

[120] Morrison, T. J. and Billett, F. 1952. 730. The salting-out of non-electrolytes. Part II. The effect of variation in non-electrolyte. *J. Chem. Soc.*, 3819–3822.

[121] Tödheide, K. and Franck, E. U. 1963. Das Zweiphasengebiet und die kritische Kurve im System Kohlendioxid–Wasser bis zu Drucken von 3500 bar. *Zeitschrift für Physikalische Chemie* 37, 5_6, 387–401.

[122] Takenouchi, S. and Kennedy, G. C. 1964. The binary system H2O-CO2 at high temperatures and pressures. *American Journal of Science* 262, 9, 1055–1074.

[123] Zawisza, A. and Malesinska, B. 1981. Solubility of carbon dioxide in liquid water and of water in gaseous carbon dioxide in the range 0.2-5 MPa and at temperatures up to 473 K. *J. Chem. Eng. Data* 26, 4, 388–391.

[124] King, M. B., Mubarak, A., Kim, J. D., and Bott, T. R. 1992. The mutual solubilities of water with supercritical and liquid carbon dioxides. *The Journal of Supercritical Fluids* 5, 4, 296–302.

[125] Wilhelm, S. 2008. Kapitel 8: Wasserchemische Berechnungen. In *Wasseraufbereitung. Chemie und chemische Verfahrenstechnik*, S. Wilhelm, Ed. VDI. Springer, Berlin, Heidelberg, 79–108.

[126] Manahan, S. E., Ed. 2000. *Environmental chemistry*. Lewis Publishers, Boca Raton, FL.

[127] Hobiger, G. 2015. *Kohlendioxid in Wasser mit Alkalinität. Berechnung und grafische Darstellung der chemischen Gleichgewichte*. SpringerLink : Bücher. Springer Spektrum, Berlin [u.a.].

[128] Lee, K. and Millero, F. J. 1995. Thermodynamic studies of the carbonate system in seawater. *Deep Sea Research Part I: Oceanographic Research Papers* 42, 11-12, 2035–2061.

[129] Millero, F. J. 1995. Thermodynamics of the carbon dioxide system in the oceans. *Geochimica et Cosmochimica Acta* 59, 4, 661–677.

[130] Millero, F. J., Graham, T. B., Huang, F., Bustos-Serrano, H., and Pierrot, D. 2006. Dissociation constants of carbonic acid in seawater as a function of salinity and temperature. *Marine Chemistry* 100, 1-2, 80–94.

[131] Millero, F. J., Pierrot, D., Lee, K., Wanninkhof, R., Feely, R., Sabine, C. L., Key, R. M., and Takahashi, T. 2002. Dissociation constants for carbonic acid determined from field measurements. *Deep Sea Research Part I: Oceanographic Research Papers* 49, 10, 1705–1723.

[132] Mojica Prieto, F. J. and Millero, F. J. 2002. The values of pK1 + pK2 for the dissociation of carbonic acid in seawater. *Geochimica et Cosmochimica Acta* 66, 14, 2529–2540.

[133] Roy, R. N., Roy, L. N., Vogel, K. M., Porter-Moore, C., Pearson, T., Good, C. E., Millero, F. J., and Campbell, D. M. 1993. The dissociation constants of carbonic acid in seawater at salinities 5 to 45 and temperatures 0 to 45°C. *Marine Chemistry* 44, 2-4, 249–267.

[134] Li, D. and Duan, Z. 2007. The speciation equilibrium coupling with phase equilibrium in the H2O–CO2–NaCl system from 0 to 250 °C, from 0 to 1000 bar, and from 0 to 5 molality of NaCl. *Chemical Geology* 244, 3-4, 730–751.

[135] Hagerman, A. E. 1987. Radial diffusion method for determining tannin in plant extracts. *Journal of Chemical Ecology* 1987, Vol. 13, No. 3, 437–449.

[136] 2013. *The Merck Index. An Encyclopedia of Chemicals, Drugs, and Biologicals.* The Royal Society of Chemistry.

[137] Maier, M., Oelbermann, A.-L., Weidner, B., Möhle, E., Renner, M., and Weidner, E. 2017. CO 2 -intensified Hydrolysis of Rutin to Quercetin – A Comparison of Experimental Data and modeled Reaction Kinetics. *Journal of CO2 Utilization* 21, 30–39.

[138] Frerichs, G., Arends, G., and Zörnig, H. 1930. *Hagers Handbuch der pharmazeutischen Praxis. Für Apotheker, Ärzte, Drogisten und Medizinalbeamte* 1. Springer Berlin Heidelberg.

[139] Frerichs, G., Arends, G., and Zörnig, H., Eds. 1938. *Hagers Handbuch der Pharmazeutischen Praxis. Für Apotheker, Arzneimittelhersteller, Drogisten, Ärzte und Medizinalbeamte* 2.

[140] Hegnauer, R. 1989. *Chemotaxonomie der Pflanzen. Eine Übersicht über die Verbreitung und die systematische Bedeutung der Pflanzenstoffe* VIII. Springer Basel AG.

[141] Hegnauer, R. 1990. *Chemotaxonomie der Pflanzen. Eine Übersicht über die Verbreitung und die systematische Bedeutung der Pflanzenstoffe* Band IX. Springer Basel AG, Basel.

[142] Council of Europe, Ed. 2004. *European Pharmacopeia 5.0*.

[143] Ainsworth, E. A. and Gillespie, K. M. 2007. Estimation of total phenolic content and other oxidation substrates in plant tissues using Folin–Ciocalteu reagent. *Nat Protoc* 2, 4, 875–877.

[144] Gathercoal, E. N. and Wirth, H. E., Eds. 1947. *Pharmacognosy* 2nd Edition. Lea and Febiger, University of Michigan.

[145] OTTO DILLE ®. *Chestnut extract.* http://www.otto-dille.de/pdf/otto-dille-de-vegetable-tanning-agent-chestnut.pdf. Accessed 19 September 2016.

[146] Silva Team. *Vegetable extracts.* http://en.silvateam.com/Products-Services/Leather/Vegetable-extracts. Accessed 19 September 2016.

[147] Tanin - Sevnica. *Leather program.* http://www.tanin.si/podstrani_eng/leather_program/chestnuts_extracts.php. Accessed 19 September 2016.

[148] Chemtan. *Chemtan Leather chemicals - Extracts.* http://www.chemtan.com/vegextract.php. Accessed 19 September 2016.

[149] Schmidt, O. T. 1955. Natürliche Gerbstoffe. In *Modern Methods of plant analysis*, K. Paech and M. V. Tracey, Eds. Volume III. Springer-Verlag, Berlin Göttingen Heidelberg, 517–548.

[150] Stafford, H. A. and Lester, H. H. 1980. Procyanidins (Condensed Tannins) in Green Cell Suspension Cultures of Douglas Fir Compared with Those in

Strawberry and Avocado Leaves by Means of C18-Reversed-phase Chromatography. *Plant Physiol.,* 66, 1085–1090.

[151] Piwowarski, J. P., Granica, S., Kosiński, M., and Kiss, A. K. 2014. Secondary metabolites from roots of Geum urbanum L. *Biochemical Systematics and Ecology* 53, 46–50.

[152] Gudej Jan, Tomczyk Michal. 2004. Determination of Flavonoids, Tannins and Ellagic acid in leaves from<Emphasis Type="Italic">Rubus</Emphasis> L. species. *Archives of Pharmacal Research,* Vol. 27, No. 11, 1114–1119.

[153] McIntyre, K. L., Harris, C. S., Saleem, A., Beaulieu, L.-P., Ta, C. A., Haddad, P. S., and Arnason, J. T. 2009. Seasonal phytochemical variation of anti-glycation principles in lowbush blueberry (Vaccinium angustifolium). *Planta medica* 75, 3, 286–292.

[154] Hokkanen, J., Mattila, S., Jaakola, L., Pirttila, A. M., and Tolonen, A. 2009. Identification of phenolic compounds from lingonberry (Vaccinium vitis-idaea L.), bilberry (Vaccinium myrtillus L.) and hybrid bilberry (Vaccinium x intermedium Ruthe L.) leaves. *Journal of Agricultural and Food Chemistry* 57, 20, 9437–9447.

[155] Okuda, T., Yoshida, T., and Hatano, T. 1992. PHARMACOLOGICALLY ACTIVE TANNINS ISOLATED FROM MEDICINAL PLANTS. In *Plant Polyphenols. Synthesis, Properties, Significance*, R. W. Hemingway and P. E. Laks, Eds. 1992, 539–569.

[156] Belgacem, M. N. and Gandini, A., Eds. 2008. *Monomers, polymers and composites from renewable resources*. Elsevier, Amsterdam, Boston.

[157] White, T., Kirby, K. S., and Knowles, E. 1952. Tannins. IV. The complexity of tannin extract composition. *J. Soc. Leather Trade Chem.,* 36, 154.

[158] Muster, G. 2014. *Nischenkultur Brombeere*. Staatliche Lehr- und Versuchsanstalt für Wein- und Obstbau Weinsberg.

[159] Fritzsche, R., Ed. 2012. *Handbuch des Arznei- und Gewürzpflanzenbaus. Band 4 Arznei- und Gewürzpflanzen A - K* 4. Verein für Arznei- und Gewürzpflanzen Saluplanta, Bernburg.

[160] Eurostat. 2016. *Anbaufläche von Erdbeeren in Deutschland bis 2014*.

[161] Abraham, H. 2015. *Kulturanleitung Frauenmantel*. http://www.fachschule-laimburg.it/download/Kulturanleitung_Frauenmantel.pdf. Accessed 21 September 2016.

[162] Kirby, K. J. 1976. *The Growth, Production and Nutrition of Rubus fruticosus L. agg. in Woodlands*. PhD, University of Oxford.

[163] PFAF. 2012. *Plants for a Future: Checklist of plants suitable for ground cover*. http://www.pfaf.org/user/cmspage.aspx?pageid=261. Accessed 7 October 2016.

[164] Landesanstalt für Landwirtschaft, Forsten und Gartenbau, Ed. 2008. *Qualität, Wirtschaftlichkeit und Nachhaltigkeit*.

[165] HDLGN. 2004. *Hessischer Ratgeber für Pflanzenbau und Pflanzenschutz*.

[166] Caruso, G., Villari, G., Melchionna, G., and Conti, S. 2011. Effects of cultural cycles and nutrient solutions on plant growth, yield and fruit quality of alpine strawberry (Fragaria vesca L.) grown in hydroponics. *Scientia Horticulturae* 129, 3, 479–485.

[167] Toews Karen L., Shroll Robert M., Wai C.M. 1995. pH-Defining Equilibrium between Water and Supercritical CO2. Influence on SFE of Organics and Metal Chelates. *Anal. Chem.,* 67, 4040–4043.

[168] Meyssami, B., Balaban, M. O., and Teixeira, A. A. 1992. Prediction of pH in model systems pressurized with carbon dioxide. *Biotechnol. Prog.* 8, 2, 149–154.

[169] R. J. Withey and E. Whalley. PRESSURE EFFECT AND MECHANISM IN ACID CATALYSIS XII. RACEMIZATION OF sec-BUTANOL.

[170] Ferreira, O. and Pinho, S. P. 2012. Solubility of Flavonoids in Pure Solvents. *Ind. Eng. Chem. Res.* 51, 18, 6586–6590.

[171] Krewson, C. F. and Naghski, J. 1952. Some Physical Properties of Rutin. *Journal of the American Pharmaceutical Association (Scientific ed.)* 41, 11, 582–587.

[172] International Plant Nutrition Institute. *Sodium Nitrate. Module 3.3-24.* http://www.ipni.net/publication/4rmanual.nsf/0/AE41667A64A7FCF285257CE0007292DA/$FILE/4RMANUAL-Module%203.3-24.pdf. Accessed 4 September 2017.

[173] Garrett, D. E., Ed. 2001. *Sodium Sulfate. Handbook of Deposits, Processing, Use.* Elsevier professional, s.l.

[174] Young, D. A., Cronjé, A., Botes, A. L., Ferreira, D., and Roux, D. G. 1985. Synthesis of condensed tannins. Part 14. Biflavanoid profisetinidins as synthons. The Acid-induced 'phlobaphene' reaction. *J. Chem. Soc., Perkin Trans. 1,* 0, 2521–2527.

[175] Buchner, N., Krumbein, A., Rohn, S., and Kroh, L. W. 2006. Effect of thermal processing on the flavonols rutin and quercetin. *Rapid communications in mass spectrometry : RCM* 20, 21, 3229–3235.

List of Figures

List of Tables

List of Equations

Appendix

Radial diffusion method

Determination of tannin content of tannic acid

Figure 45: HPLC - Chromatogram of Tannic acid and pentagalloylglucose

The sum of the peak areas before RT PGG and after RT PGG was calculated and the real tannin content of tannic acid was determined and summarized in Table 25

Table 25: Determination of tannin content - tannic acid

Peak Area		
	bis Retentionszeit PGG nichtgerbend	ab einschließlich Retentionszeit PGG gerbend
	4,71988	1287,42151
	572,19739	286,98239
	13,63265	3031,41431
	555,94391	4492,01025
	9,17835	1,13E+04
	7,91461	
	9,92561	
	14,79307	
	32,84187	
	210,20715	
	48,25754	
	41,71663	
	42,86685	
	17,21663	
	37,91093	
	787,23553	
Summe	2406,5586	20429,82846
Anteil	**10,54**	**89,46**

Detection limit of RDM
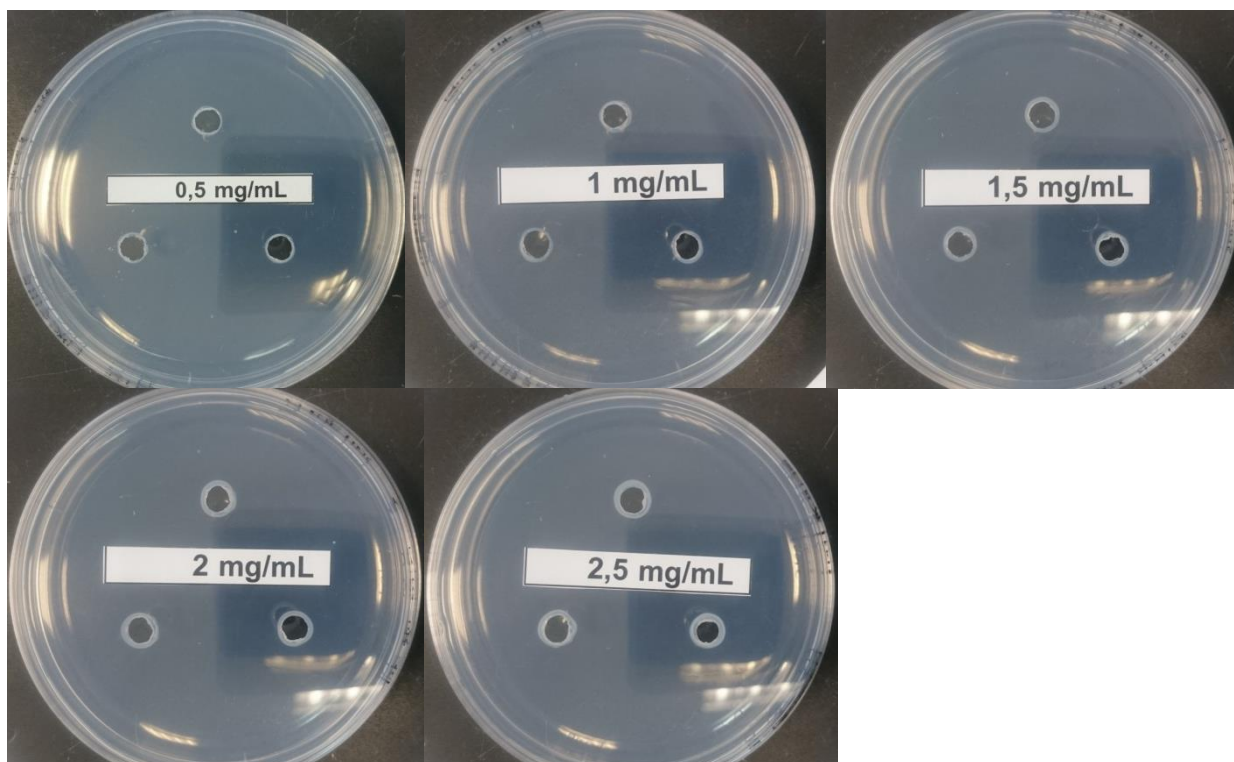
Determination of calibration – water / BSA

Concentration [mg/mL]	plate	pixel²	Scale [pixel/cm]	Area [cm²]	Mean [cm²]	SD [cm²]
	1	20510	157,84	0,82		
5,04	2	20292	157,84	0,81	0,81	0,02
	3	19403	157,84	0,78		
	4	29713	157,29	1,20		
10,01	5	31332	158,88	1,24	1,24	0,04
	6	32042	158,56	1,27		
	7	40611	158,56	1,62		
15,05	8	40220	158,56	1,60	1,59	0,03
	9	38939	158,56	1,55		
	10	47504	158,56	1,89		
20,01	11	48626	158,56	1,93	1,92	0,03
	12	48896	158,56	1,94		
	13	56603	158,56	2,25		
25,05	14	57009	160,02	2,23	2,22	0,03
	15	57239	161,5	2,19		
	16	65679	161,5	2,52		
30,10	17	62282	161,5	2,39	2,46	0,07
	18	64228	161,5	2,46		
	19	60527	161,5	2,32		
34,98	20	74978	161,5	2,87	2,73	0,36
	21	77817	161,5	2,98		

	22	92580	161,5	3,55		
40,02	23	87660	161,5	3,36	3,39	0,15
	24	86323	162,98	3,25		
	25	100216	161,55	3,84		
45,22	26	101773	161,55	3,90	3,89	0,04
	27	102423	161,55	3,92		
	28	117470	161,5	4,50		
50,03	29	116492	162,89	4,39	4,38	0,13
	30	112439	162,89	4,24		
	31	130180	162,89	4,91		
55,23	32	121944	162,89	4,60	4,70	0,18
	33	121791	162,89	4,59		
	34	145760	162,89	5,49		
60,19	35	138321	165,79	5,03	5,32	0,25
	36	149509	165,79	5,44		
	37	153361	165,79	5,58		
65,07	38	157985	165,79	5,75	5,54	0,23
	39	145655	165,79	5,30		
	40	149558	165,79	5,44		
70,20	41	157272	165,79	5,72	5,47	0,24
	42	149232	168,66	5,25		
	43	195459	168,66	6,87		
75,48	44	195205	168,66	6,86	6,66	0,35
	45	180893	170,1	6,25		
80,04	46	185004	171,54	6,29	6,44	0,15

| | 47 | 194063 | 171,54 | 6,60 |
| | 48 | 192211 | 172,98 | 6,42 |

Extractions – screening of European medicinal herbs and spice plants

Moisture content of European medicinal herbs and spice plants

Plant	Crucible empty [g]	Crucible full [g]	Crucible after drying [g]	Water [%]
Arctostaphylos uva-ursi	12,277	17,6687	17,2343	8,06
Origanum vulgare	13,5338	15,8611	15,6307	9,90
Potentilla erecta	10,7025	17,7861	16,9948	11,17
Agrimonia euparia	10,7537	12,6272	12,4415	9,91
Fragaria	9,3752	10,4342	10,3265	10,17
Salicis folium	12,6696	15,6737	15,4094	8,80
Geum urbanum	14,4419	19,8371	19,2118	11,59
Alchemilla vulgaris	13,9224	15,531	15,3568	10,83
Rubi idaei	13,5468	15,654	15,4399	10,16

Rheum palmatum	13,0182	17,9998	17,5092	9,85
Vaccinium vitis-ideae	9,5614	11,509	11,3528	8,02
Vaccinium myrtillus	13,3003	15,3681	15,1826	8,97
Rubi fruticosus	14,145	15,6038	15,4624	9,69
Melissa officinalis	13,5973	14,6015	14,494	10,71
Mentha piperita	13,6325	14,9641	14,8112	11,48
Potentilla anserina	12,5302	13,972	13,8183	10,66

Calculation of amount tannin from calibration curve:

$$measured\ ring\ area = 0.283 + 3.915 \cdot amount\ of\ tannic\ acid$$
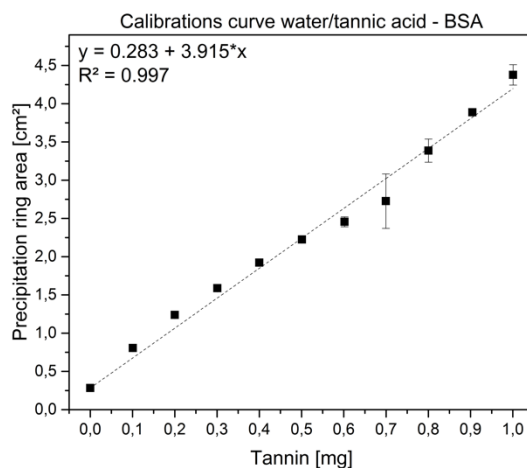
Calculation of tannin content in dried plant:

$Tannin\ content\ [w\%]$

$$= \left(\frac{Tannin\ content\ calculated\ from\ calibration\ curve\ [mg] \cdot 0.895\ (real\ tannin\ content)}{Pipette\ volume\ [mL]} \right.$$

$$\left. \cdot \frac{\frac{Amount\ solvent\ afer\ extraction\ [g]}{Density\ solvent\ [g]}}{1000\ (g\ into\ mg)} \right) \cdot \frac{100}{weighed\ plant\ [g] \cdot \left(1 - \frac{moisture\ content}{100} \right)}$$

Raw data screening– radial diffusion method

Arctostaphylos uva-ursi

Date	16.10.2014	1	2	3
Weight beaker:		117,98	134,45	132,24
Weighed portion plant		10	10,2	9,99
Weighed portion solvent		100,34	100,26	100,69
Ratio		1:10	1:10	1:10
Extraction time		1h	1h	1h
Total weight		246,96	261,67	259,6
Weight after extraction		245,7	260,95	259,1

Plate 1 [mm]		Plate 2 [mm]		Plate 3 [mm]	
0°	90°	0°	90°	0°	90°
15,58	15,66	16,34	16,64	16,5	16,39
16,5	16,47	16,98	17,07	16,47	16,54
16,06	15,93	16,59	16,29	16,06	16,2

Origanum vulgaris

Date	14.10.2014	1	2	3
Weight beaker:		134,71	120,12	134,3
Weighed portion plant		10,02	10	10
Weighed portion solvent		100,16	100,25	103,97
Ratio		1:10	1:10	1:10
Extraction time		1h	1h	1h
Total weight		261,59	247,02	267,03
Weight after extraction		260,65	245,57	265,93

Plate 1 [mm]		Plate 2 [mm]		Plate 3 [mm]	
0°	90°	0°	90°	0°	90°
8	7	8	7	8	7
8	7	8	7	8	7
8	7	8	7	8	7

Melissa officinalis

Date	15.10.2014	1	2	3
Weight beaker:		126,37	132,25	126,68
Weighed portion plant		10,12	9,92	10,06
Weighed portion solvent		101,31	99,99	103,63
Ratio		1:10	1:10	1:10
Extraction time		1h	1h	1h
Total weight		256,45	258,48	257,07
Weight after extraction		254,07	258,23	256,23

Plate 1 [mm]		Plate 2 [mm]		Plate 3 [mm]	
0°	90°	0°	90°	0°	90°
8,62	8,14	7,79	7,84	7,6	7,76
8,12	8,15	8,07	7,96	7,45	7,58
7,94	8,02	8,54	8,29	7,65	7,66

Potentilla anserine

Date	16.10.2014	1	2	3
Weight beaker:		132,45	120,26	135,88
Weighed portion plant		10,24	5,05	5,22
Weighed portion solvent		151,03	110,23	105,38
Ratio		1:10	1:10	1:10
Extraction time		1h	1h	1h
Total weight		293,72	252,62	264,87
Weight after extraction		292,84	251,29	264,22

Plate 1 [mm]		Plate 2 [mm]		Plate 3 [mm]	
0°	90°	0°	90°	0°	90°
10,29	10,05	8,71	8,58	9,02	9,13
10,13	10,02	8,95	8,57	9,15	9
10,11	10,15	8,86	8,85	9,07	9,15

Agrimonia

Date	20.10.2014	1	2	3
Weight beaker:		120,03	134,54	132,01
Weighed portion plant		10,26	10,07	10,09
Weighed portion solvent		100,31	100,20	106,77
Ratio		1:10	1:10	1:10
Extraction time		1h	1h	1h
Total weight		247,08	261,37	267,43
Weight after extraction		246,8	260,71	267,34

Plate 1 [mm]		Plate 2 [mm]		Plate 3 [mm]	
0°	90°	0°	90°	0°	90°
10,83	10,28	10,41	10,13	10,02	10,24
-	-	10,13	9,84	10,07	10,07
10,47	10,12	10,03	10,03	10,1	10,18

Alchemilla vulgaris

Date	20.10.2014	1	2	3
Weight beaker:		134,7	132,33	134,38
Weighed portion plant		10,04	9,99	10,23
Weighed portion solvent		100,25	100,58	100,03
Ratio		1:10	1:10	1:10
Extraction time		1h	1h	1h
Total weight		261,73	259,49	262,94
Weight after extraction		261,05	259,15	262,53

Plate 1 [mm]		Plate 2 [mm]		Plate 3 [mm]	
0°	90°	0°	90°	0°	90°
11,36	11,68	11,05	11,01	11,65	11,88
10,98	11,1	11,01	11,1	11,87	11,61
11,19	11,39	11,1	11,22	11,31	11,44

Rheum plantanum

Date	20.10.2014	1	2	3
Weight beaker:		135,66	120,12	135,67
Weighed portion plant		10,14	10,03	10,32
Weighed portion solvent		100,02	100,28	100,19
Ratio		1:10	1:10	1:10
Extraction time		1h	1h	1h
Total weight		263,91	246,99	262,65
Weight after extraction		263,45	245,97	261,43

Plate 1 [mm]		Plate 2 [mm]		Plate 3 [mm]	
0°	90°	0°	90°	0°	90°
13,92	13,53	12,93	12,95	14,62	14,08
12,82	12,88	13,29	13,21	14,12	13,97
12,56	12,56	12,66	12,69	14,28	14,18

Fragaria

Date	21.10.2014	1	2	3
Weight beaker:		134,51	132,24	134,3
Weighed portion plant		10,17	10,07	10,13
Weighed portion solvent		100	101,85	100,11
Ratio		1:10	1:10	1:10
Extraction time		1h	1h	1h
Total weight		263,15	260,89	261,15
Weight after extraction		262,18	260,08	261

Plate 1 [mm]		Plate 2 [mm]		Plate 3 [mm]	
0°	90°	0°	90°	0°	90°
11,17	10,87	11,36	11,27	11,25	11,29
11,11	11,12	11,14	11,18	11,58	11,45
10,9	11,06	11,09	11,07	11,72	11,27

Vaccinium vitis-idaea

Date	21.10.2014	1	2	3
Weight beaker:		120,29	135,71	120,27
Weighed portion plant		10,05	10,06	10,2
Weighed portion solvent		100,45	100,10	100,42
Ratio		1:10	1:10	1:10
Extraction time		1h	1h	1h
Total weight		247,35	262,38	249,37
Weight after extraction		246,91	261,67	248,61

Plate 1 [mm]		Plate 2 [mm]		Plate 3 [mm]	
0°	90°	0°	90°	0°	90°
11,36	11,59	11,82	11,69	11,77	11,69
11,57	11,85	11,95	11,82	11,86	12,11
11,84	11,55	11,79	11,59	11,93	11,64

Geum urbanum

Date	21.10.2014	1	2	3
Weight beaker:		132,2	120,15	135,18
Weighed portion plant		10,07	10	10,53
Weighed portion solvent		100,09	100,23	100,46
Ratio		1:10	1:10	1:10
Extraction time		1h	1h	1h
Total weight		260,82	246,91	262,48
Weight after extraction		259,87	245,57	261,69

Plate 1 [mm]		Plate 2 [mm]		Plate 3 [mm]	
0°	90°	0°	90°	0°	90°
12,72	12,35	12,77	12,76	13,11	13,24
11,69	12,69	13,19	13,22	13,24	13,2
12,78	12,76	13,09	13,38	13,57	13,66

Rubi fruticosus

Date	22.10.2014	1	2	3
Weight beaker:		120,51	134,64	120,32
Weighed portion plant		10,03	10,21	9,97
Weighed portion solvent		100,09	100,04	100,19
Ratio		1:10	1:10	1:10
Extraction time		1h	1h	1h
Total weight		247,34	261,34	248,88
Weight after extraction		246,44	260,58	248,26

Plate 1 [mm]		Plate 2 [mm]		Plate 3 [mm]	
0°	90°	0°	90°	0°	90°
12,32	12,7	12,13	12,54	12,75	12,77
12,92	12,61	12,61	12,59	12,57	12,31
12,88	13,15	13,09	12,76	12,64	12,68

Rubi idaei

Date	22.10.2014	1	2	3
Weight beaker:		134,78	135,75	134,9
Weighed portion plant		10,13	9,96	10,05
Weighed portion solvent		100,3	108,80	100,02
Ratio		1:10	1:10	1:10
Extraction time		1h	1h	1h
Total weight		261,84	271,05	263,58
Weight after extraction		261,39	270,04	262,58

Plate 1 [mm]		Plate 2 [mm]		Plate 3 [mm]	
0°	90°	0°	90°	0°	90°
10,85	10,83	10,78	10,85	11,17	11,1
11,09	10,82	10,62	10,94	10,9	11,12
10,61	10,82	10,95	10,78	11,22	11,17

Vaccinium myrtillus

Date	22.10.2014	1	2	3
Weight beaker:		132,3	120,19	132,2
Weighed portion plant		10,19	10	9,89
Weighed portion solvent		100,24	101,08	100,14
Ratio		1:10	1:10	1:10
Extraction time		1h	1h	1h
Total weight		261,03	247,66	259
Weight after extraction		260,33	247,11	258,49

Plate 1 [mm]		Plate 2 [mm]		Plate 3 [mm]	
0°	90°	0°	90°	0°	90°
10,41	10,16	10,08	10,27	10,15	10,41
10,28	10,27	10,3	10,05	10,38	10,38
10,08	10,08	10,23	10,15	10,26	10,41

Salicis folium

Date	23.10.2014	1	2	3
Weight beaker:		120,21	135,68	120,1
Weighed portion plant		10,08	10,01	10,15
Weighed portion solvent		100,19	100,10	100,12
Ratio		1:10	1:10	1:10
Extraction time		1h	1h	1h
Total weight		249,02	262,4	246,86
Weight after extraction		248,03	261,08	244,62

Plate 1 [mm]		Plate 2 [mm]		Plate 3 [mm]	
0°	90°	0°	90°	0°	90°
8,92	8,69	8,78	8,79	8,65	8,89
8,93	8,46	8,7	8,79	8,53	8,56
8,53	8,97	8,9	8,59	8,59	8,57

Potentilla erecta

Date	22.10.2014	1	2	3
Weight beaker:		126,63	126,92	126,88
Weighed portion plant		10,11	10,25	9,99
Weighed portion solvent		100,13	101,48	100,26
Ratio		1:10	1:10	1:10
Extraction time		1h	1h	1h
Total weight		255,19	255,22	253,84
Weight after extraction		254,92	254,45	252,73

Plate 1 [mm]		Plate 2 [mm]		Plate 3 [mm]	
0°	90°	0°	90°	0°	90°
21,26	21,61	21,6	21,8	21,61	21,14
21,59	21,55	22,05	22,32	21,39	21,36
21,59	21,45	21,78	21,77	21,48	21,29

Determination of dry matter of extracts and tannin content

Plant	Crucible	Mass after glowing [g]	Adding 20ml of extract [g]	Mass after drying [g]	Mass of extract [g]	Dry matter [g]	Dry matter [%]
Origanum vulgare	16M	26,2727	46,4447	26,8936	20,1721	0,6209	3,078
	13M	26,8971	47,0231	27,5198	20,1264	0,6227	3,093
Salicis folium	18M	25,0347	45,1628	25,5967	20,1282	0,562	2,792
	12M	23,8226	43,8908	24,3873	20,0687	0,5647	2,814
Fragaria	1M	26,332	46,4661	26,8972	20,1343	0,5652	2,807
	11M	26,0682	46,1454	26,6368	20,0778	0,5686	2,832
Melissa officinalis	14M	25,7332	45,9221	26,3566	20,1891	0,6234	3,088
	6M	25,4029	45,5115	26,0284	20,1088	0,6255	3,111
Rubi fruticosus	5M	25,1829	45,2905	25,6789	20,1079	0,496	2,467
	19M	25,3344	45,4601	25,8348	20,1257	0,5004	2,486
Vaccinium myrtillus	3M	27,3447	47,3927	27,7766	20,0483	0,4319	2,154
	15M	24,9189	45,0126	25,4133	20,0343	0,4944	2,468
Potentilla anserina	18M	25,0347	45,0542	25,3341	20,0194	0,2994	1,496
	15M	24,9789	45,0413	25,2808	20,0622	0,3019	1,505
Agrimonia eupatoria	5M	25,1829	45,2146	25,5705	20,031	0,3876	1,935
	19M	25,3344	45,3247	25,7237	19,9897	0,3893	1,948
Vaccinium vitis-idaea	14M	25,7332	45,8619	26,3687	20,1283	0,6355	3,157
	16M	26,2727	46,3677	26,9093	20,0944	0,6366	3,168
Alchemilla vulgaris	13M	26,8971	47,069	27,445	20,1712	0,5479	2,716
	11M	26,0682	46,2142	26,6188	20,1455	0,5506	2,733
Mentha piperita	6M	25,4029	45,6617	26,1334	20,258	0,7305	3,606
	1M	26,332	46,5584	27,0647	20,2258	0,7327	3,623
Potentilla erecta	6M	25,4029	45,5186	25,9135	20,1156	0,5106	2,538
	14M	25,7332	45,8655	26,2439	20,1322	0,5107	2,537
Geum urbanum	16M	26,2727	46,3566	26,7396	20,0838	0,4669	2,325
	3M	27,3447	47,4813	27,8109	20,1365	0,4662	2,315
Arctostaphylos uva-ursi	18M	25,0347	45,2313	25,8564	20,1962	0,8217	4,069
	1M	26,332	46,5339	27,1588	20,2013	0,8268	4,093
Rubi idaei	5M	25,1829	45,3314	25,6824	20,1482	0,4995	2,479
	19M	25,3344	45,4501	25,8372	20,1152	0,5028	2,500
Rheum palmatum	12M	23,8226	32,1228	24,0309	8,2997	0,2083	2,510
	13M						

Determination of tannin content from additional extractions

Fragaria

Date	02.02.2015	1
Weight beaker:		135
Weighed portion plant		10,23
Weighed portion solvent		100,18
Ratio		1:10
Extraction time		1h
Total weight		262,05
Weight after extraction		261,51

Plate 1 [mm]	
0°	90°
15,38	15,53
15,3	15,7
15,51	15,37

Potentilla erecta

Date	04.02.2015	1
Weight beaker:		132,18
Weighed portion plant		10,06
Weighed portion solvent		100,21
Ratio		1:10
Extraction time		1h
Total weight		258,97
Weight after extraction		258,4

Plate 1 [mm]	
0°	90°
17,26	17,14
17,85	17,99
17,49	17,43

Arctostaphylos uva-ursi

Date	04.02.2015	1
Weight beaker:		132,3
Weighed portion plant		10,16
Weighed portion solvent		100,49
Ratio		1:10
Extraction time		1h
Total weight		259,41
Weight after extraction		258,77

Plate 1 [mm]	
0°	90°
18,88	18,9
19,11	18,7
19,35	19,26

Geum urbanum

Date	04.02.2015	1
Weight beaker:		120,15
Weighed portion plant		10,19
Weighed portion solvent		100,28
Ratio		1:10
Extraction time		1h
Total weight		249,04
Weight after extraction		248,64

Plate 1 [mm]	
0°	90°
15,39	15,25
14,83	14,97
15,18	15,08

Vaccinium myrtillus

Date	02.02.2015	1
Weight beaker:		132,34
Weighed portion plant		10,08
Weighed portion solvent		103,23
Ratio		1:10
Extraction time		1h
Total weight		262,13
Weight after extraction		261,45

Plate 1 [mm]	
0°	90°
9,86	9,77
9,86	10,12
9,84	9,86

Rubi fruticosus

Date	02.02.2015	1
Weight beaker:		119,82
Weighed portion plant		10,04
Weighed portion solvent		100,08
Ratio		1:10
Extraction time		1h
Total weight		246,54
Weight after extraction		246,12

Plate 1 [mm]	
0°	90°
18,9	18,93
18,87	19,11
18,51	18,39

Origanum vulgaris

Date	02.02.2015	1
Weight beaker:		132,44
Weighed portion plant		10,15
Weighed portion solvent		100,19
Ratio		1:10
Extraction time		1h
Total weight		261,23
Weight after extraction		260,65

Plate 1 [mm]	
0°	90°
8,58	8,49
8,6	8,37
8,33	8,41

Melissa officinalis

Date	02.02.2015	1
Weight beaker:		120,32
Weighed portion plant		9,96
Weighed portion solvent		100,66
Ratio		1:10
Extraction time		1h
Total weight		247,29
Weight after extraction		246,54

Plate 1 [mm]	
0°	90°
10,18	10,38
10,28	10,17
10,28	10,26

Vaccinium vitis-idaea

Date	02.02.2015	1
Weight beaker:		117,85
Weighed portion plant		10,02
Weighed portion solvent		100,13
Ratio		1:10
Extraction time		1h
Total weight		246,28
Weight after extraction		245,64

Plate 1 [mm]	
0°	90°
11,38	11,19
11,03	11,3
11,24	11,25

Salicis folium

Date	03.02.2015	1
Weight beaker:		120,12
Weighed portion plant		10,01
Weighed portion solvent		100,31
Ratio		1:10
Extraction time		1h
Total weight		248,85
Weight after extraction		248,5

Plate 1 [mm]	
0°	90°
8,58	8,49
8,6	8,37
8,33	8,41

Alchemilla vulgaris

Date	03.02.2015	1
Weight beaker:		131,89
Weighed portion plant		10,11
Weighed portion solvent		100,26
Ratio		1:10
Extraction time		1h
Total weight		258,72
Weight after extraction		258,48

Plate 1 [mm]	
0°	90°
17,35	17,34
18,02	17,57
18,3	18,14

Agrimonia eupatoria

Date	03.02.2015	1
Weight beaker:		132,33
Weighed portion plant		10,03
Weighed portion solvent		100,19
Ratio		1:10
Extraction time		1h
Total weight		259,02
Weight after extraction		258,44

Plate 1 [mm]	
0°	90°
9,56	9,78
9,61	9,78
9,22	9,56

Potentilla anserina

Date	03.02.2015	1
Weight beaker:		132,33
Weighed portion plant		10,03
Weighed portion solvent		100,19
Ratio		1:10
Extraction time		1h
Total weight		259,02
Weight after extraction		258,44

Plate 1 [mm]	
0°	90°
10,43	10,52
10,26	10,27
10,28	10,44

Mentha piperita

Date	03.02.2015	1
Weight beaker:		120,17
Weighed portion plant		10,06
Weighed portion solvent		100,31
Ratio		1:10
Extraction time		1h
Total weight		246,83
Weight after extraction		246,35

Plate 1 [mm]	
0°	90°
8,84	9,06
8,35	8,51
8,76	8,78

Rubi idaei

Date	04.02.2015	1
Weight beaker:		120,13
Weighed portion plant		10,1
Weighed portion solvent		100,15
Ratio		1:10
Extraction time		1h
Total weight		249,04
Weight after extraction		248,11

Plate 1 [mm]	
0°	90°
12,59	12,63
12,96	12,71
12,05	12,15

__Rheum palmatum__

Date	04.02.2015	1
Weight beaker:		134,72
Weighed portion plant		10,06
Weighed portion solvent		100,4
Ratio		1:10
Extraction time		1h
Total weight		261,66
Weight after extraction		261,11

Plate 1 [mm]	
0°	90°
12,98	12,85
13,12	13,18
13,26	13,44

Raw data - hydrolysis

Table 26: CO_2-intensified hydrolysis without inertization

Date	Parameter	HPLC Results [mg/L]					
		Compound	0_0	2h	4h	6h	8h
08.10.2015	363K, 150 bar	Rutin	42,39	43,83	43,64	43,26	42,57
		Quercetin	0,00	0,00	0,00	0,00	0,00
09.10.2015	363K, 150 bar	Rutin	42,53	43,72	43,40	43,55	42,32
		Quercetin	0,00	0,00	0,00	0,00	0,00
12.10.2015	363K, 150 bar	Rutin	42,65	44,54	43,62	43,91	43,40
		Quercetin	0,00	0,00	0,00	0,00	0,00
13.10.2015	388K, 150 bar	Rutin	43,40	41,16	34,85	30,94	26,47
		Quercetin	0,00	1,60	3,51	5,43	6,69
14.10.2015	388K, 150 bar	Rutin	42,58	38,93	34,44	31,26	27,71
		Quercetin	0,00	1,74	3,71	5,67	7,28
15.10.2015	388K, 150 bar	Rutin	42,47	40,11	35,05	31,31	28,00
		Quercetin	0,00	1,78	3,64	5,68	7,17
22.09.2015	413K, 150 bar	Rutin	41,75	14,80	6,33	2,60	1,18
		Quercetin	0,00	5,59	7,82	8,30	5,41

23.09.2015	413K, 150 bar	Rutin	42,38	15,21	6,00	2,07	0,90
		Quercetin	0,00	5,88	7,23	5,45	3,88
24.09.2015	413K, 150 bar	Rutin	42,38	15,89	6,32	2,29	1,08
		Quercetin	0,00	5,30	6,54	5,72	2,89

Table 27: CO_2-intensified hydrolysis - temperature dependence

Date	Parameter	HPLC Results [mg/L]				
		Compound	0_0	2h	4h	6h	8h
18.02.2016	373K, 150 bar	Rutin	42,38	40,99	39,77	38,44	37,60
		Quercetin	0,00	0,42	0,72	1,37	2,12
26.02.2016	373K, 150 bar	Rutin	42,10	39,68	38,14	37,20	35,85
		Quercetin	0,00	0,00	0,00	0,00	0,00
25.02.2016	393K, 150 bar	Rutin	41,93	31,38	23,31	17,46	12,90
		Quercetin	0,00	0,00	0,00	0,00	0,00
01.03.2016	393K, 150 bar	Rutin	41,75	33,24	26,24	20,66	16,76
		Quercetin	0,00	0,90	1,38	2,31	3,52
04.03.2016	393K, 150 bar	Rutin	41,96	36,29	27,44	22,06	17,42
		Quercetin	0,00	2,61	5,63	8,42	11,05
29.02.2016	433K, 150 bar	Rutin	41,93	1,09	0,00	0,00	0,00
		Quercetin	0,00	12,72	12,95	14,53	15,26
02.03.2016	433K, 150 bar	Rutin	42,19	1,20	0,00	0,00	0,00
		Quercetin	0,00	17,55	18,97	20,12	20,20
07.03.2016	433K, 150 bar	Rutin	42,13	1,59	0,38	0,00	0,00
		Quercetin	0,00	14,25	16,01	16,73	17,76

Table 28: CO$_2$-intensified hydrolysis - pressure dependence

Date	Parameter	Compound	0_0	2h	4h	6h	8h
					HPLC Results [mg/L]		
19.11.2015	150 bar, 413K	Rutin	40,04	14,63	5,72	2,19	0,99
		Quercetin	0,00	8,95	15,44	18,02	19,83
06.01.2016	150 bar, 413K	Rutin	46,86	17,47	7,22	3,21	1,57
		Quercetin	0,00	10,52	17,78	20,12	22,92
19.01.2016	150 bar, 413K	Rutin	49,15	16,72	6,73	2,51	0,83
		Quercetin	0,00	10,82	18,75	21,59	25,30
04.02.2016	100 bar, 413K	Rutin	44,64	19,25	7,96	3,22	1,33
		Quercetin	0,00	7,47	14,15	17,25	19,46
05.02.2016	100 bar, 413K	Rutin	44,42	16,18	5,50	2,08	0,73
		Quercetin	0,00	10,48	16,72	18,17	19,63
03.02.2016	100 bar, 413K	Rutin	44,09	17,43	7,29	3,10	1,36
		Quercetin	0,00	6,35	11,11	15,39	16,98
11.02.2016	50 bar, 413K	Rutin	44,03	19,78	9,19	4,43	2,20
		Quercetin	0,00	5,54	10,53	14,81	16,99
12.02.2016	50 bar, 413K	Rutin	44,17	21,41	10,37	5,06	2,71
		Quercetin	0,00	6,18	12,03	16,46	19,07
15.02.2016	50 bar, 413K	Rutin	43,83	19,63	8,82	3,93	1,84
		Quercetin	0,00	5,58	10,02	14,61	16,88
14.01.2016	25 bar, 413K	Rutin	46,69	31,25	22,41	17,08	13,83
		Quercetin	0,00	3,62	7,40	9,58	12,22
10.02.2016	25 bar, 413K	Rutin	44,05	25,20	15,18	9,68	6,50
		Quercetin	0,00	1,10	3,52	7,12	8,76
04.12.2015	4 bar, 413K	Rutin	37,56	33,10	30,11	27,55	25,44

		Quercetin	0,00	2,02	2,82	4,17	5,50
13.01.2016	4 bar, 413K	Rutin	46,26	40,92	37,38	34,88	32,34
		Quercetin	0,00	0,67	1,46	3,03	4,24
17.02.2016	4 bar, 413K	Rutin	43,44	39,95	37,25	34,71	33,26
		Quercetin	0,00	0,35	1,10	1,56	3,78

Table 29: CO$_2$-intensified hydrolysis of Fragaria extract

Date	Parameter	HPLC Results [mg/L]					
		Compound	0_0	2h	4h	6h	8h
11.03.2016	150 bar, 413K	Quercetin	0,96	65,28	47,59	35,57	27,63
14.03.2016	150 bar, 413K	Quercetin	1,36	64,56	46,24	37,00	30,35
15.03.2016	150 bar, 413K	Quercetin	1,45	65,51	52,54	39,58	29,89

Table 30: Strong and weak acid hydrolysis of Fragaria extract

Date	Acid	HPLC Results [mg/L]							
		C	0_0	1h	2h	3h	4h	6h	8h
14.03.16	HCl	Q	1,70	67,33	79,93	109,79	118,92	123,02	123,75
14.03.16	HCl	Q	1,72	92,07	107,10	112,82	106,05	100,01	102,44
14.03.16	HCl	Q	1,68	94,51	111,42	127,92	125,92	110,20	95,56
15.03.16	HAc	Q	1,75	6,00	10,12		17,76	25,71	30,91
15.03.16	HAc	Q	1,71	7,29	12,34		21,49	31,86	37,31
15.03.16	HAc	Q	1,58	5,41	8,26		16,46	27,23	33,40

C = Compound; Q = Quercetin

Table 31: RDM of Fragaria extract treated with CO$_2$-intensified hydrolysis, strong and weak acid hydrolysis

Date	P	C	0_0	1h	2h	3h	4h	6h	8h
					RDM [mm]				
11.03.16	150 bar, 413K	T	14,26		14,26		13,52	13,32	13,39
14.03.16	150 bar, 413K	T	14,99		14,96		10,69	10,70	10,41
15.03.16	150 bar, 413K	T	12,19		11,72		11,41	10,92	10,75
14.03.16	HCl	T	14,99	15,61	14,70	14,81	12,17	12,36	11,49
14.03.16	HCl	T	14,99	15,22	14,46	13,61	13,47	11,46	10,63
14.03.16	HCl	T	14,99	14,65	14,56	13,67	13,40	11,22	11,08
15.03.16	HAc	T	12,19	12,67	12,69		12,69	12,90	13,02
15.03.16	HAc	T	12,19	12,33	12,49		12,34	12,35	12,65
15.03.16	HAc	T	12,19	12,73	12,33		12,49	12,44	12,30

P = Parameter (Acid or Pressure and Temperature); C = Compound; T = Tannins

Table 32: CO$_2$-intensified hydrolysis of Arctostaphylos uva-ursi extract

Date	Parameter	C	0_0	2h	4h	6h	8h
				HPLC Results [mg/L]			
08.03.2016	150 bar, 413K	Q	1,73	126,89	131,00	120,88	103,47
09.03.2016	150 bar, 413K	Q	1,78	128,82	126,04	124,78	95,19
10.03.2016	150 bar, 413K	Q	1,74	133,02	151,24	127,09	117,46

C = Compound; Q = Quercetin

Table 33: Strong and weak acid hydrolysis of Arctostaphylos uva-ursi extract

Date	Acid	HPLC Results [mg/L]							
		C	0_0	1h	2h	3h	4h	6h	8h
08.03.16	HCl	Q	1,88	203,77	273,98	292,29	297,42	256,37	243,65
08.03.16	HCl	Q	1,81	233,19	276,33	166,38	269,78	242,14	227,66
08.03.16	HCl	Q	1,88	219,37	223,64	166,16	248,50	238,90	218,12
09.03.16	HAc	Q	1,94	4,60	9,64		16,79	24,99	31,78
09.03.16	HAc	Q	1,84	6,05	36,97		20,55	32,36	41,82
09.03.16	HAc	Q	1,85	6,39	12,51		23,85	35,15	44,73

C = Compound; Q = Quercetin

Table 34: RDM of Arctostaphylos uva-ursi extract treated with CO_2-intensified hydrolysis, strong and weak acid hydrolysis

Date	P	RDM [mm]							
		C	0_0	1h	2h	3h	4h	6h	8h
08.03.16	150 bar, 413K	T	19,48		11,11		10,36	9,84	9,64
09.03.16	150 bar, 413K	T	18,55		10,85		10,10	10,02	10,07
10.03.16	150 bar, 413K	T	18,72		11,34		10,15	9,20	9,70
08.03.16	HCl	T	19,48	17,64	16,41	14,70	13,94	12,24	12,04
08.03.16	HCl	T	19,48	17,64	15,99	14,27	13,59	11,98	10,87
08.03.16	HCl	T	19,48	17,22	15,65	13,21	12,27	11,43	10,77
09.03.16	HAc	T	18,55	18,19	18,29		17,84	17,69	17,17

09.03.16	HAc	T	18,55	17,95	17,90		17,10	16,92	17,02
09.03.16	HAc	T	18,55	18,26	17,84		16,81	16,88	17,22

P = Parameter (Acid or Pressure and Temperature); C = Compound; T = Tannins

Table 35: RDM of tannic acid solution treated with CO$_2$-intensified hydrolysis, strong and weak acid hydrolysis

Date	P	RDM [mm]							
		C	0_0	1h	2h	3h	4h	6h	8h
16.03.16	150 bar, 413K	T	10,19		8,80		0,00	0,00	0,00
17.03.16	150 bar, 413K	T	13,43		10,42		9,02	0,00	0,00
18.03.16	150 bar, 413K	T	12,85		10,49		7,64	0,00	0,00
16.03.16	HCl	T	10,19	10,33	10,29	9,92	9,81	9,65	8,98
16.03.16	HCl	T	10,19	10,22	10,12	9,85	9,76	10,04	9,88
16.03.16	HCl	T	10,19	9,96	10,21	9,87	9,75	10,06	9,98
17.03.16	HAc	T	13,43	13,86	13,72		13,64	14,25	13,76
17.03.16	HAc	T	13,43	13,89	13,59		13,69	14,82	14,33
17.03.16	HAc	T	13,43	13,38	14,05		14,07	14,67	14,34

P = Parameter (Acid or Pressure and Temperature); C = Compound; T = Tannins

Matlab Code

```
%gemessene Konzentrationen Quercetin Druck

cQdata0 = [0 5.2 8.9 14.3 21.9];

cQdata25 = [0 10.3 24.1 37.1 46.5];

cQdata50 = [0 26.5 49.8 70.2 81];

cQdata100 = [0 36.8 63.7 77.1 85];

cQdata150 = [0 45 77.2 88.8 100];

c0 = 8.18974E-05; %Rutin Konzentration c0=50mg/L Mrutin=610,52 mg/mmol

%gemessene Rutin Konzentrationen Druck

cRdata0 = [100 89.58 82.24 76.22 71.41];

cRdata25 = [100 62.07 41.24 29.28 22.2];

cRdata50 = [100 46.07 21.5 10.16 5.11];

cRdata100 = [100 39.69 15.59 6.32 2.57];

cRdata150 = [100 35.94 14.46 5.81 2.5];

H+_0 = 1.90e-05;

H+_25 = 1.98e-04;

H+_50 = 2.76e-04;

H+_100 = 3.66e-04;

H+_150 = 4.23e-04;

cA0 = 100;

%Zeit

tdata = [0 2 4 6 8];

%Funktion Quercetinbildung

fun1 = @(k,tdata)cA0*((1-exp(-(k(1)+k(2))*H+_0/c0*tdata)-k(2)/(k(3)-
k(1)-k(2))*(exp(-(k(1)+k(2))*H+_0/c0*tdata)-exp(-
k(3)*H+_0/c0*tdata))));

%Funktion Quercetinbildung

fun2 = @(l,tdata)cA0*((exp(-(l(1)+l(2))*H+_0/c0*tdata)));

%Grenzensetzung

lb = [x.x,x.x,x.x];

ub = [x.x,x.x,x.x];

lb1 = [x.x,x.x];
```

```matlab
ub1 = [x.x,x.x];
%Startpunkte
k0=[x.x,x.x,x.x];
l0=[x.x,x.x];
kQ = lsqcurvefit(fun1,k0,tdata,cQdata0,lb,ub);
kR = lsqcurvefit(fun2,l0,tdata,cRdata0,lb1,ub1);
%Plot
times = linspace (tdata(1), tdata(end));
plot(tdata, cQdata0, 'ko', times, fun1(kQ,times), 'b')
legend('data', 'Fitted exponential')
title('Pressure 0 bar')
%Reaktionskonstante Quercetin
kQ
%Reaktionskonstante Rutin
kR
```

CO$_2$-intensified hydrolysis of rutin - preliminary experiments

In Figure 46 CO$_2$–intensified hydrolysis of rutin in a mixture of ethanol / water is shown. For both compounds a pseudo reaction order of 0 was observed. A higher amount of rutin was hydrolyzed than the amount of formed quercetin. Apparently, the effect of an CO$_2$–intensified hydrolysis is hindered in an alcoholic atmosphere [31]. One explanation could be that the formation of carbonic acid is disrupted and therefore the pH value is too high to hydrolyze glycosides in a greater extend.
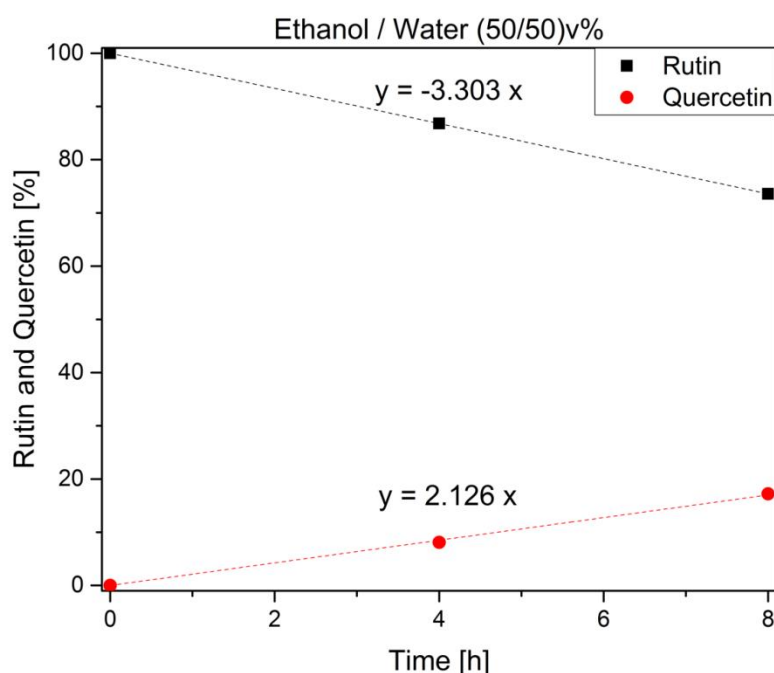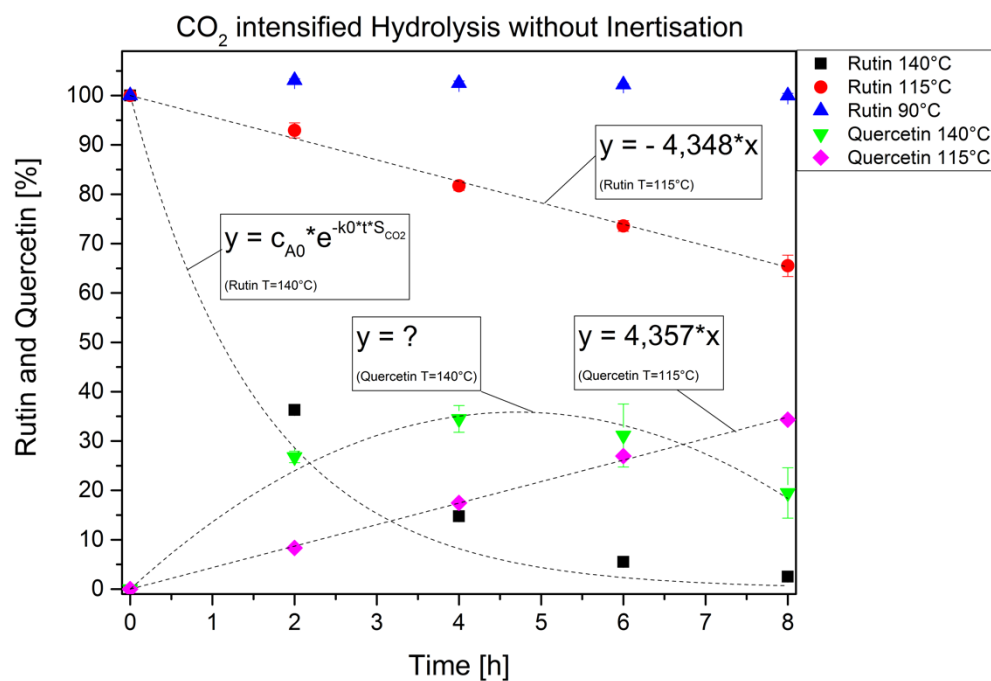

Figure 46: CO2 - intensified Hydrolysis of 0.2 g/L rutin dissolved in ethanol / water (50 v% / 50 v%) at 413.15 K and 150 bar

These findings of the preliminary experiments showed the disrupting behavior of ethanol in a CO$_2$–intensified hydrolysis. Subsequently, the use of ethanol will be abandoned for the next series of experiments and therefore the hydrolysis behavior

should be investigated at 363.15 K, 388.15 K and 413.15 K. The maximum solubility of rutin is decreasing to 0.05 g/L by using water as reaction solvent. The concentration of 0.05 g/L is adequate due to detection limit of 0.001 g/L by analyzing with HPLC. The amount of rutin solution in the high pressure view cell will be increased to 40 mL and the amount of samples will be enhanced by taking samples every 2 hours.

CO_2-intensified hydrolysis of rutin without inertization

In Figure 47 the CO_2–intensified hydrolysis without inertization at 150 bar and 363.15 K, 388.15 K and 413.15 K is shown. CO_2–intensified hydrolysis at 363.15 K resulted in no change of the concentration of rutin. Consequently, no detectable amount of quercetin could be found. This is in accordance to hydrolysis experiments with weak acid at 363.15 K - temperature was too low to initiate hydrolysis of glycosides. A linear degradation of rutin was observed at 388.15 K. Both courses follow a pseudo reaction rate of 0 order. 30% of the initial amount of rutin was equimolar hydrolyzed to 30% of quercetin. At 413.15 K rutin degraded almost completely, whereas quercetin increased within the first four hours and started to decrease after four hours. The degradation of rutin followed a first reaction order. For quercetin a higher reaction order was observed. This means that quercetin starts to decompose after 4 hours at 413.15 K. Buchner et. al [175] investigated decomposition reactions of glycosides and ascertained that oxygen has a high impact on decomposition of quercetin. For these experiments no inert gas was used to replace the containing air in the high pressure view cell.

Figure 47: CO₂-intensified hydrolysis of rutin without inertization at 150 bar and 363.15 K, 388.15 K and 413.15 K

Out of these findings, it was decided to use inert gas to flush the high pressure view cell to remove the remaining air. CO_2 will be used for that purpose as CO_2 is used to lower the pH value for hydrolysis reaction.

Curriculum vitae

Personnel Data

Name: Markus Maier

Date of birth: 21.04.1986

Place of birth: Weiz, Austria

Studies

10.2006 – 05.2013	Chemical and Process Engineering Bachelor and Masters University of Technology Graz, Austria
05.2011 – 08.2011	Summer exchange Program Rutgers University, New Jersey, USA
08.2011 – 08.2012	Chinese Language and Chinese Culture Dalian University of Foreign Languages, Dalian, China

School

09.1992 – 07.2000	Primary and Secondary modern school Anger bei Weiz, Austria
09.2000 – 06.2005	Austrian Matura Höhere Technische Bundeslehranstalt Weiz, Austria

Military Service

09.2005 – 10.2006	Military Service Kirchnerkaserne Graz / KFOR 14 - Kosovo

Employment History

Since 01.2017	IPAT-Program: Assistant Plant Manager C4 Refining Evonik Performance Materials GmbH, Performance Intermediates, Marl, Germany
06.2013 – 12.2016	Project Employee / Researcher Fraunhofer UMSICHT, Oberhausen, Germany